Morphological modelling of the gravel revetment on artificial composite beaches

H.T. Rijper

Technische Universiteit Delft

Deltares
Enabling Delta Life

TU Delft

Boskalis

Morphological modelling of the gravel revetment on artificial composite beaches

by

H.T. Rijper

in partial fulfilment of the requirements for the degree of

Master of Science
in Civil Engineering

at the Delft University of Technology,
to be defended publicly on Wednesday 28 March 2018 at 14:30.

Student number:	4149211	
Thesis committee:	Prof. dr. ir. S. G. J. Aarninkhof,	TU Delft
	Dr. ir. B. Hofland,	TU Delft
	Dr. ir. R. T. McCall,	Deltares
	Ir. T.F. van der Biezen,	Royal Boskalis Westminster N.V.

An electronic version of this thesis is available at `http://repository.tudelft.nl/`.

Cover photo is taken during the DynaRev experiment in Hannover
September 2017 - A wave overtops the revetment and reaches the back sand slope.

SUMMARY

This thesis discusses the morphological modelling of the gravel revetment on artificial composite beaches. A composite beach is a combination of a sandy lower beach and a gravel upper beach. These beaches are found in nature, but can also be created artificially by placement of a gravel structure on a sandy beach. Artificial composite beaches are widely acknowledged as an effective type of shore protection against runup and overtopping (Blenkinsopp, 2016), but an assessment of such a beach with a numerical model has not been attempted yet.

Therefore this work explores to what extent the morphological developments of these artificial beaches can be modelled with a numerical model. The numerical models that were used in this work are XBeach and XBeach-G. The aim is to reproduce the short term (3 to 6 hours) cross-shore morphological developments of the DynaRev experiments (a series of physical model experiments to investigate the stability of an artificial composite beach under sea-level rise), with a focus on the beach section on which the gravel revetment is placed. The first step was to find the relevant processes that are missing in the currently available numerical models. The missing processes were identified by combining knowledge acquired through the modelling of composite beaches with the currently available models, substantiated by analysis of the DynaRev experiments and literature research.

It was concluded that the numerical models were lacking two important processes: namely the absence of a gravel transport formulation in XBeach and transport of sand in the gravel revetment. The missing processes were implemented into XBeach and the updated model's performances were verified with the DynaRev experiments as benchmark. The implementation of the XBeach-G gravel transport formulation in coherence with the existing XBeach code for sand transport required under-the-hood adaptations to improve the switches that are already in place for multiple sediment fractions. It was found that a combination of sand transport and gravel transport is possible, but this combination presents difficulties regarding suspended sediment transport in combination with the hydrodynamics and the groundwater dynamics.

The second process was transport of sand in the gravel revetment. This was first analysed by looking at the initial transport rates of sand inside the revetment with a newly introduced equation for transport of sand inside a filter layer (Jacobsen et al., 2017). It was shown that transport fluxes of sand inside the revetment are likely to occur as results of the groundwater dynamics. To see bed level changes due to these transport fluxes this transport equation needs to be implemented into the XBeach code. This was not possible with the current architecture of XBeach and the way it accounts for multiple fractions. Therefore a new accounting system for multiple fractions was introduced in this work and implemented in XBeach, named the two-line model. In this experimental model sand transport gradients in the revetment are translated into visible sinking of the revetment (erosion) and settling of sand within the gravel revetment (deposition). In the model's current state the erosive locations appear to match with the DynaRev observations, whereas locations where deposition occurs are no match. The two-line model was sensitive and showed instabilities, mainly due to high groundwater velocities that were caused by wave breaking in the model. The results of the experimental model can possibly be improved by including vertical groundwater velocities to model sand transports, possibly also in combination with the addition of suspended sediment transport of sand inside the revetment.

PREFACE

This thesis is the result of work executed at Deltares and Boskalis and concludes the degree Master of Science Civil Engineering (Hydraulic Engineering) at Delft University of Technology. I am very proud of the work presented in this thesis and I could not have done this without the help of many people.

My sincere appreciation goes out to my commission. Many students describe graduating to be a stressful and though time during the master, but my commission showed me that the opposite is true. Every meeting we've had gave me much energy and joy, which helped me throughout the last 7.5 months. I might miss graduating the coming months!

First of all I want to thank Robert McCall (Deltares) for the time and effort he invested in me. Our pleasant trip to Hannover showed me how much you like your field of study and I will never forget how excited you were when we were setting up the first model of the DynaRev experiment from scratch (and actually seemed to work). That enthusiasm give me motivation to work on the subject. Secondly my thanks go out to Tim van der Biezen (Boskalis). Many of my modelling skills I acquired during my internship and graduation I learned from you or by copying your Matlab scripts. Whenever my head was too busy with the model, our meetings were often eye-openers and lastly thank you for often reviewing my reports. I am very grateful that Bas Hofland (TU Delft) wanted to join my commission. You were full of ideas that could contribute to my report and many of them made it to the final report. I also appreciated the critical feedback as well as the hidden smiley in chapter number three. Lastly I would like to thank the chairman of my commission, namely Stefan Aarninkhof (TU Delft). I find it admirable that you find the time to have personal and useful conversations with your students, while having such a busy agenda. I really appreciated our 40 minute conversation over the phone brainstorming about many different subjects. Lastly I think that your guidance throughout the process of graduating really contributed to what needed to be studied.

The work performed in this thesis would not have been possible without the help of Chris Blenkinsopp and Paul Maxime Bayle from the Univerisity of Bath on the DynaRev experiments. Also I would like to thank Dano Roelvink (UNESCO-IHE), Niels Jacobsen (Deltares) and Jaap van Thiel de Vries (Boskalis) for the useful brainstorms.

Besides my commission I need to thank the Hydronamici of Boskalis. Thanks all the help, activities, drinks and 11'en during my thesis work and internship, I have really enjoyed my time at the department. Of course I would like to thank all of my fellow graduates from Boskalis and Deltares. Without the help of our coffee breaks and conversations about nonsense I would have gone mad. Last 2.5 years I have had the pleasure of working with many nice people at the TU Delft, those who feel addressed: thank you! Most of all I will remember the time spent with my friends from Flood Proof Myanmar. I have learned a lot from you and hope to work with you guys again in the future! I would really like to thank all of my (former) housemates for at times giving me the feeling was actually capable of doing something. I treasure my time at Noordeinde: the last 5.5 years were a blast and I consider everyone as a dear friend.

Last but not least I owe many thanks to my family. I am very grateful to have been supported both emotionally and financially throughout my entire study. "Try your best, but most of all enjoy yourself", I have not taken it for granted!

Huub Rijper
Delft, March 2018

CONTENTS

LIST OF FIGURES

LIST OF TABLES

LIST OF SYMBOLS

Symbol	Unit	Description
A_{sb}	-	Bed-load coefficient
A_{ss}	-	Suspended-load coefficient
C	$m^{\frac{1}{2}}s^{-1}$	Chezy coefficient
C	-	Depth averaged concentration
C_1	$m^3s^{-1}m^{-1}$	Calibration constant
C_{eq}	m^3m^{-3}	Depth averaged equilibrium concentration
$C_{eq,s}$	m^3m^{-3}	Depth averaged equilibrium concentration (suspended load)
$C_{eq,b}$	m^3m^{-3}	Depth averaged equilibrium concentration (bed-load)
D	m	Characteristic grain size
D_h	m^2s^{-1}	Horizontal diffusion coefficient for sediment
D_{50}	m	Median grain size
D_*	-	Dimensionless grain size
H	m	Wave height
H	m	Groundwater head
H_b	m	Wave height at wave breaking
L	m	Wave length
Re	-	Reynolds number
S	ms^{-1}	Surface water-groundwater exchange flux
T	s	Wave period
T_s	s	Adaptation time
U	ms^{-1}	Depth averaged flow velocity
U_{cr}	ms^{-1}	Critical velocity
U_{crc}	ms^{-1}	Critical velocity for currents
U_{crw}	ms^{-1}	Critical velocity due to waves
c_f	-	Dimensionless friction coefficient
d	m	Fraction size
g	ms^{-2}	Gravitational acceleration
h	m	Water depth
k	m	Characteristic roughness height
n_p	-	Porosity
p_{atm}	$kgm^{-1}s^{-2}$	Atmospheric pressure
q_b	$m^3s^{-1}m^{-1}$	Volumetric bed-load transport rate, excluding pore space
$\bar{q}$	m^2s^{-2}	Depth-averaged normalized dynamic pressure
s	-	Density of sand relative to that of water
t	s	Temporal coordinate
u	ms^{-1}	Flow velocity
$u_{\parallel}$	ms^{-1}	Filter velocity parallel to sediment bed
u^E	ms^{-1}	Eulerian flow velocity
v_{mg}	ms^{-1}	Velocity magnitude
w	ms^{-1}	Vertical velocity
w_s	ms^{-1}	Sediment fall velocity
x	m	Horizontal coordinate
Δ	-	Relative submerged weight of sediment
Ψ	-	Mobility number
Ψ_{cr}	-	Slope corrected critical mobility number
Ψ_{cr0}	-	Critical mobility number
Ω	-	Dimensionless fall velocity

β	$^\circ$	Beach slope angle
ζ	m	Free surface elevation
θ	-	Shields parameter
θ_{cr}	-	Critical Shields parameter for the initiation of transport
ν	$m^2 s^{-1}$	Kinematic viscosity of water
ν_h	$m^2 s^{-1}$	Horizontal viscosity
ξ	-	Iribarren number
ρ	kgm^{-1}	Density
τ_b	$kgm^{-1}s^{-2}$	Bed shear stress
τ_{bd}	$kgm^{-1}s^{-2}$	Bed shear stress due to drag
τ_{bi}	$kgm^{-1}s^{-2}$	Bed shear stress due to inertia
ϕ	$^\circ$	Slope of bed relative to direction of flow
ϕ	$^\circ$	Angle of repose
ϕ_r	$^\circ$	Angle of repose

1

INTRODUCTION

1.1. BACKGROUND

Beaches come in many shapes and forms. Everyone is familiar with sandy beaches, which are found all over the world. Less prominent are beaches that consist of bigger grains, which are named gravel beaches. In England and Wales one third of the beaches is of a gravel nature (Fuller and Randall, 1988). Even less prominent are the so-called mixed-sand-gravel and composite beaches. These beaches are a combination of sandy and gravel beaches. Mixed-sand-gravel beaches consist of mixed medium of both sand and gravel throughout the entire cross-section of the beach, while on composite beaches sand and gravel are separated. Offshore, composite beaches consist of a sandy slope and onshore a gravel slope is found.

Beaches play an essential role in protecting the hinterland. Beaches and dunes protect the hinterland from flooding and therefore prevent societal damages. Within coastal management a distinction is made between *soft* and *hard* engineering. Soft engineering aims to protect the hinterland by maintaining beaches sandy. Soft engineering maintenance is almost always done through local beach nourishments. This method is often used in areas where recreation and environment is of importance, see Van Thiel De Vries et al. (2016) for sandy strategies. Hard engineering on the other hand makes use of hard structures to manage a certain coastal areas. For hard structures one can think of seawalls, groynes, breakwaters or rip rap. They take up less space while maintaining the same level of safety as for soft structures, these structures are commonly found around areas of high economical and/or societal value such as a harbour or densely populated urban areas.

In the recent decades a certain type of shore protection has been mentioned to be of interest: dynamic revetments. This is a mix between a soft and hard engineering measure. These revetments, which consist of gravel and are placed on a sandy beach, resemble the earlier mentioned composite beaches as they are composed of a sandy beach slope and separate gravel slope. The potential of this type shore protection has been widely acknowledged throughout the years (Allan et al., 2005). Gravel revetments are known for their dynamic stability and allow the absorption of wave energy through groundwater dynamics. From experience it is known they perform well in preventing runup and overtopping (Blenkinsopp, 2016). From data presented by Allan et al. (2004) it was found that dunes fronted by composite gravel beaches experienced erosion rates that were typically 20 - 40 % of the rates experienced by adjacent pure sand beaches. The gravel stones of these beaches typically have a smaller grain size than large armouring stones, which makes dynamic revetments economically interesting. Lastly the placement of the gravel material does not need to be very precise. The stones can be dumped and they adapt to the wave conditions, as they form a dynamic revetment (Allan et al., 2005).

An assessment of the resilience and strength of a beach is needed when designing a beach or when beaches need maintenance. To do so coastal engineers use several types of models. *Process-based models* are models that simulate beach processes using the physics behind these processes. *Empirical models* are the precursors of the process-based models and can be applied with a certain range of applicability. These empirical models are often established by fitting certain formulas to observations. Therefore empirical models most often work well for situations that are similar to the situations with which they have been fitted. Process-based models on the other hand are more universally based, as physics do not change for different situations.

XBeach (Roelvink et al., 2009) is a process-based model that can model hydrodynamic and morphodynamic processes for sandy beaches. Ever since its release the model has been tested, validated, improved and it has been used in practice. As XBeach was developed it opened up opportunities to model gravel beaches, for which only empirical models were present. McCall (2015) created an adaptation of XBeach called XBeach-Gravel, also known as *XBeach-G*.

1.2. RELEVANCE

As XBeach is only able to model sandy beaches and XBeach-G only gravel beaches, neither of these models is designed to model composite beaches or sandy beaches with dynamic revetments. XBeach-G has been used to model a mixed-sand-gravel beach by Bergillos et al. (2016) and was successful, but this was done by assuming only gravel was present. The gravel fraction dominated the morphodynamic response of the beach. Furthermore a transport formulation was used that uses a best fit, which means this model could only be used in areas where data is present. Furthermore Pedrozo-Acuña et al. (2007) have applied a numerical-empirical model to mixed-sand-gravel beaches, but this model is also limited. It does not allow for the separation of sand and gravel and considers it to be one single fraction. Lastly an attempt was made to model composite beaches with empirical models. Here Karunarathna et al. (2012) compared two beach sites, a sand beach and a composite beach, in order to investigate their morphodynamic differences. In this research the long-term cross-shore morphodynamic variability was assessed by comparing the time-mean beach profiles with equilibrium profiles of Dean (1991) and Vellinga (1983). There are a few big restrictions to these empirical formulations, the biggest being that these profiles can only predict profile variability up to the water level and that these formulations predict equilibrium states. In reality beaches are always dynamic.

Modelling composite beaches has not been explored extensively yet, despite the potential of similar artificial beaches. Furthermore the behaviour of artificial composite beaches is not yet fully understood. Therefore a series of large scale experiments have been conducted called DynaRev. Besides gaining knowledge into the dynamics of composite beaches, research on modelling this type of beach includes many types of processes that are of interest for the application of gravel in sandy environments. Gravel is used to protect cables and pipelines on sand beds, provide local scour protection or even help facilitate beaching of large vessels on intertidal zones. In other words, a study on the modelling of composite beaches increases the general knowledge on large-scale interactions of mixed-sand-gravel bodies.

1.3. OBJECTIVES

The objective of this report is based on the demand for knowledge on sand-gravel interactions and the potential of application of a model that is able to correctly reproduce the morphodynamics of (artificial) composite beaches. The work is the first step to the generic modelling of these beaches. The experimental results from DynaRev are suitable as a reference case and have been used for the start of modelling (artificial) composite beaches.

The research question for this thesis is:

*To what extent can the **morphological developments** of the artificial beach of the DynaRev experiments be modelled with a **numerical model**?*

The scope of the research is narrowed down as follows:

Morphological developments:
The scope is limited to modelling of the cross-shore and short-term response of the DynaRev beach. Furthermore the research is limited to the morphological active surf zone and swash, excluding bar morphodynamics and is focussed on sand-gravel interactions. Changes in bed slopes and bed elevation are assessed in order to qualify how the model performs.

Numerical model:
The numerical models of the XBeach family are used for this thesis, namely XBeach and XBeach-G. In this report both XBeach and XBeach-G have been mentioned as two different models, but in reality XBeach-G is part of the XBeach software. For clarity these models have been treated as two separate

models that share characteristics, but needed to be specified separately because of their distinct modelling purposes.

Accompanied with this research question the following sub-questions are proposed:

1. How do the current numerical models perform regarding the modelling of composite beaches?
2. What are the current limitations of the numerical models regarding modelling of composite beaches?
3. Which processes can and have to be added to or adapted in the numerical models in order to model composite beaches?
4. How do the additional processes improve the numerical model results?

1.4. APPROACH

The approach for this thesis is visualised in Figure 1.1. In order to model the morphological developments of composite beaches one must know all about the processes present at these beaches. In Chapter 2 background information on composite beaches is provided. Chapter 3 discusses modelling of sandy and gravel beaches. In Chapter 4 observations of composite beaches from experiments that were performed in Hannover, named *DynaRev*, are discussed. These experiments provided detailed measurements of developments of a composite beach. In Chapter 5 the performances of XBeach and XBeach-G are assessed based on the DynaRev experiments. The *performance study* answers the first sub-question regarding the performance of modelling composite beaches with current numerical models. In Chapter 6 the information gathered from the literature study, DynaRev experiment and performance study is combined to make conclusions on limitations of the numerical models. This chapter on *process identification* answers the second sub-question. Furthermore Chapter 6 also discusses the processes to be added to the current models, answering the third sub-question. The processes to be added are discussed in Chapter 7 and Chapter 8, which are on *modelling with multiple fractions* and *sand transport in the gravel revetment*. From these two chapters and Chapter 9, in which a new two-line model is proposed, the last sub-question can be answered. After a discussion in Chapter 10 several conclusions are made is Chapter 11. Finally a variety of recommendations is provided in Chapter 12.

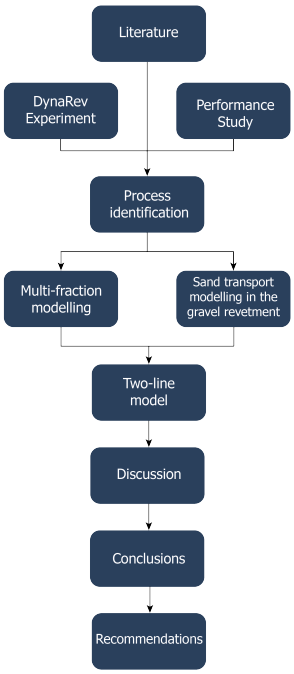

Figure 1.1: Approach of report

1.5. THESIS OUTLINE

This report contains the following chapters:

Chapter 2: in which background information about composite beaches is given
Chapter 3: in which background information about modelling is given
Chapter 5: in which the performance of current models is analysed
Chapter 6: in which the relevant processes are identified
Chapter 7: in modelling with multiple fraction is elaborated
Chapter 8: in which sand transport in the gravel revetment is discussed
Chapter 9: in which a new two-line model is proposed
Chapter 10: provides a critical discussion
Chapter 11: provides several conclusions
Chapter 12: provides several recommendations

2

COMPOSITE BEACHES

What is a composite beach?

This chapter discusses the characteristics of beaches and in particular the characteristics of composite beaches. Some terminology is provided and background information of processes occurring at beach sites is discussed.

First some main beach characteristics are discussed in section 2.1 after which section 2.2 discusses composite beaches in more detail.

2.1. BEACH CHARACTERISTICS

The most important distinction to be made between several beach states for the scope of this research are the differences *reflective* and *dissipative* beaches. Beaches are highly dynamic such that various morphodynamic regimes (or beach states) have been classified according to their overall appearance (Bosboom and Stive, 2015). A dimensionless parameter $\Omega = \frac{H_b}{w_s T}$ is used to identify these states, with H_b being the wave height at breaking, w_s the fall velocity of the sediment and T the wave period. Reflective beaches have an $\Omega < 1$ and are characterized by a relative steep slope (Bosboom and Stive, 2015). The sediments present at the beach are relatively coarse. These beaches are called reflective as they reflect waves, which means not all energy is dissipated with wave breaking but is reflected offshore. Dissipative beaches on the other hand are characterized by a mild slope and the sediments present are relatively fine. At these beaches the dimensionless fall velocity Ω is found to be larger than 6. These beaches are called dissipative as they dissipate almost all of the wave energy through wave breaking.

2.1.1. CLASSIFICATIONS

In nature a wide variety of beaches are found. Composite beaches are classified as gravel beaches. Three different types of gravel beaches can be distinguished, namely pure gravel beaches, mixed-sand-gravel beaches and composite gravel beaches. These beaches have been classified and described by Jennings and Shulmeister (2002). Some key elements of these beaches are discussed below in order to distinguish what makes a composite beach different the other gravel beaches. In these classification Iribarren numbers are mentioned, which give an indication how reflective or dissipative a beach is, see section A.2.1.

- **Pure gravel beaches**:
  Pure gravel beaches (Figure A.3) are the steepest gravel beaches of the three classified gravel beaches. These beaches are reflective and have steep beachfaces of about $\tan\beta = 0.1 - 0.25$. This steep beachface can be maintained due to the high permeability of the gravel, which accentuates the asymmetry of the swash (Quick and Dyksterhuis, 1994). The Iribarren numbers found at these beaches are around $1.6 - 4.0$.

- **Mixed-sand-gravel beaches**:
  Mixed-sand-gravel beaches (MSG) (Figure A.4) are composed of sand and gravel over the entire cross

section. The beach slope ranges from $\tan\beta = 0.04 - 0.12$ and the Iribarren numbers found at these beaches are around $0.7 - 1.95$. Jennings and Shulmeister (2002) mention that at MSG beaches the sand and gravel are mixed over the entire profile including the in the vertical. They do mention that it occurs that there is sediment sorting in the top sediment layer. When this sediment sorting is pronounced it is more likely that the beach can be classified as a composite beach.

- **Composite beaches**:
  Compared to MSG beaches composite beaches are not composed of mixed-sand-gravel sediment over the enter cross section, see Figure 2.1. Due to hydraulic sorting these beaches are composed of two parts. At the landward side the beach is composed of gravel with a slope of about $\tan\beta = 0.1 - 0.15$ and at the seaward side the beach is composed of sand with a slope of about $\tan\beta = 0.03 - 0.1$.

  During low tide the waves experience a relatively flat dissipative sandy beach and these are typically spilling waves. With high tide the waves become reflective because the change in beach slope. At high tide Iribarren numbers are found to be about $0.5 - 1.8$.

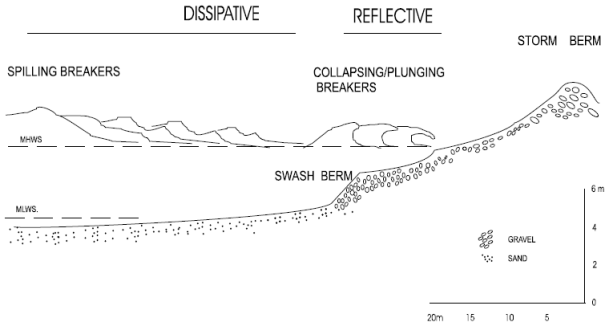

Figure 2.1: Representation of a composite beach (Jennings and Shulmeister, 2002)

Figure 2.2: A composite beach by the name Short Beach, Oregon (picture by J. Spesard)

2.1.2. COMPOSITE BEACHES AS FOUND IN NATURE

A comprehensive study on gravel beaches on the coast of Oregon was performed by Allan et al. (2005). Most of these gravel beaches also consisted of a sandy beach in front of the gravel, therefore they can be considered to be composite beaches. On the composite beaches as found on the Oregon coast, the sandy lower beach is exposed at all tidal stages during summer, only becoming submerged in the winter when storms occur and much of that sand has moved to offshore bars, allowing the waves to reach the gravel ridge at mid- to high-tides (Allan et al., 2005). Jennings and Shulmeister (2002) did show in their classification that composite beaches that the gravel upper beach can be expected to be exposed during most high waters. The slopes of the sandy lower beach and gravel upper beach vary for each beach. Grain sizes of gravel found at these beaches vary from 30 mm to 128 mm. These grain sizes were found to be uniform in size and the sorting of

the sediments was classified as well sorted to moderately well sorted. On average the gravel beaches were found to have a slope of 10.9° (1/5.19).

2.1.3. ARTIFICIAL COMPOSITE BEACHES

Several artificial composite beaches have been constructed throughout the decades are discussed below. These artificial composite beaches are often made by placing a dynamic revetment onshore. The documented dynamic revetments by Allan et al. (2005) had varying grains sizes .

Several of these dynamic revetments are found in relatively low wave-energy environments. The first example is a dynamic revetment placed on the shore of Vancouver, Canada. This revetment was made from cobbles and performed relatively well (Allan et al., 2005), (Downie and Saaltink, 1983). Another dynamic revetment is found in Flathead Lake, Montana. Here a structure was made from stones ranging from grain sizes from 5 to 25 mm. The structure effectively reduced the erosion, however some gravel stones were lost due to oblique wave approach (Allan et al., 2005), (Lorang, 1991). Another interesting example is the dynamic revetment constructed at Cape Lookout State Park, Oregon and was constructed to prevent erosion of the shores, see Figure 2.3. This dynamic revetment consists of mean grain sizes varying from 39.4 to 55.7 mm.

In a report by Allan et al. (2005) it was analysed what the grain size would typically be best for a dynamic revetment. It was concluded that dynamic revetments should consist of gravel stones with a median grain size around 64 mm. This conclusion was based on the observation made from naturally occurring beaches around the southern coast of Oregon and their performances.

Figure 2.3: Dynamic revetment at Cape Lookout State Park, Oregon

2.2. DYNAMICS OF COMPOSITE BEACHES

In this section the dynamics of composite beaches are elaborated and several relevant processes are introduced.

First the sandy lower beach and its dynamics are discussed, then the upper gravel beach and lastly several sand-gravel interactions are discussed.

2.2.1. SANDY LOWER BEACH

As was described in section 2.1.1, the sandy slope of the composite beaches are typically dissipative. Dissipative beaches are highly energetic and the energy is dissipated through wave breaking over a wide surf zone. In the surf zone waves get higher due to shoaling. Shoaling is caused by a change in water depth, which is gentle in the surf zone. Once a wave grows in size it reaches a certain steepness, after which the wave breaks when it reaches a maximum steepness.

In the surfzone a *undertow* is present, which is a relatively large return current directed seaward (Bosboom and Stive, 2015). This undertow is a result of the breaking of waves (which is caused by a vertical imbalance in the cross-shore momentum terms), where mass transport is large towards the coasts. The undertow is of

importance regarding transports of sediments.

Dissipative beaches are lastly characterized by having a *bar*. During energetic conditions these bars move offshore, while they move onshore during less energetic conditions (Bosboom and Stive, 2015). Long-shore bar-trough systems are mentioned by Jennings and Shulmeister (2002) to potentially develop at composite beaches, but their development is out of the scope of this thesis.

2.2.2. GRAVEL UPPER BEACH

As was described by Jennings and Shulmeister (2002) the upper gravel beach of a composite beach falls within the reflective domain. The amount of reflection is still depended on the percolation of the gravel slope, as was mentioned by Mason et al. (1997) who studied the differences between composite and sandy beaches. Gravel beaches have a high permeability and groundwater flow is of importance. Wave energy is dissipated through turbulence within the gravel upper beach.

Field studies at a composite gravel beach show that the groundwater table is dependent on the underlying sand layer (Mason et al., 1997). In these researches little is mentioned about the depth at which this sand layer lies, as this probably varies for each beach site and is difficult to measure.

2.2.3. REFLECTION AT COMPOSITE BEACHES

In the paper by Mason et al. (1997) the reflection of composite beaches is compared with sandy beaches. Figure 2.4 shows measurements of reflection FDRF (Frequency-Dependent Reflection Function). High FDRF values correspond to high reflection and low values to low reflection. The open symbols correspond to a sandy beach and the filled symbols to a composite beach (with both sand and gravel slopes). The figure show the reflection for different wave frequencies. For composite beaches the reflection of swell waves (low frequency) is highly sensitive to the Irribarren number and therefore the beach gradient. This is not the case of wind waves, which are reflected for which the reflection stayed the same for different Iribarren numbers.

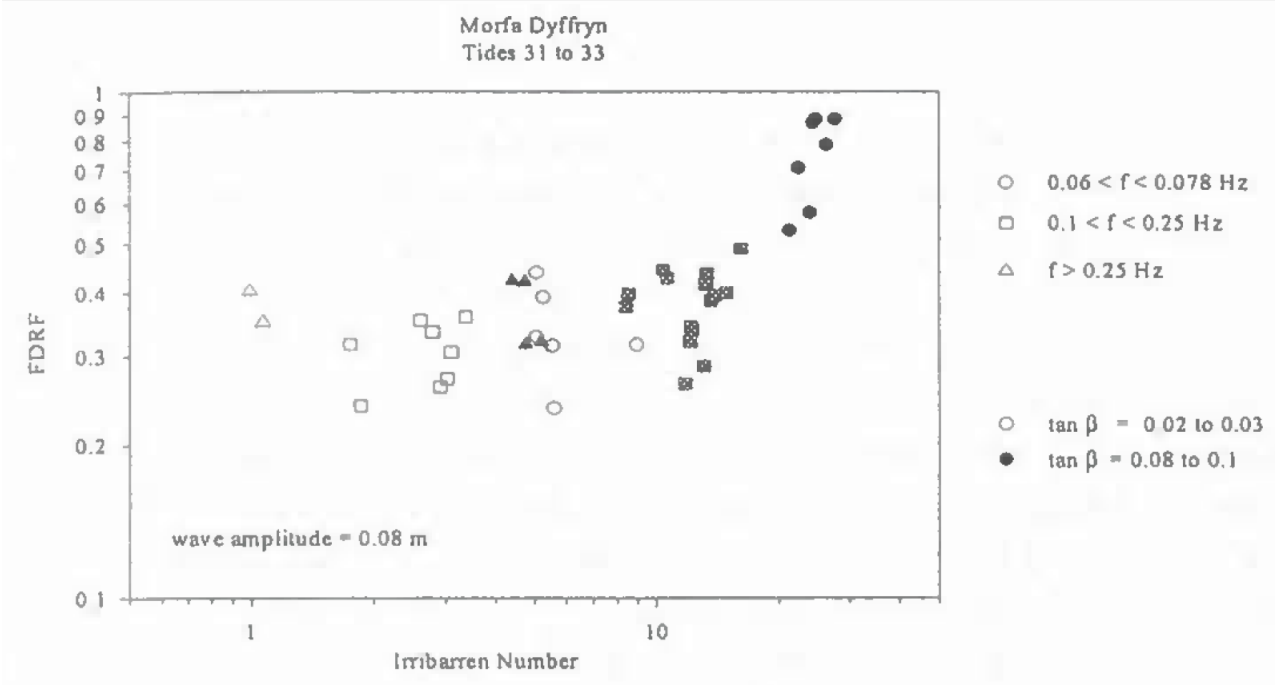

Figure 2.4: Irribarren Number vs. FDRF for constant wave amplitude and beach gradient of 0.02 to 0.03 (open symbols) and 0.08 to 0.1 (filled symbols) (Mason et al., 1997)

2.2.4. SAND-GRAVEL INTERACTIONS

2.2.4.1 INTERFACES

In order to explore the processes present at composite beaches the following interfaces have been identified: water-sand, water-gravel and gravel-sand.

- Interface I: *Water and sand*
  At this interface sand particles are transported through both suspended and bed-load transport. These types of transport occur when the water reaches a certain threshold velocity. Several types of formulations for calculating these transports are known and are discussed in section 3.2.2 where they are implemented in XBeach.

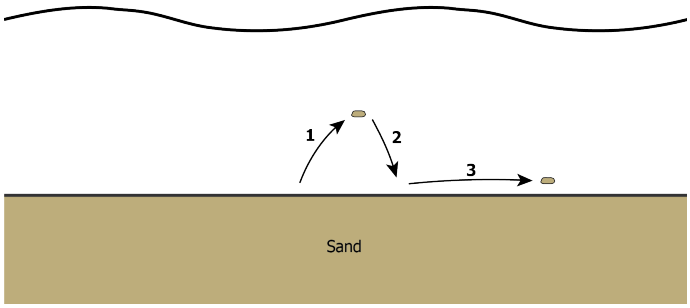

Figure 2.5: Interface I: (1) Resuspension of sand particles (2) Settling of sand particles (3) Bed-load transport of sand particles

- Interface II: *Water and gravel*
  Interface II describes the interaction between water and gravel. Gravel is only transported through bed-load transport and calculating the transport has a different approach with regard to the transport of sand. This is discussed in section 3.2.3 where it is implemented in XBeach-G.

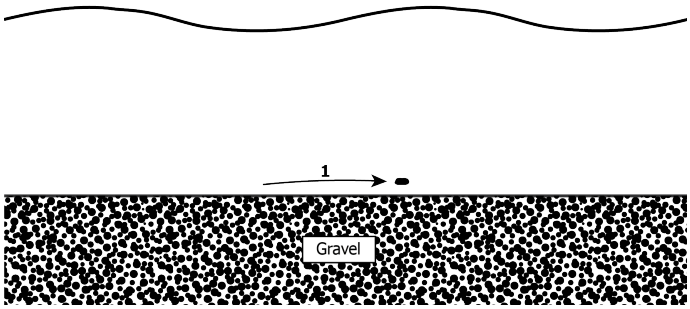

Figure 2.6: Interface II: (1) Bed-load transport of gravel particles

- Interface III: *Gravel and sand*
  The third interface describes the transport of sand below gravel. As this type of transport is not implemented in XBeach its formulations has been discussed shortly.

  Jacobsen et al. (2017) did research on the hydraulic loading at the interface between an open filter (gravel) and base material (sand). When the loading is large enough to mobilize sediment at this interface the sediment transport function is given as:

$$q_b = C_1 \left(\Psi - \Psi_{cr}\right)^{1.5} \frac{u_{\parallel}}{||u_{\parallel}||_2} \tag{2.1}$$

  In which q_b describes the sediment transport along the direction of a velocity vector adjacent to the bed. C_1 is a calibrated constant by Jacobsen et al. (2017). The mobility parameter Ψ is given as:

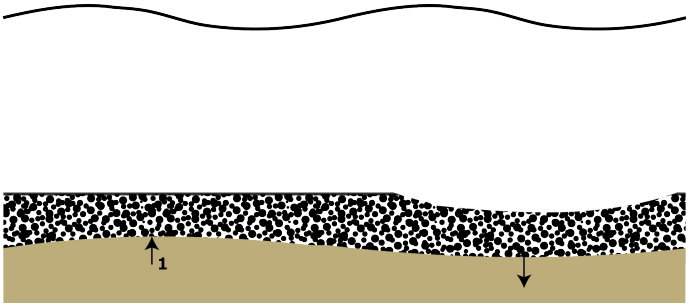

Figure 2.7: Interface III: (1) Transport of sand underneath gravel layer

$$\Psi = \frac{||u_{\parallel}||_2^2}{(s-1)\,gd} \tag{2.2}$$

Here and in function 2.1 $u_{\parallel}$ is the horizontal filter velocity and s is the relative weight of the sand compared with water. The slope corrected critical mobility parameter is described to be:

$$\Psi_{cr} = \Psi_{cr0}\frac{\sin(\phi_r - \phi)}{\sin\phi_r} \tag{2.3}$$

In which Ψ_{cr0} is a critical mobility number which is calibrated, ϕ_r is the angle of repose and ϕ is the slope of the bed relative to the flow.

2.2.4.2 ARMORING, HIDING AND EXPOSURE

In multi-fraction beds some additional effects should be discussed that are not present in uniform beds, namely armoring, hiding and exposure. *Armoring* occurs when smaller particles (sand) are eroded and coarser particles are immobile and do not erode. This leads to the development of a armor layer that prevents the further pick up of finer particles that lay underneath the armor layer (Van Rijn, 2007c).

Hiding of a sediment is a phenomena that occurs when a certain particle has a higher critical shear stress in a non-uniform bed compared with a uniform bed. A particle hides between bigger particles and therefore has a higher critical shear stress. The opposite is when a particle is more exposed compared with a uniform bed. This is called *exposure* and for exposure the critical shear stress becomes lower. Sand particles between gravel particles in theory would then have a higher critical bed shear stress and gravel particles would have smaller critical bed shear stresses. Several studies have been done on this phenomena, see Van Rijn (2007c) for a comprehensive summary of these studies.

2.2.5. GROUNDWATER FLOW

At the gravel upper beach groundwater flow is present. Through groundwater flow energy is dissipated, which influences the overwash and run-up at the beach. Two formulations for groundwater flow through a porous medium are discussed.

2.2.5.1 GROUNDWATER FLOW EQUATIONS

The well known equation that describes the flow of an incompressible fluid through a porous (homogeneous) medium is the Law of Darcy (1856):

$$\nabla H = -\frac{1}{K}\vec{U} \tag{2.4}$$

In which K described the hydraulic conductivity of a medium and H is the hydraulic head. The hydraulic conductivity K describes how easily water flows through a certain medium. This equation only holds for laminar flow. Once the flow increases it might become turbulent and then Darcy's Law does not apply any more. Whether flow is turbulent or laminar is described with the Reynolds number for flow through a bed:

$$Re = \frac{|U|D_{50}}{n_p \nu} \tag{2.5}$$

Here $|U|$ is the depth averaged absolute velocity, D_{50} the median grain size of the mediu, n_p is the porosity of the medium and ν is the kinematic viscosity of water. High flow velocities gives higher Reynold numbers and the flow can be described to be turbulent if Re is large enough. For turbulent flow the Darcy-Forchheimer equation can be used (Forchheimer, 1901). Here the simplified Darcy-Forchheimer equation is known:

$$\nabla H = -a\vec{U} - b\vec{U}\left|\vec{U}\right| \tag{2.6}$$

In which a is a coefficient describing the hydraulic conductivity, similarly to equation 2.4, and b is a friction coefficient which is the turbulent contribution to the equation. This equation can be expanded with an inertial term.

2.2.5.2 HYDRAULIC CONDUCTIVITY OF SEDIMENTS

In both Darcy as well as the Darcy-Forchheimer equation the hydraulic conductivity K is of importance. This variable largely depends on the permeability of the medium present. In a gravel environment large values for K are found and smaller values are found for less permeable sediments such as sand. In a mixture of gravel and sand this K can change rapidly. A mixture of 20% medium sand to gravel reduced the hydraulic conductivity to around a third of the gravel alone (Mason et al., 1997). Appendix A.2.2 provides information about the hydraulic conductivities of mixed-sand-gravel mediums.

3

PROCESS-BASED MODELLING

How do you model these beaches?

This chapter discusses the process based models XBeach and XBeach-G. These models share many of the same equations and both models are of equal importance. Mostly the equations that are implemented in XBeach are discussed and with these equations remarks are made about their implementation in XBeach-G. Remarks are made in the case equations are present in XBeach-G only.

In section 3.1 the hydrodynamics behind XBeach and XBeach-G are discussed followed by the morphodynamics in section 3.2. The groundwater dynamics are discussed in section 3.3, some remarks are made on the numerical implementation in section 3.4 and finally in section 3.5 an overview of comparisons between XBeach and XBeach-G is given.

3.1. HYDRODYNAMICS

In order to understand process-based models like XBeach and XBeach-G it is important to know how the physics are implemented in the models. Therefore some of the base principles and corresponding assumptions with regard to the implementation are elaborated.

The XBeach model is able to run in three hydrodynamic settings, namely:

- Stationary mode
- Surf-beat mode (in-stationary)
- Non-hydrostatic mode (wave resolving)

The stationary mode is the most basic mode in which XBeach can run. The mode neglects infra gravity waves and is out of the scope of this research. In surf-beat mode models the effects of short waves are resolved by modelling the short wave variations on the wave group scale. In this way the long waves, that are associated with wave groups, are resolved. These long waves are of importance as they have a large contribution to the erosion and avalanching. The non-hydrostatic mode models a depth-averaged flow using the NLSWE and includes a non-hydrostatic pressure (Smit et al., 2010). This mode allows the modelling of all waves, including short waves.

The main advantage of the non-hydrostatic model is that is better in modelling run-up due to short waves and is better at modelling the effects of overwash than the surf-beat mode (McCall, 2015). Furthermore wave asymmetry and skewness of waves are resolved by the model instead of empirical formulations as in surf-beat mode. McCall (2015) validated gravel beaches with XBeach-G in the non-hydrostatic mode and currently research is done to validate morphodynamics of sandy beach in the

non-hydrostatic mode.

The scope of this research is limited to the non-hydrostatic mode only. This means that the surf-beat mode and corresponding equations are not elaborated in the following sections, although they are mentioned. Instead the non-hydrostatic mode is elaborated for XBeach and XBeach-G. The motivation for this decision is the fact that XBeach-G only works in the non-hydrostatic mode. For reflective beaches (gravel beaches in XBeach-G) the hydrodynamics need to be resolved in the swash, which is not done in the surfbeat mode. As composite beaches are partly reflective the non-hydrostatic mode is therefore necessary. The hydrodynamics of non-hydrostatic mode have been validated for dissipative beaches (Smit et al., 2010) in XBeach. McCall (2015) validated the non-hydrostatic mode for XBeach-G from data collected from 4 gravel beaches and an experiment. XBeach-G was capable of reproducing the hydrodynamics on gravel beaches, in particular with regard to wave transformation, wave run-up and initial wave overtopping (McCall, 2015).

3.1.1. NON-LINEAR SHALLOW WATER EQUATIONS

The non-linear shallow water equations, the equations that describe the flow of water, are based on the Navier-Stokes equations. These equations are depth-averaged and are one-dimensional for this thesis. With the development of XBeach-G it is also possible to include groundwater exchanges in these equations for both XBeach and XBeach-G.

The non-linear shallow water equations are:

$$\frac{\partial \zeta}{\partial t} + \frac{\partial hu}{\partial x} + \underbrace{S}_{\text{Introduced with XBeach-G}} = 0 \tag{3.1}$$

$$\frac{\partial u}{\partial t} + \underbrace{u\frac{\partial u}{\partial x}}_{\text{Advective term}} - \underbrace{\nu_h \frac{\partial^2 u}{\partial x^2}}_{\text{Viscousity term}} = \underbrace{-\frac{1}{\rho}\frac{\partial\left(\rho\bar{q}+\rho g\zeta\right)}{\partial x}}_{\text{Pressure term}} - \underbrace{\frac{\tau_b}{\rho h}}_{\text{Bottom friction}} \tag{3.2}$$

In these equations u describes the depth-averaged cross-shore velocity, ζ is the free surface elevation, h is the total water depth, S stands for the surface water-groundwater exchange. Furthermore ν_h is the horizontal viscosity, ρ is the density of water, $\bar{q}$ is the so called depth-averaged dynamic pressure normalized by density, g is the gravitational constant and finally τ_b is the shear stress due to bottom friction.

The bed shear stress τ_b is described as a product of the current velocity, water density and a dimensionless friction coefficient c_f:

$$\tau_b = \rho c_f u|u| \tag{3.3}$$

In XBeach-G this bed shear stress is calculated in a different manner, as is discussed in section 3.2.3. The dimensionless friction coefficient can be calculated by defining a Chézy value:

$$c_f = \sqrt{\frac{g}{C^2}} \tag{3.4}$$

3.2. MORPHODYNAMICS

In this chapter the morphodynamics as implemented in XBeach and XBeach-G are discussed. Due to the scope of the report and the limits of XBeach(-G) only non-cohesive material and corresponding physics are discussed.

3.2.1. SEDIMENT TRANSPORT PROCESSES

XBeach calculates the bed-load transport and suspended load transport with the advection-diffusion equation, see section 3.2.2. XBeach-G only calculates bed-load transport as gravel material does not act as a suspended sediment. This approach for the calculation of bed-load transport is discussed in section 3.2.3.

3.2.2. ADVECTION-DIFFUSION EQUATION

Many numerical models, including XBeach, use depth-averaged sediment transport equations. XBeach uses the advection-diffusion equation, which can be found by integrating a simplified concentration equation over the the water depth.

XBeach solves the equilibrium concentration for the bed and suspended load separately, but their formulations are very similar. The 2D-depth averaged advection-diffusion equation for XBeach is given as (Galappatti and Vreugdenhil, 1985):

$$\frac{\partial hC}{\partial t} + \frac{\partial hCu}{\partial x} + \frac{\partial hCv}{\partial y} + \frac{\partial}{\partial x}\left(D_h h \frac{\partial C}{\partial x}\right) + \frac{\partial}{\partial y}\left(D_h h \frac{\partial C}{\partial y}\right) = \frac{hC_{eq} - hC}{T_s} \tag{3.5}$$

In a 1D environment that equation is simplified to:

$$\frac{\partial hC}{\partial t} + \frac{\partial hCu}{\partial x} + \frac{\partial}{\partial x}\left(D_h h \frac{\partial C}{\partial x}\right) = \frac{hC_{eq} - hC}{T_s} \tag{3.6}$$

In Equation 3.6 h represents the water depth, C the depth averaged sediment concentration, u the flow velocity, D_h is the sediment diffusion coefficient, C_{eq} is the equilibrium sediment concentration and lastly T_s is the so-called adaptation time.

The adaptation time T_s can describe how quickly sediments react to a change of hydrodynamics, provided that there is a mismatch between the concentration C and equilibrium concentration C_{eq}. If T_s is small the sediment concentration responds quickly to the change of hydrodynamics. This is the opposite when T_s is large. This adaptation time can be calculated with:

$$T_s = \max\left(0.05\frac{h}{w_s}, T_{s,min}\right) \tag{3.7}$$

In Equation 3.7 w_s is the fall velocity as suggested by Ahrens (2000):

$$\begin{aligned} w_s &= \alpha_1\sqrt{\Delta g D_{50}} + \alpha_2\frac{\Delta g D_{50}^2}{\nu} \\ \alpha_1 &= 1.06\tanh\left(0.016A^{0.50}\exp\left(-120/A\right)\right) \\ \alpha_2 &= 0.055\tanh\left(12A^{-0.59}\exp\left(-0.0004A\right)\right) \end{aligned} \tag{3.8}$$

Here A is the Archimedes buoyancy index $A = \Delta g d^3/\nu^2$ which was introduced by Hallermeier (1981).

3.2.2.1 TRANSPORT FORMULATIONS

The last term of Equation 3.6 contains the concentration equilibrium variable C_{eq}, which can be calculated with the following formulations:

- Soulsby-Van Rijn (Soulsby, 1997), (Van Rijn, 1984).

- Van Thiel-Van Rijn (Van Thiel De Vries, 2009).

The latter is the default of XBeach and is preferred in models including overwash (De Vet, 2014). The formulations Soulsby-Van Rijn are similar but a bit different from the Van Thiel-Van Rijn formulations, as they also calculate a drag coefficient and the critical velocity did not include a differentiation between the contributions of currents and waves. The formulas of Van Rijn (2007a,b) are depth-averaged and wave-averaged in order to account for oscillatory motions. Below the Van Thiel-Van Rijn ((Van Rijn, 2007a,b),(Van Thiel De Vries, 2009)) formulas are discussed.

The equilibrium concentration C_{eq} from Equation 3.6 can be calculated for bed-load ($C_{eq,b}$) and suspended load ($C_{eq,s}$):

$$\begin{aligned} C_{eq,b} &= \frac{A_{sb}}{h}\left(\sqrt{v_{mg}^2 + 0.64u_{rms,2}^2} - U_{cr}\right)^{1.5} \\ C_{eq,s} &= \frac{A_{ss}}{h}\left(\sqrt{v_{mg}^2 + 0.64u_{rms,2}^2} - U_{cr}\right)^{2.4} \end{aligned} \tag{3.9}$$

In which the bed- and suspended load coefficients are:

$$\begin{aligned} A_{sb} &= 0.015h\frac{(D_{50}/h)^{1.2}}{\left(\Delta g D_{50}\right)^{0.75}} \\ A_{ss} &= 0.012D_{50}\frac{D^{-0.6}}{\left(\Delta g D_{50}\right)^{1.2}} \end{aligned} \tag{3.10}$$

Furthermore the critical velocity U_{cr} is described by (Van Rijn, 2007a) to be a weighted summation of critical velocities due to currents and waves:

$$\begin{aligned} U_{cr} &= \beta U_{crc} + (1-\beta)U_{crw} \\ \beta &= \frac{v_{mg}}{v_{mg} + u_{rms}} \end{aligned} \tag{3.11}$$

In Equation 3.11 U_{crc}, the critical velocity for currents, is based on Shields (1936):

$$U_{crc} = \begin{cases} 0.19D_{50}^{0.1}\log 10\left(\frac{4h}{D_{90}}\right) & \text{for } D_{50} \leq 0.0005m \\ 8.5D_{50}^{0.6}\log 10\left(\frac{4h}{D_{90}}\right) & \text{for } D_{50} \leq 0.002m \\ 1.3\sqrt{\Delta g D_{50}}\left(\frac{h}{D_{50}}\right)^{1/6} & \text{for } D_{50} > 0.0005m \end{cases} \tag{3.12}$$

Lastly the critical velocity due to waves is described by Komar and Miller (1975):

$$U_{crw}\begin{cases} 0.24\left(\Delta g\right)^{2/3}\left(D_{50}T_{rep}\right)^{1/3} & \text{for } D_{50} \leq 0.0005m \\ 0.95\left(\Delta g\right)^{0.57}\left(D_{50}\right)^{0.43}T_{rep}^{0.14} & \text{for } D_{50} > 0.0005m \end{cases} \tag{3.13}$$

In the non-hydrostatic mode $u_{rms} = 0$, which means $\beta = 1$. This means that the critical velocity is solely based on the critical velocity for currents U_{crc}.

3.2.3. BED-LOAD TRANSPORT IN XBEACH-G

Several formulations for the bed-load transport in XBeach-G have been investigated by McCall (2015). Formulations studied were Meyer-Peter and Muller (1948), Engelund and Fredsøe (1976), Nielsen (2002) and Wong and Parker (2006), but in the end Van Rijn (2007a) turned out to be the most accurate formulation for bed-load transport. For this reason only Van Rijn (2007a) is discussed in detail, while the other formulations are shortly addressed.

3.2.3.1 BED SHEAR STRESS

In order to calculate the bed-load transport, the bed shear stress τ_b has to be calculated. For XBeach-G McCall (2015) added a term to the bed shear stress and changed the computation of the drag coefficient. The bed shear stress is described to have two terms, namely a drag term and an inertia term:

$$\tau_b = \underbrace{\tau_{bd}}_{\text{Drag}} + \underbrace{\tau_{bi}}_{\text{Inertia}} \tag{3.14}$$

Here the bed shear stress due to drag is the same as for XBeach, namely:

$$\tau_{bd} = c_f \rho u |u| \tag{3.15}$$

Here the dimensionless friction factor c_f is defined differently for XBeach-G than for XBeach, namely with the description of Conley and Inman (1994) that accounts for the effects of infiltration and exfiltration (McCall, 2015). This dimensionless friction factor is defined as:

$$\begin{aligned} c_f &= c_{f,0}\left(\frac{\Phi}{e^{\Phi}-1}\right) \\ c_{f,0} &= \frac{g}{\left(18\log\left(\frac{12h}{k}\right)\right)^2} \end{aligned} \tag{3.16}$$

Within Equation 3.16, Φ is the so called non-dimensional ventilation parameter, k is the characteristic roughness height and h is the water depth.

The bed shear stress due to inertia is defined through an analogy of the force exerted by water on a sphere in un-stationary flow and is defined to be:

$$\tau_{bi} = \rho c_m c_v c_n D_{50} \frac{\partial u}{\partial t} \tag{3.17}$$

A restriction of Equation 3.17 is the fact that can only implement the D_{50} of one fraction. This creates issues when modelling with multiple fractions, when the inertia term for the bed friction is used. Furthermore McCall (2015) notes that Equation 3.17 ignores the advective acceleration term to the total inertia force on the particles in the bed and the equation does not explicitly account for relative velocity differences between the surface water flow and sediment motion.

3.2.3.2 SEDIMENT TRANSPORT

The equation for bed-load transport requires the Shields parameter:

$$\theta = \frac{\tau_b}{\rho g \Delta_i D_{50}} \tag{3.18}$$

In which:

$$\Delta_i = \Delta + \alpha \frac{S}{K} \tag{3.19}$$

The Shields parameter θ of Equation 3.18 is depended on the bed shear stress calculated from Equation 3.14 and a parameter Δ_i for the relative effective weight calculated in Equation 3.19. In the calculation for the relative effective weight the effect of vertical groundwater pressure gradients is accounted for.

In order to account for bed slope effects the Shields parameter is adapted to create the effective Shields parameter (Fredsøe and Deigaard, 1992):

$$\theta' = \theta \cos\beta \left(1 \pm \frac{\tan\beta}{\tan\phi}\right) \tag{3.20}$$

Here β is the local angle of the bed and ϕ is the angle of repose of the sediment.

With the bed shear stress and effective Shields parameter calculated the bed-load transport as proposed by Van Rijn (2007a) is calculated by:

$$q_b = \gamma D_{50} D_*^{-0.3} \sqrt{\frac{\tau_b}{\rho}} \frac{\theta' - \theta_{cr}}{\theta_{cr}} \frac{\tau_b}{|\tau_b|} \tag{3.21}$$

In this equation q_b is the volumetric bed-load transport, γ is a calibration factor set to be 0.5, D_* is the non-dimensional grain size and θ_{cr} is the critical Shields parameter. The non-dimensional grain size D_* is defined by $D_* = D_{50}\left(\frac{\Delta g}{\nu^2}\right)^{1/3}$. The critical Shields parameter is the value for which the sediment is put into motion (initiation of transport). McCall (2015) used the relation of Soulsby and Whitehouse (1997):

$$\theta_{cr} = \frac{0.30}{1 + 1.2 D_*} + 0.055\left(1 - e^{-0.020 D_*}\right) \tag{3.22}$$

3.2.3.3 OTHER TRANSPORT FORMULATIONS

In the formulation by Meyer-Peter and Muller (1948) (MPM) the equation for the bed-load transport is a bit different from Equation 3.21. MPM turned out to overestimate the morphodynamic response. Nielsen (2002) proposed an adoption of the MPM formulations. Here the friction velocity u_* computes the Shields parameter, in which this friction velocity is depended on expansion and contraction in swash, pressure gradients effects and the presence of turbulent fronts (McCall, 2015). An issue with Nielsen's model is the fact that the user has to calibrate the settings to the model, which is not preferable. In the case of Engelund and Fredsøe (1976) (EF) equation for bed-load transport also looks similar to Equation 3.21. This equation uses a probabilistic fraction that is based on empirical value θ. For EF the morphodynamic response was also overestimated. Lastly Wong and Parker (2006) also proposed an adaptation of MPM, but the results found by McCall (2015) turned to be less accurate than Van Rijn (2007a).

3.2.4. BED SLOPE EFFECTS

The slope of a bed has influence on the sediment transport: it influences local near-bed flow velocity, it could influence the rate and direction of the transport once the sediment is in motion and the slope might change the threshold conditions for the initiation of motion (Walstra et al., 2007).

These effects are taken into account by changing the magnitude of the sediment transport, which is default in XBeach. Further elaboration on different adaptations to the sediment transport equations due to bed slope effects are out of the scope of this report.

3.2.5. AVALANCHING

In order to account for the erosion of regions where the beach face is too steep avalanching has been implemented in XBeach and XBeach-G. This collapse of a sediment is dependent on the angle of repose of this sediment. When the bed slope is larger than the angle of repose avalanching down slope avalanching occurs.

3.2.6. BED COMPOSITION

XBeach has the ability to take into account multiple fractions. Multiple bed layers are defined in the model, each layer having its own distribution of the sediment fraction pb over the vertical and horizontal. Only the top layer is allowed to erode sediments and preserves its thickness. The second layer is a variable layer and interacts with the bottom layers and top layer, as the variable layer adapts to the erosion of the top layer. To the authors knowledge this accounting of fractions has not been used yet in any studies.

Armoring and sorting is simulated with the bed composition ability of XBeach. Coarse sediments may be deposited on top of fine sediment after which erosion of the coarse sediment is needed to expose the fine sediment again, effectively armoring the bed (Roelvink et al., 2015).

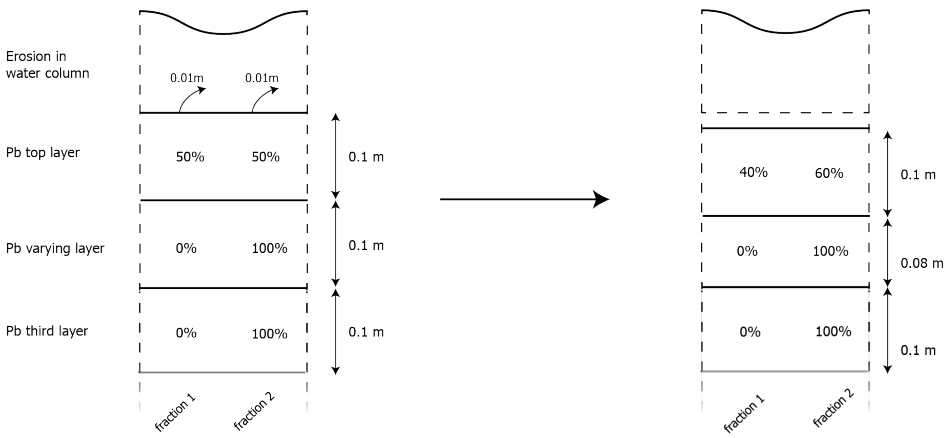

Figure 3.1: Representation of bed composition in XBeach - The left shows an initial situation with 2 fractions of equal proportion in the top layer. In the lower layers only the second fraction is present. In the water column both the fractions are eroded. In the right panel on can see how this changes the distribution in the top layer and how the second varying layer adapts its thickness.

3.2.7. BED LEVEL UPDATE

In XBeach and XBeach-G the equations for bed level update (or bed level change) differ slightly. In XBeach this is for a 1D situation described as:

$$\frac{\partial z_b}{\partial t} + \frac{f_{mor}}{(1-n_p)} \frac{\partial q_b}{\partial x} = 0 \tag{3.23}$$

Here f_{mor} is a morphological acceleration factor, n_p is the porosity and q_x is the sediment transport rate in the x-direction. In XBeach-G this f_{mor} is not applicable and Equation 3.23 reduces to the simple Exner equation:

$$\frac{\partial z_b}{\partial t} + \frac{1}{(1-n_p)} \frac{\partial q_b}{\partial x} = 0 \tag{3.24}$$

3.3. GROUNDWATER DYNAMICS

This section describes the non-hydrostatic groundwater model as implemented in XBeach and XBeach-G. The groundwater dynamics are only of relevance for parts of the beach where infiltration is significant. This means that the groundwater module is more relevant for gravel beaches than it is for sandy beaches.

The groundwater model is able to simulate groundwater flow in saturated permeable gravel beaches, infiltration of surface water into the unsaturated beach, exfiltration of groundwater from the saturated beach and exfiltration of groundwater at the groundwater exit point on the back barrier (McCall, 2015). Further details on the groundwater model are provided by McCall (2015).

3.3.1. GOVERNING EQUATIONS

Three equations (or set of equations) are used in the groundwater model. Firstly equation for mass continuity equation is described to be:

$$\nabla \vec{U} = 0 \tag{3.25}$$

In which:

$$\vec{U} = \begin{bmatrix} u \\ v \\ w \end{bmatrix} \tag{3.26}$$

The equations of motion differ for laminar and turbulent flow. For laminar flow the Darcy's law is applied (Darcy, 1856), in which K described the hydraulic conductivity of a medium and H is the hydraulic head:

$$\nabla H = -\frac{1}{K(Re)} \vec{U} \tag{3.27}$$

$$H = z + \frac{p}{\rho g} \tag{3.28}$$

The difference for laminar and turbulent flow calculated through the hydraulic conductivity K, which is:

$$K(Re) = \begin{cases} K_{lam} \sqrt{\frac{Re_{crit}}{Re}} & \text{for } Re > Re_{crit} \\ K_{lam} & \text{for } Re \leq Re_{crit} \end{cases} \tag{3.29}$$

The groundwater model is depth averaged, but H in Equation 3.28 is dependent on the depth. Therefore a quasi-3D modelling approach is applied in order to estimate groundwater head variation, see Figure 3.2.

After imposing several conditions and integrating over the depth the depth-averaged ground water head can be written as:

$$\bar{H} = H_{bc} - \frac{2}{3}\beta h_{gw}^2 \tag{3.30}$$

As was stated there is also a flow interaction at interface between surface water and/or ground water level. Three types of exchanges with the surface water can be distinguished:

- Infiltration S_{inf}, which occurs only where the groundwater *is not* connected to the surface water. This occurs at unsaturated locations at the beach.

$$S_i = K\left(\frac{1}{\rho g}\frac{p|_{z=\xi}}{wf} + 1\right) \tag{3.31}$$

- Exfiltration S_{exf}, which also occurs only where the groundwater *is not* connected to the surface water.

$$S_e = n_p \frac{\partial\left(\xi - \zeta_{gw}\right)}{\partial t} \tag{3.32}$$

- Submarine exchange S_{sub}

$$S_s = 2\beta h_{gw} K \tag{3.33}$$

These three exchange terms exchange information with the surface water or groundwater level. If the groundwater level *is not* connected to the surface water:

$$n_p \frac{\partial \zeta_{gw}}{\partial t} = w + S_i + S_e \tag{3.34}$$

The surface water level is updated to be:

$$\frac{\partial \zeta}{\partial t} = -S_i - S_e \tag{3.35}$$

When the groundwater level *is* connected to the surface water, only transport due to submarine exchange occurs:

$$n_p \frac{\partial \zeta_{gw}}{\partial t} = w + S_s = 0 \tag{3.36}$$

$$\frac{\partial \zeta}{\partial t} = -S_s \tag{3.37}$$

3.4. NUMERICAL IMPLEMENTATION

The non-hydrostatic mode of XBeach and XBeach-G have the same numerical schemes. The surface flow is solved using a predictor-corrector scheme by MacCormack (1969). The numerical model is elaborated by Smit et al. (2010) and can be studied for detailed information.

3.5. COMPARISON XBEACH AND XBEACH-G

Last sections many resemblances but also differences between XBeach and XBeach-G were mentioned. This section provides a clear representation of differences between XBeach and XBeach-G.

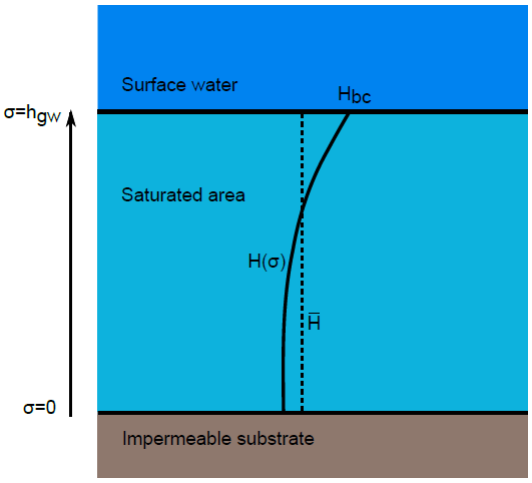

Figure 3.2: Schematic representation of quasi-3D groundwater head approximation (McCall, 2015)

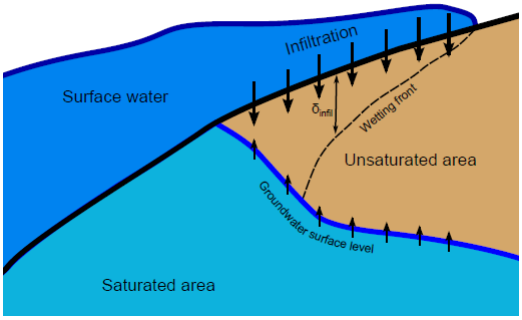

Figure 3.3: Example of infiltration (McCall, 2015)

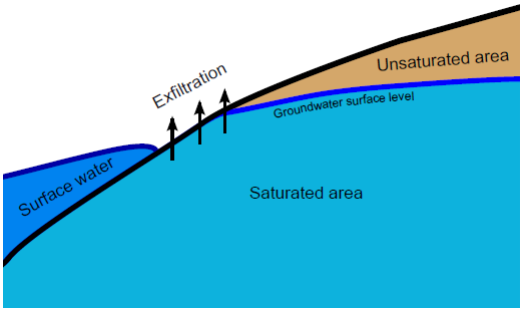

Figure 3.4: Example of exfiltration (McCall, 2015)

In Figure 3.5 one can see a simplified loop that is used by XBeach to calculate the morphological changes in the model. First the hydrodynamics are solved, providing a flow velocity u. Then the sediment transport for sand is calculated: q_s for suspended sediment and q_b for bed-load transport. With these sediment transports a bed level change Δz_b is calculated and the loop starts again for a new time step.

Figure 3.6 shows the same loop, but now for XBeach-G. First the hydrodynamics (u) are solved. Then the groundwater dynamics are calculated. The groundwater head $\bar{H}$ is calculated from using depth of a predefined aquifer and the groundwater velocities $u_{\parallel}$ are calculated from this groundwater head and a hydraulic conductivity K. The groundwater dynamics then feeds back information to the hydrodynamics. Then the bed-load transport for the gravel q_b are calculated, after which the bed is updated and the loop starts again.

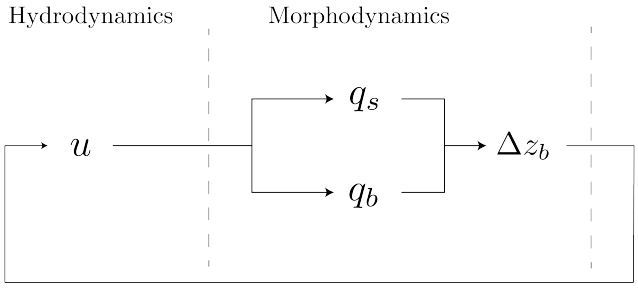

Figure 3.5: Model simplification of XBeach

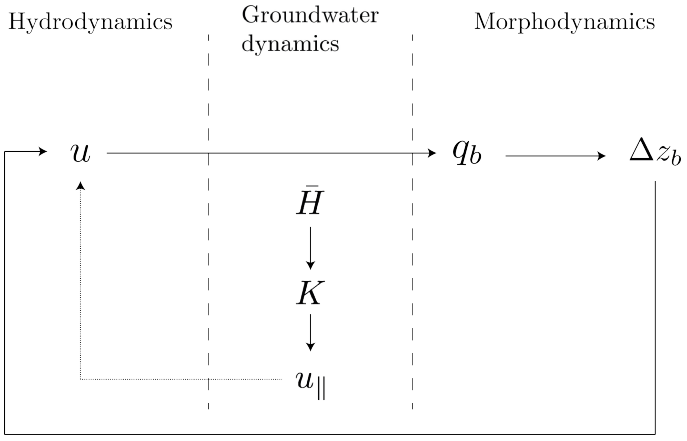

Figure 3.6: Model simplification of XBeach-G

4

DynaRev Experiments

What happened in the flume?

In this chapter the experiments that have been used for this report to evaluate the performance of the process-based models are discussed. The information about the experiments has been retrieved from the proposal for the experiment by Blenkinsopp (2016). Furthermore information is gained from a study visit at these experiments in Hannover and from correspondence with some of the conductors of the experiments.

Section 4.1 discusses the research scope of the experiments, setup of the experiments and overview of the tests and in section 4.2 the observations of these conducted test are described.

4.1. Experimental overview

The DynaRev experiments were established in order to gain fundamental knowledge about the performance of dynamic coastal protections to a rising sea level and erosive wave conditions. The DynaRev experiments are distinguished by two separate experiments. During the first experiment a planar sandy beach was subjected to erosive waves without the construction of a gravel revetment. In the second experiment the same planar beach was subjected to similar waves, but now with a gravel revetment on the beach. The results of these two experiments are used to compare the performance of a beach with a dynamic revetment in comparison with a regular sandy beach. A secondary aim of the experiments was to obtain information about sediment transports over the bar. Modelling these bars are out of the scope of this thesis, but the observations of the bar dynamics are still of interest as the bar might influence the hydrodynamics.

4.1.1. Experimental set-up

The experiments took place in Hannover at the Grosser Wellen Kanal (GWK, Large Wave Flume). A cross-section of the flume with a section of the first experiment is shown in Figure 4.1. To ensure the hydrodynamics and sediment transport remained unaffected by the bed of the flume the toe of the beach profile was constructed to have a width of 25 meters and a thickness of 0.5 meters. This can be seen in Figure 4.2. The initial water level was at 4.5 meters above the flume base.

The first experiment, which is referred to as *DynaRev - Sand*, consisted of a planar beach with an initial slope of $1:15$. The median diameter D_{50} of the sand was 0.3 mm, which was the standard sand available at the facility.

For the second experiment, which is referred to as *DynaRev - Gravel*, a gravel revetment was placed on top of a developed beach. After some initial tests with just a sandy beach, the gravel revetment was constructed on top of the beach profile that had formed, see Figure 4.2. The dynamic revetment had an initial mean slope of 1 : 6.5 and was constructed of gravel with a D_{50} of 50 mm.

Different instrumentations were used during the experiments. For the hydrodynamics 2D laser scanners were mounted above the flume to obtain high-resolution measurements of the surface water elevation and wall mounted current meters were present. The morphology was measured with with a profiler and for the exposed beach high resolution measurements were done with laser scanners. For this thesis the measurements from the profiler were available, but for future research the detailed laser measurements with data about the hydrodynamics and morphodynamics have become available. Lastly overwash events was manually noted each time a wave overtopped the crest of the revetment.

Wave set	Profiles	H_s (m)	T_p (s)	Water level (m)	Duration (s)
DR0	DR0_1 - DR0_14	0.8	6	4.5	72000
Gravel revetment was placed					
DR1	DR1_1 - DR1_9	0.8	6	4.6	25200
DR2	DR2_1 - DR2_7	0.8	6	4.7	25200
DR3	DR3_1 - DR3_7	0.8	6	4.8	25200
DR4	DR4_1 - DR4_11	0.8	6	4.9	61200
DRE1	DRE1_1 - DRE1_3	0.9	6	4.9	7200
DRE2	DRE2_1 - DRE2_4	1.0	7	4.9	7200
DRE3	DRE3_1 - DRE3_3	1.0	8	4.9	3600
DRR1	DRR1_1 - DRR1_2	0.8	6	4.9	7200
Extra gravel was added					
DRN1	DRN1_1 - DRN1_2	0.8	6	4.9	7200
DRN2	DRN2_1 - DRN2_2	1.0	8	4.9	2400
DRN3	DRN3_1 - DRN3_2	0.8	6	4.9	7200
DRN4	DRN4_1 - DRN4_2	1.0	9	4.9	2400
DRN5	DRN5	1.2	8	4.9	1200
DRN6	DRN6	0.8	6	4.9	3600

Table 4.1: *DynaRev - Gravel* wave sets - During each series multiple profiles have been measured in order to evaluate the dynamics of the profile

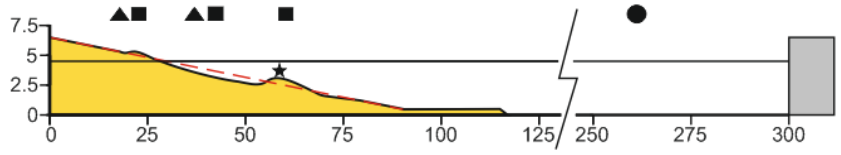

Figure 4.1: First experiments - Primary instrumentation to be operated during the experiments. (Blenkinsopp, 2016) - Triangle = camera, Square = Lidar, Star = bar dynamics rig, Circle = three-probe array.

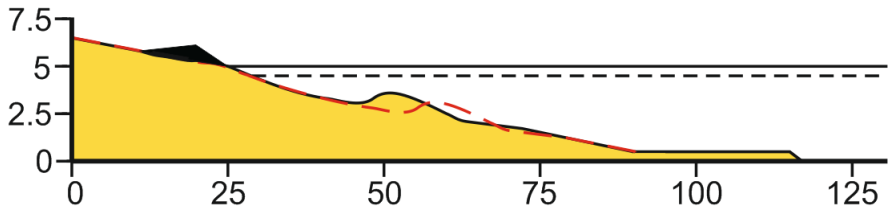

Figure 4.2: Second experiments - Cross section of experiment during resilience testing (Blenkinsopp, 2016) - Dotted line is original water level, black is the new water level after sea level rise. The red dotted line represent the initial bed level before sea level rise.

4.1.2. OVERVIEW OF TESTS

Table 4.1 give an overview of all the tests that have been performed at the GWK with the gravel revetment. The experiments with the sandy beach are shortly adressed, for more details see Appendix B.1. Each experiment several wave sets were imposed on the beach, which are discussed in the following sections.

4.1.2.1 DYNAREV - SAND

The imposed sets of waves on the sandy beach varied from intensity and had different wave heights. Furthermore each wave set the water level rose 0.1 m in order to study the effects of sea level rise. Additionally resilience tests were performed, see Appendix B.1 for more information.

4.1.2.2 DYNAREV - GRAVEL

The first set DR0 was intended to create a natural sandy beach with a bar. This started with a planar profile beach with a slope of 1 : 15. After DR0 the dynamic revetment was constructed on top of the final profile of DR0. The profile of DR0 had to be manually adapted in order to create the correct slope from the drawing board underneath the dynamic revetment, but also to ensure sufficient gravel material was used to make sure the revetment could function accordingly. The berm of the revetment had a width of about 3 meters. Landward of the revetment the sandy beach profile continued. After the profile with the revetment was constructed 4 sets of waves were imposed on the beach, namely set DR1 to DR4. For each set the water level was again increased with 0.1 m per set. Hereafter 3 sets of resilience testing (DRE1 - DRE3) were conducted by increasing the wave height and wave period. Lastly the front slope of the revetment was increased in volume by adding more gravel stones at a slope of 1 : 3.5. Then some tests were performed that allowed erosion followed by accretion, namely sets DRN1 to DRN6.

4.2. OBSERVATIONS FROM EXPERIMENTS

The measured profiles of the tests show how the beaches responded to the waves they were subjected to. In Figure 4.3 the beach profiler that was used to measure the bathymetry is shown. Once more both experiments are discussed separately.

4.2.1. OBSERVATIONS DYNAREV - SAND

Elaborated observations from DynaRev - Sand are discussed in Appendix B.1. During the tests is was found that the planar beach had developed into a beach with an offshore bar. Furthermore onshore erosion had occurred. With each water level rise the onshore erosion increased.

Figure 4.3: Bed profiler during GWK experiments

4.2.2. OBSERVATIONS DYNAREV - GRAVEL

As the profiler only measures elevation, it is not possible to make distinctions from the results between materials present. By looking at slope changes and at the initial toe location it is still possible to infer where the dynamic revetment is located within a certain range. For clarity the location of the initial location of the toe of the revetment has been shown in the figures. Figure 4.4a shows the profile development from sets DR1 to DR4. In Figure 4.4b the resilience testing and testing with additional gravel can be seen (set DRE1 to DRN6).

During the first tests the revetment seemed to retreat landward and the slope of this revetment steepened. Furthermore the bar system had grown in size. From observations after set DR4 it was seen that the transition from sand to gravel remained at the same location as the initial toe, see Figure B.5. In front of the toe gravel stones were found to be buried beneath the sand as one single layer of gravel stones. During DR3 15 overwash events were noted each 30 minutes and for DR4 150 overwash events were noted. For both wave sets the crest was located around 5.4 meters elevation.

Observations made during the experiment that the revetment seemed to sink are supported by Figure 4.4a. The front of the revetment has sunk a bit more after each wave set. Some gravel stones were observed to be offshore of the initial toe of the revetment, but not enough to explain the observed volume loss. It is therefore unlikely that the sinkage is caused by the erosion of the gravel stones. A possible explanation could be that the sand below the revetment was able to erode due to groundwater flow within the revetment. This would also explain the significant growth of the sand bar offshore, as sand below the revetment is mobilised and can be transported offshore. The latter can be motivated by checking the volume balance of the profiles. Table B.2 shows the volume changes of the profiles during 4 waves sets. In order to differentiate between several areas of the cross section, the profile has been split up into several sections. These sections correspond to the section transitions shown in Figure 4.5.

Figure 4.6 shows the relative volume changes of these sections during all of the experiments with gravel. The first dotted vertical line corresponds to the start of DR1 (see sudden volume increase at revetment caused by placement of gravel), the second to DR2, third to DR3, fourth to DR4 and the blue dotted line to the extra placement of gravel during resilience testing. Measuring errors are marked with red circles. Some general observations can be made from these graphs. During the first 20 hours of testing the beach (without gravel revetment) eroded quickly. The sand bar grows in volume and this volume can mostly be contributed to erosion of sand from the area between the sand bar and revetment. Little erosion occurs at the revetment. Things change when gravel is placed at the revetment location and when the water level is elevated each wave set. The volume change of sand between the sandbar and revetment seems to reach a stable state. The sandbar on the other hand keeps on growing in volume. The source of the volume gain is most probably due to volume loss at the revetment. As can be seen the rate of volume change at the revetment gets larger with the increase of the water level (the increases of the water level occur between $t = 20$ hrs and $t = 40$ hrs). During the resilience testing the volume loss at the revetment continues and one could argue whether this volume change seems to seems stabilise towards the end of the experiment. The latter can not be confirmed as the experiments had to be ended.

The volume losses between the sand bar and revetment were to be expected, as the planar beach had yet to form a natural stable sandy beach. With the introduction of the gravel revetment and the slowly rising water level the beach tries to find a new stable profile. Every water level increase is an impulse that triggers volume losses at the beach. One could also argue whether wave height and or wave period differences could also trigger these volume losses; larger waves and longer wave periods lead to larger run-ups and could potentially mobilise sediments.

As can be seen in Table B.2 the total cross section gains and loses volume depending on the wave set. This is most probably due to 2D effects in the flume or measurements errors. When taking this volume into account as an inaccuracy and comparing this inaccuracy with the other sections width and volume loss, one can compare the inaccuracy over a certain section width with the measured volume change. Table B.3 shows the score of these volume losses compared with the inaccuracies.

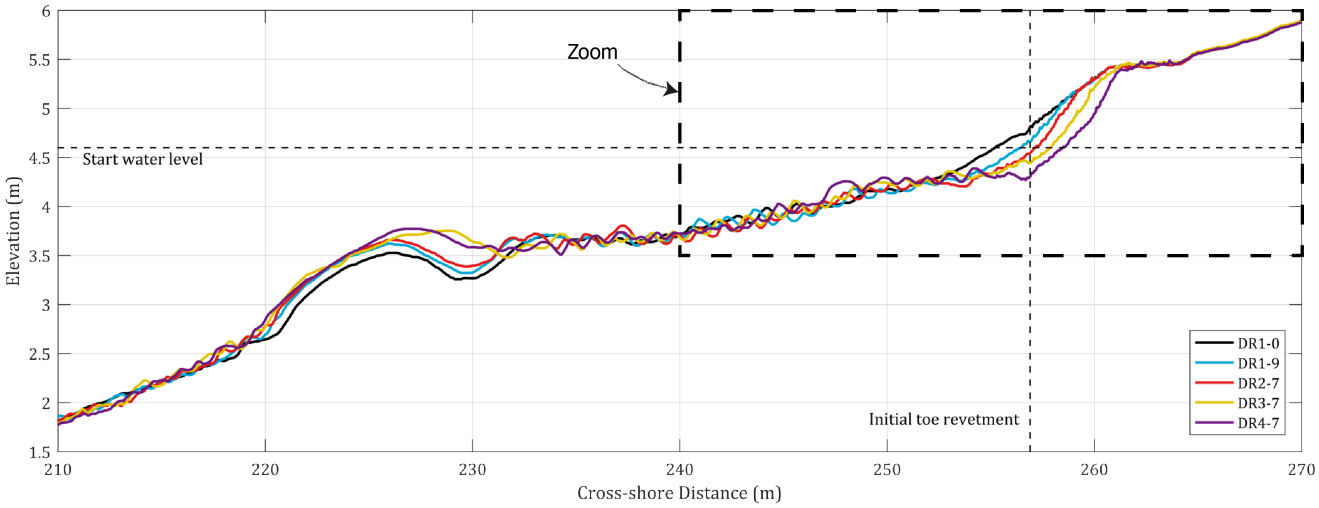

(a) Observed changes between DR1 and DR4

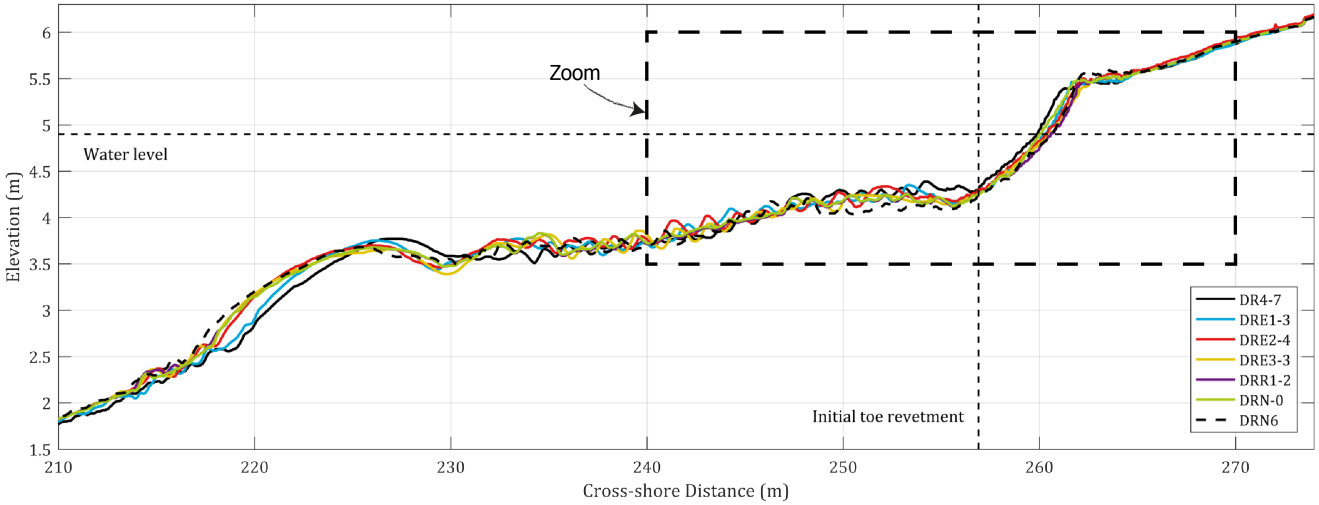

(b) Observed changes between DR4 and DRN

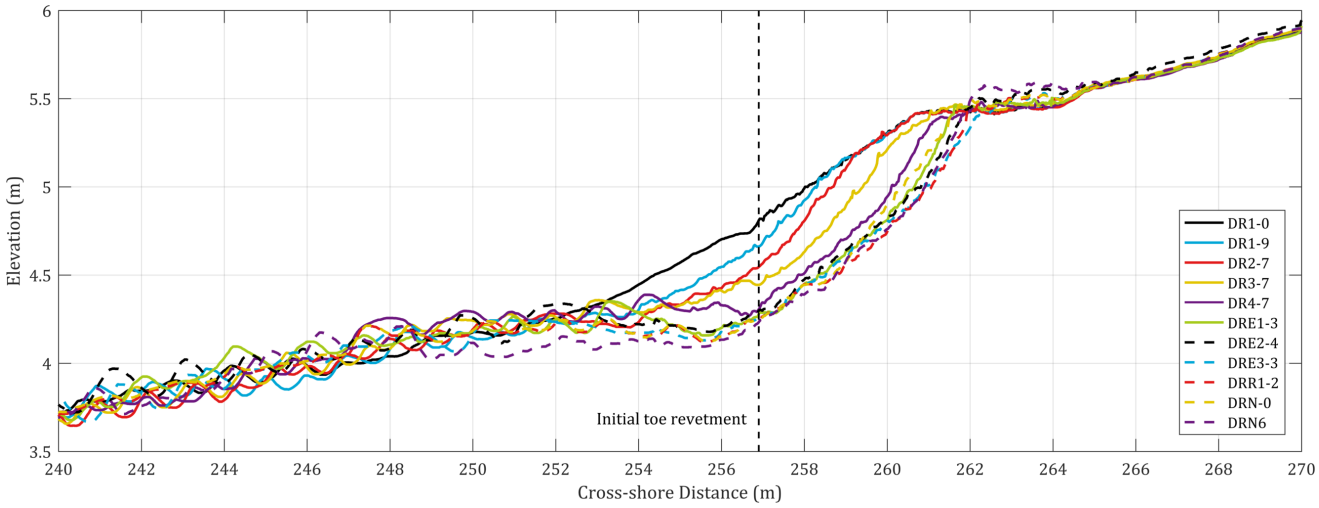

(c) Zoom of observed changes between DR1 and DRN

Figure 4.4: Observations from DynaRev - Gravel

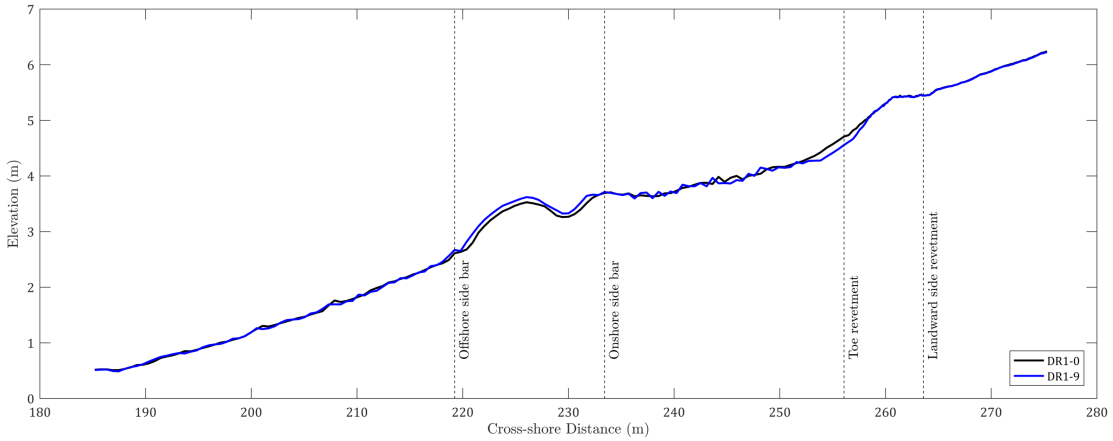

Figure 4.5: Section differences of profile

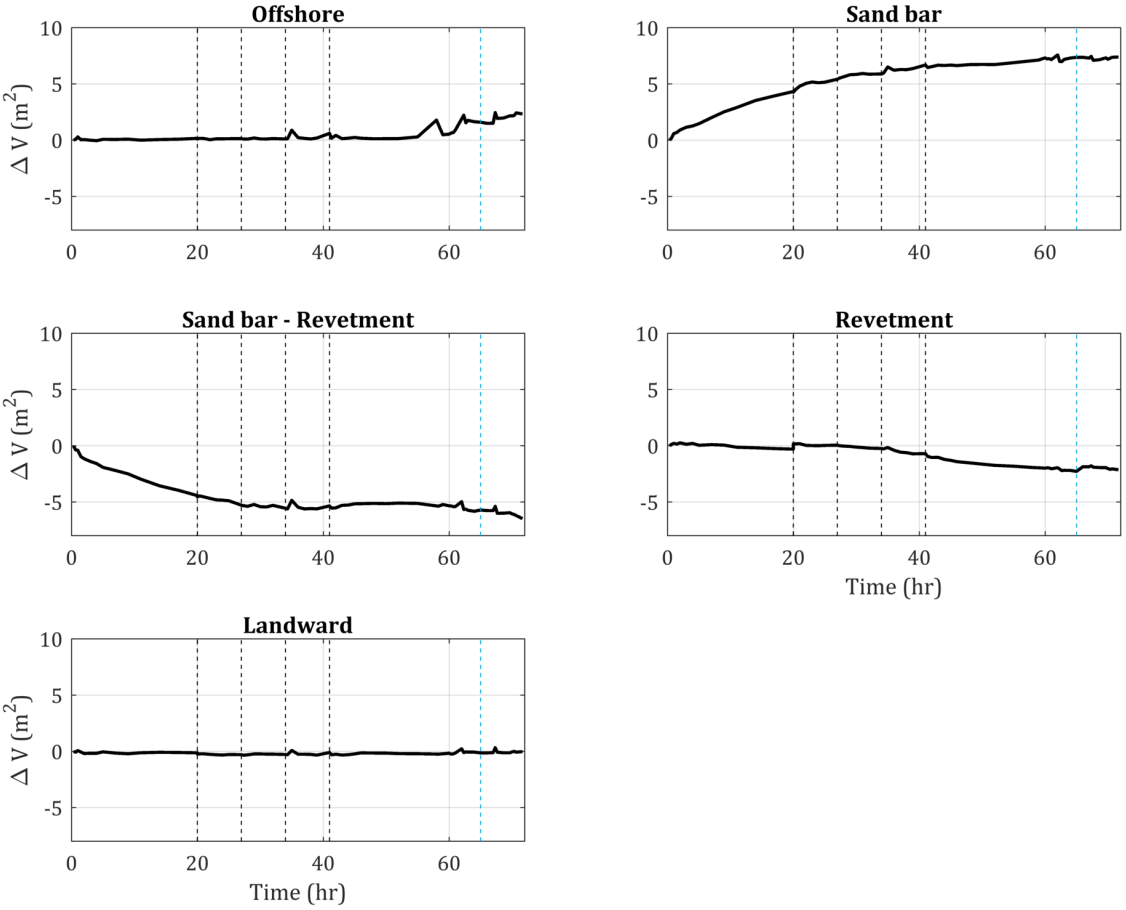

Figure 4.6: Volume development - First black dotted line = start DR1, second black dotted line = start DR2, third black dotted line = start DR3, fourth black dotted line DR4, blue dotted line = extra placement of gravel.

4.2.2.1 ANALYSIS OF THE REVETMENT

The shape of the body of the man-made revetment is of interest regarding the modelling with groundwater flow. To gain insight into the development of the revetment a short analysis has been conducted. The shape of this revetment has changed during the testing which can be clarified from the erosion of sand below the revetment, as was discussed in section 4.2.2.

There is no clear data about the shape of the revetment after its construction, but some data have been

retrieved from correspondence with the executors of the experiment. As was mentioned in section 4.1.2 the sand bed was adapted in order to facilitate space for the revetment. The slope of the sand bed was constructed to be 1 : 15. At the back of the revetment a sand step was constructed. In order to stabilise the stones at the front of the revetment the revetment was deepened to 15 cm. In Appendix B Figure B.6 pictures of the adapted sand bed is shown. The amount of gravel placed on this bed was 9.37 m^3 and with a flume width of 5 metres this implies that the surface area of a cross section of the revetment would be 1.87 $m^3 m^{-1}$. With the revetment surface was area was put in the model setup with a slope of 1 : 15 and local start depth of 15 cm, the revetment was found to have a large cross section of 2.27 $m^3 m^{-1}$. In order to match the cross section volume of the model setup to the surface area volume as it was constructed, the slope of the model setup was corrected to 1 : 11.75. This gave a model surface area of the revetment of 1.86 $m^3 m^{-1}$. This sand bed is shown in blue in Figure 4.7.

In order to gain insight into what happened to the sand slope below the revetment in between the start and end of testing some stones were removed after series DR4-7. The stones were removed just behind and in front of the crest and the depth from the top of the revetment till the bottom of the revetment were measured. Figure 4.7 shows where the sand bed was measured to be below the measured elevation of DR4-7, where the elevation is shown as data points.

In between the DRR and DRN sets extra gravel stones were added to the front face of the revetment. About 2.5 m^3 of gravel was added, which corresponds to about 0.5 m^2 for a cross section. At the end of the last set of waves the revetment was removed from the sand bed and the bed was measured, see Figure B.7 for a picture. The profiles are shown in Figure 4.7 and show what the revetment looked like at the end of testing. From the figure it can be seen that the toe of revetment has shifted landward and that the crest has built up to about 5.6 meters. The sand bed itself has a S-curve and was steepest below the crest. The largest part of the sand bed had a slope of about 1 : 7.2 meters. The surface area of the revetment at the end of testing was 1.6338 $m^3 m^{-1}$.

If it is assumed that indeed 1.87 $m^3 m^{-1}$ of gravel was present at the start of the testing and if indeed 1.6338 $m^3 m^{-1}$ of gravel was found at the end of testing, a volume $(1.87 - 1.633) + 0.5 = 0.737 m^3 m^{-1}$ still needs to be accounted for. Figure B.7 shows how the revetment was removed in order to take the measurements of the bottom. As can be seen a single layer of gravel has not been excavated. The thickness of this layer was about 0.08 meters, which (together with the length of the influenced revetment, reaching from 256.9 m to 265 m) leads to an extra revetment volume of $8.1 m \cdot 0.08 m = 0.65 m^3 m^{-1}$. This leaves $0.74 - 0.64 = 0.1 m^3 m^{-1}$ of mass loss of gravel at the revetment, which is assumed to be buried in front of the revetment.

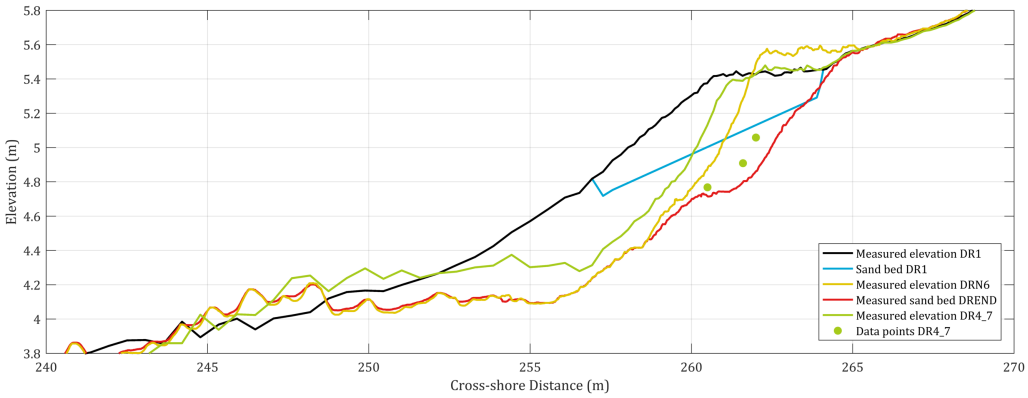

Figure 4.7: Cross section of the revetment

4.3. Conclusions

As has been described many things occurred during the DynaReve experiments. Two things can be considered to be of most significance from the DynaRev-Gravel experiment. This is sketched in Figures 4.8 and 4.9, showing the initial profiles (black) of DR1 and DR4 and their final profiles (red).

The first significant observation was the offshore transport of sand in combination with gravel steeping. This is especially significant for DR1, which is the case where the revetment was first exposed to waves. The second observation was the significant erosion of sand from underneath the revetment, which is especially significant for DR4. Here the water level is in contact with the revetment, which has been observed to be a trigger for erosion of sand inside the revetment.

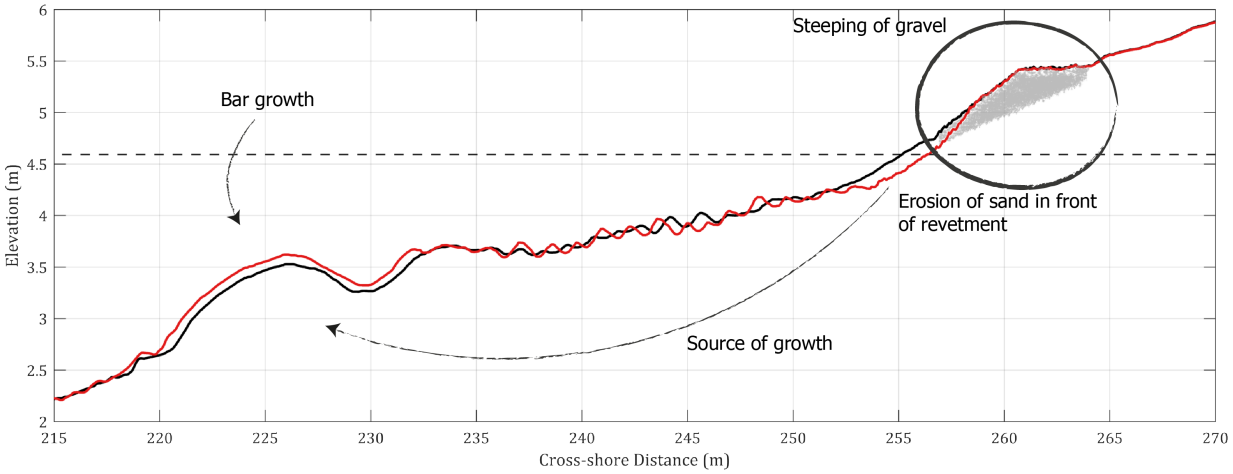

Figure 4.8: Developments at DR1

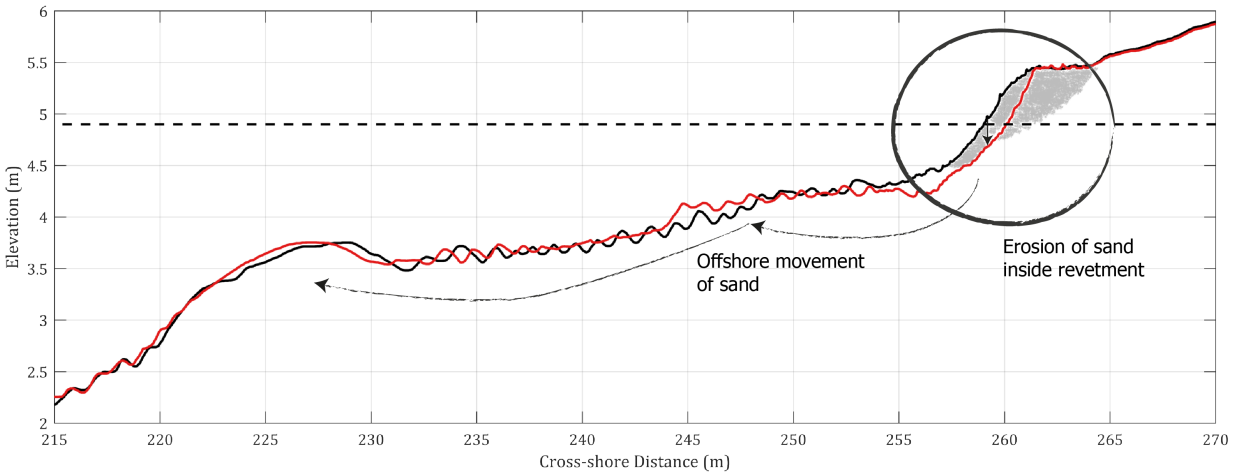

Figure 4.9: Developments at DR4

5

MODELLING PERFORMANCES

How do the current models perform?

This chapter discusses the current performances of process based models regarding the modelling of the artificial composite beach of DynaRev.

First the modelling approach is discussed in section 5.1. This is followed by the model setup in section 5.2. The XBeach performances are discussed in section 5.3 and the XBeach-G performances are discussed in section 5.4. Some conclusions are provided in section 5.5.

5.1. APPROACH

The performances of XBeach and XBeach-G are assessed separately in this chapter. In order to assess these performances the models have been run with different settings besides the main settings which are discussed in section 5.2.

The profile development from two wave sets of the DynaRev experiment are assessed for the two models. The first wave set is DR1, where the profile development from DR1_0 to DR1_9 is attempted to be modelled. Significant erosion was found in front of the revetment during this wave test. The effects of this erosion on the revetment are of interest for this thesis. The second wave set that is used for the performance of the model case is DR4. The profile development from DR3_7 (start profile of wave set DR4) to DR4_10 (last profile measurement without errors) is of interest as it was found that significant volume loss was found at the revetment.

Distinctions are made where sediment is able to erode and where it is not. This makes sense as XBeach and XBeach-G can respectively only model sand or gravel. This means that when one wants to model the sandy part of the beach it also models the revetment to be made of sand. This sandy revetment will then erode in the model which gives faulty results. This could also be the other way around if one wants model to solely with gravel. Therefore locations are specified where erosion is not possible. These location are specified and explained in the performance sections of XBeach and XBeach-G.

5.2. MODEL SETUP

In order to asses the performances of the models, first the model is set up. Data about hydrodynamics and specific characteristics of the gravel that could be used for setting up the model were scarce for thesis. Because of a lack of data several assumptions are made and sensitivities of the model are identified. Some remarks are made about the boundary conditions and some aspects of modelling with

groundwater flow are mentioned.

The XBeach models were run with a median particle size of D_{50} of 0.3 mm and the XBeach-G models were run with a median particle size of D_{50} of 50 mm. The domain had varying grid sizes, which were calculated with a non-hydrostatic modelling purpose. The grid size has a maximum of 1 m and a minimum of 0.1 m, which resulted in small grid sizes close to and at the beach/revetment. An example of of the model setup is shown in Figure 5.1 and an example of a model input can be found in Appendix C.2.

The only concrete data that could be used to validate the hydrodynamics that were present for this thesis were the amount of overwash events during wave sets DR3-7 and DR4-7 and the surface water elevations at several locations.

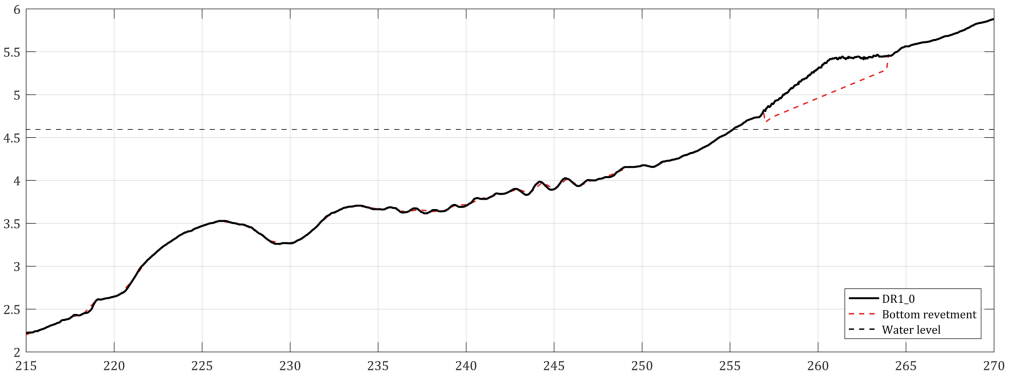

Figure 5.1: Model setup

5.2.1. BOUNDARY CONDITIONS

The size of the domain of the model is similar to the domain that was measured with the profiler for the DynaRev tests. Increasing the domain of the model to match the length of the flume has been considered, but discarded due to a significant increase in computational costs. The first grid cell is located at 185.2 m and the last at 275.3 m. The boundary conditions of the models that are used to asses the performance of XBeach and XBeach-G are determined from the conditions present during the wave sets and are retrieved from table 4.1. These conditions are imitated by the wave paddle, which is located at 0 m, 185 meters away from the model boundary. The boundary conditions setup is shown in table 5.1. Appendix C.1.1 discusses comparison between the model input for the hydrodynamics and measured surface water elevation. The data indicates that the current setup underestimates the wave height, but this might be caused by energy reflected on the beach. In order to see how much the imposed wave height influences the performance study and to take into account the possible underestimation of the wave height, the response of the beach to two other wave heights are assessed. These wave height are 0.7 m and 0.9 m.

Variable	Value
H_{m0}	0.7, 0.8, 0.9 m
f_p	0.1667 s^{-1}
mainang	270 °
γ_{jps}	3.3 (-)
s	1200 (-)
f_{nyq}	2 Hz

Table 5.1: Jonswap setup for DR1_0

5.2.2. GROUNDWATER FLOW

The groundwater flow in XBeach and XBeach-G relies on the hydraulic conductivity of the medium present. The hydraulic conductivity also relies on the critical Reynolds number, which dictates when flow within the medium becomes turbulent as is discussed in section 3.3.1. A short analysis on the hydraulic conductivity in the model has been conducted in order to compare it with the amount of counted overwash events during the experiments, see Appendix C.1.2.

From this analysis it was found the model hydrodynamics were relatively sensitive to the hydraulic conductivity. Furthermore it was found that the size of the revetment did influence the amount of overwash events, but not as considerable as the influence of the hydraulic conductivity K.

The exact hydraulic conductivity of the gravel present is unknown and from literature a range of values for different types of fractions are found. As this hydraulic conductivity has been found to be sensitive to the hydrodynamics of the model, the model runs for the performance study considers multiple hydraulic conductivities. The model runs with groundwater flow (and therefore K) consider three values for K, namely 0.2, 0.3 and 0.4 ms^{-1}.

5.3. XBEACH PERFORMANCES

This section discusses the performances of XBeach regarding the modelling of the composite beaches. An overview of the XBeach performance test is shown in Table 5.2.

As the non-hydrostatic mode of XBeach has not been fully validated yet for sand transport, it is of interest if to see how XBeach performs for the sandy reference case of DynaRev. This has also been done in test S0 and the results are discussed in Appendix C.3.

Tests S1 to S4 are performance test of profile development during DR1. Test S5 to S7 are the performance test that have been done for wave set DR4. To make distinctions between the sandy beach and gravel revetment non-erodible structures have been specified. For tests S1 and S5 the non-erodible structure is located at the revetment such that only the sandy beach can erode. For S2 and S6 only the revetment area could be eroded. The revetment area is defined to be from 256.9 m to 264 m. In tests S3 and S7 the entire cross section could be eroded, meaning no non-erodible structures were defined.

For the performance tests of XBeach multiple wave heights have been modelled in order to see the sensibility of the morphodynamic results to these imposed wave heights. In the performance results these differences have been visualised by showing the range of results of the model. For these model a wave height of 0.8 m is modelled and the range of results follows from model runs with a wave height of 0.7 and 0.9 m, see Table 5.1.

Test	Model	Reference wave set	Transport formulation	Sediment available for pick-up at	D_{50} (mm)
S0	XBeach	SB0	Van Thiel-Van Rijn	Entire cross section	0.3
S1	XBeach	DR1	Van Thiel-Van Rijn	Beach	0.3
S2	XBeach	DR1	Van Thiel-Van Rijn	Revetment	50
S3	XBeach	DR1	Van Thiel-Van Rijn	Entire cross section	0.3
S5	XBeach	DR4	Van Thiel-Van Rijn	Beach	0.3
S6	XBeach	DR4	Van Thiel-Van Rijn	Revetment	50
S7	XBeach	DR4	Van Thiel-Van Rijn	Entire cross section	0.3

Table 5.2: XBeach performance tests

5.3.1. MODEL PERFORMANCES OF DR1 - S1 – S4

Figures 5.2a, 5.2b and 5.2c show the performance of XBeach on composite beaches.

Test S1 in figure 5.2a shows a beach where erosion at the revetment is not allowed in the model. Erosion occurs mainly in front of the revetment. Sediments are deposited only a few meters offshore and the offshore bar has decreased in size. Overall the entire profile of the beach, which initially had some ripples, has been smoothed. Near the toe of the revetment the erosion the results from the model come close to the measured elevation change. The range of results with respect to the different wave heights is not significant.

In test S2 erosion at the revetment was only possible. The grain size in the model was increased to the grain size of the gravel. As can be seen in figure 5.2b the revetment is eroded and deposited about 10 meters down slope. The erosion at the revetment from the model is much larger compared with the measured erosion. The range of results with respect to the different wave heights is again not significant.

Lastly from test S3, where full erosion of the beach was possible, it can be seen that the profile retreats landward and that the slope of the profile steepens. Furthermore for this model the profile has also been smoothed just as for test S1. Also for these test the range of results due to different wave heights is not significant.

The XBeach model make quite some errors regarding modelling of the composite beach. First of all the offshore bar is eroded instead of accreted. This is a well known issue of XBeach and research on this subject is out of the scope of this report. Regarding the erosion at and near the revetment it can be seen that the revetment erodes quite significantly in the models. The XBeach models that were run only used one sand fraction and therefore the gravel is modelled as if it was sand. The sand fraction combined with the absence of groundwater flow can explain the significant erosion near the revetment: the erosion is of larger volume and reaches more landward. For the second test S2 the erosion at the revetment is too large for the grain size that is present. This is the exact reason why McCall (2015) introduced gravel transport formulations to XBeach, making XBeach-G. Finally from the results of the tests it is apparent that sand transport from around 245 to 255 to the offshore is missing. This can possibly be contributed to a mismatch between the hydrodynamics of the undertow of the model and the transport equations.

5.3.2. MODEL PERFORMANCES OF DR4 - S5 – S7

The modelling of the performances of XBeach for the wave set DR4 perform the same for as DR1. The results are not discussed in detail, as they resemble the performance of XBeach on DR1. A short description is provided in this section. The performances of test S5, S6 and S7 can found found in Appendix C, respectively figure C.9a, figure C.9b and figure C.9c.

The test with only beach erosion (S5) the sand bar has been eroded. In front of the toe of the revetment some erosion of sand seems to be missing, but is a limited amount. Test S6 with revetment erosion shows severe erosion of the revetment, which was expected for a XBeach transport formulation for gravel without groundwater flow. Total erosion of the beach was possible for S7, from which the results show large erosion of the beach and revetment. This was also to be expected as this test model the revetment as sand, which causes larger runup and larger erosion rates.

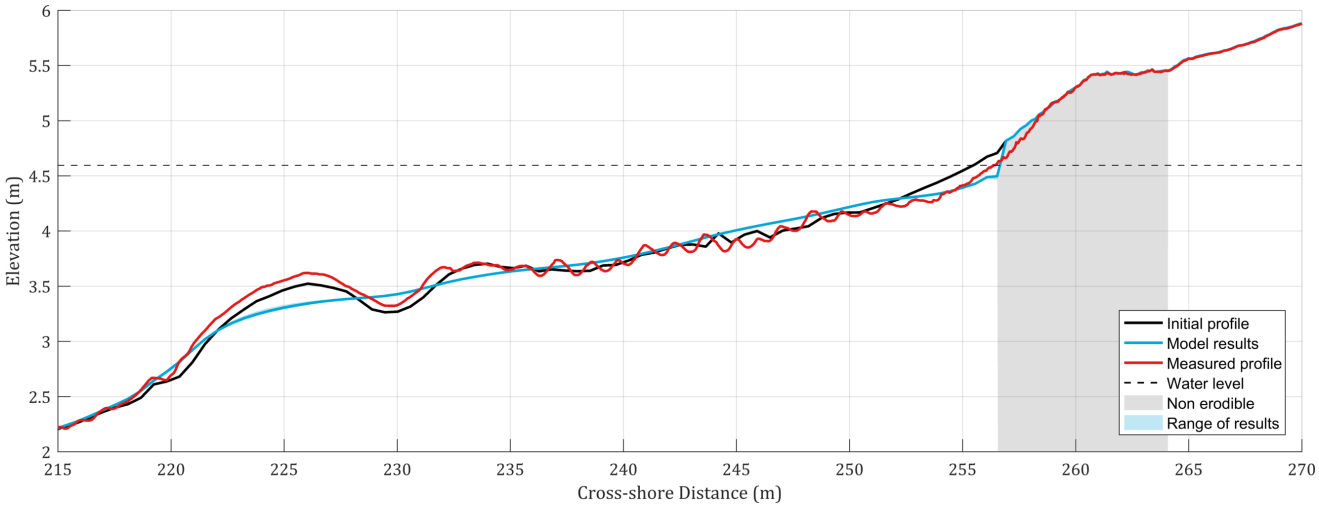

(a) Test S1 - Only beach erosion was possible.

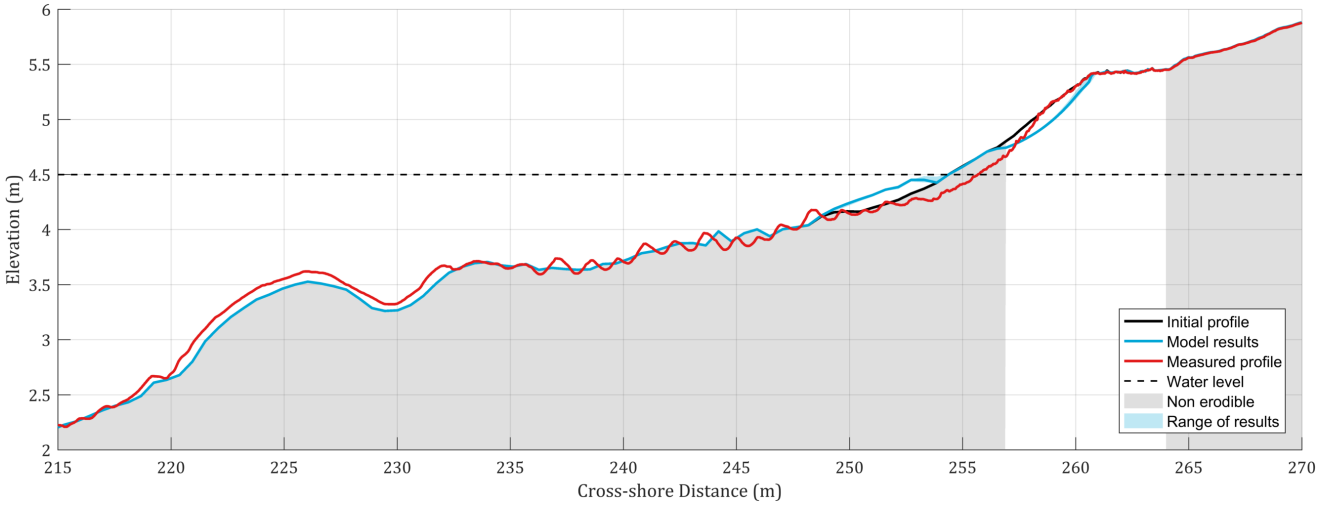

(b) Test S2 - Only revetment erosion

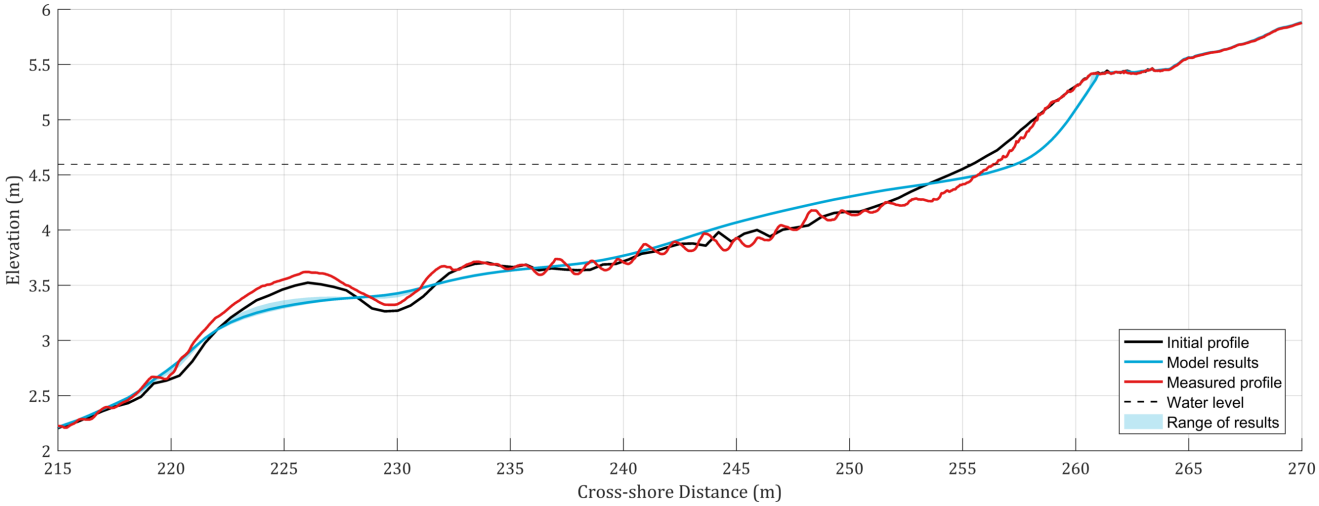

(c) Test S3 - Erosion over entire cross section

Figure 5.2: XBeach performances

5.4. XBEACH-G PERFORMANCES

The XBeach-G performances tests have also been split up into model runs for DR1 and for DR4. Two different transport formulations were run, namely Nielsen and Van Rijn, with a median particle size of D_{50} of 50 mm. The XBeach-G model runs included groundwater flow. For the XBeach-G performance results a range of results is presented that are obtained by running the same model with different hydraulic conductivities K.

An overview of the performance tests is given in Table 5.3. Tests G1, G2, G4 and G5 give insight into the performance of two different transport formulation of XBeach-G, where erosion was only possible at the revetment. Tests G3 and G6 on the other hand show how XBeach-G perform if the entire beach is able to erode.

Test	Model	Reference wave set	Transport formulation	Sediment available for pick-up at	D_{50} (mm)
G1	XBeach-G	DR1	Nielsen - $\varphi = 25°$	Revetment	50
G2	XBeach-G	DR1	Van Rijn	Revetment	50
G3	XBeach-G	DR1	Van Rijn	Entire cross section	50
G4	XBeach-G	DR4	Nielsen - $\varphi = 25°$	Revetment	50
G5	XBeach-G	DR4	Van Rijn	Revetment	50
G6	XBeach-G	DR4	Van Rijn	Entire cross section	50

Table 5.3: XBeach-G performance tests

5.4.1. MODEL PERFORMANCES OF DR1 - G1 – G3

Figure 5.3a (test G1) and figures 5.3b (test G2) show zoomed views of the cross-section near the revetment. The results of the formulation of Nielsen are very similar to the results with the Van Rijn formulation. Both show a slight increase of the slope near the bottom of the revetment and the profile slightly wiggles. The influence of different hydraulic conductivities is not evident as the range of results can barely be observed.

The test with full erosion of the beach G3 in figure 5.3c shows severe accretion of gravel stones. The offshore bar has fully eroded and the shore-face has advanced seaward. Even though this is obviously not a model run that could come close to the measured profile results, this result is of interest because it shows what the model does with offshore gravel, namely bringing the material onshore.

The XBeach-G model seems to enhance accretion of gravel material and is steepening the beach slope. Something that the model does not take into account is the development of the bottom of the revetment. The sand bottom below the revetment is fixed in time and space, while it still influences the groundwater flow. This does not mean that the revetment depths do not change. For locations where gravel is eroded and the revetment depth has thus decreased the soil saturates quicker for groundwater flow. The other way around for locations where gravel has accreted the revetment depth has thus increased. Though this might be of influence for the hydrodynamics, it might not be as important for the morphodynamics. From the tests it could be seen that different the range of results for different K's was very little. This could possible be the same for different revetment depths.

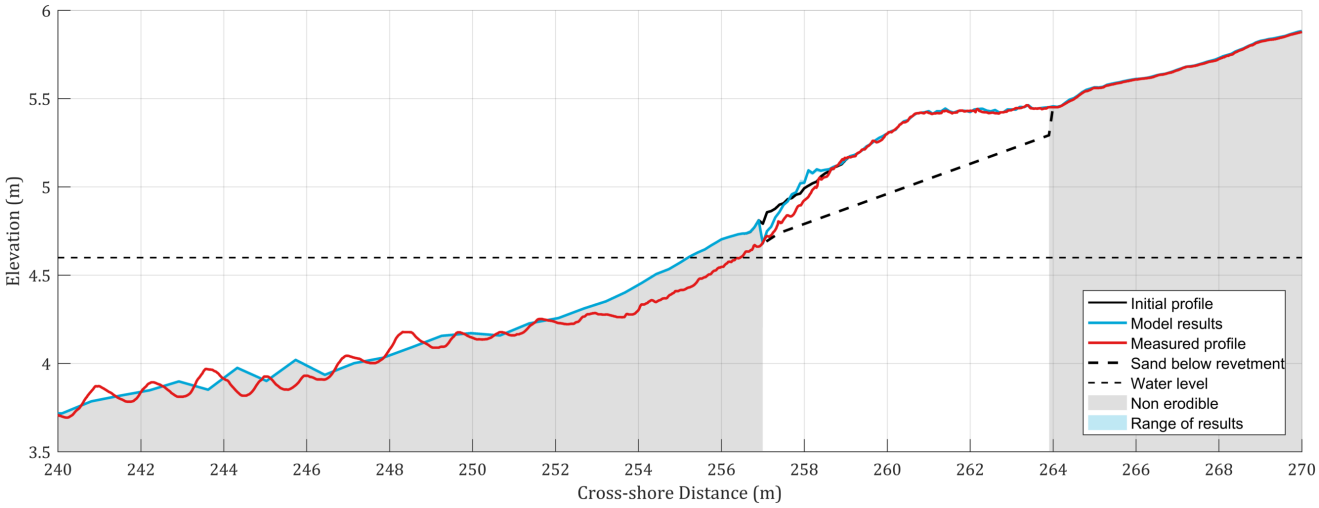

(a) Test G1 - Nielsen ($\varphi = 25°$) - Only revetment erosion

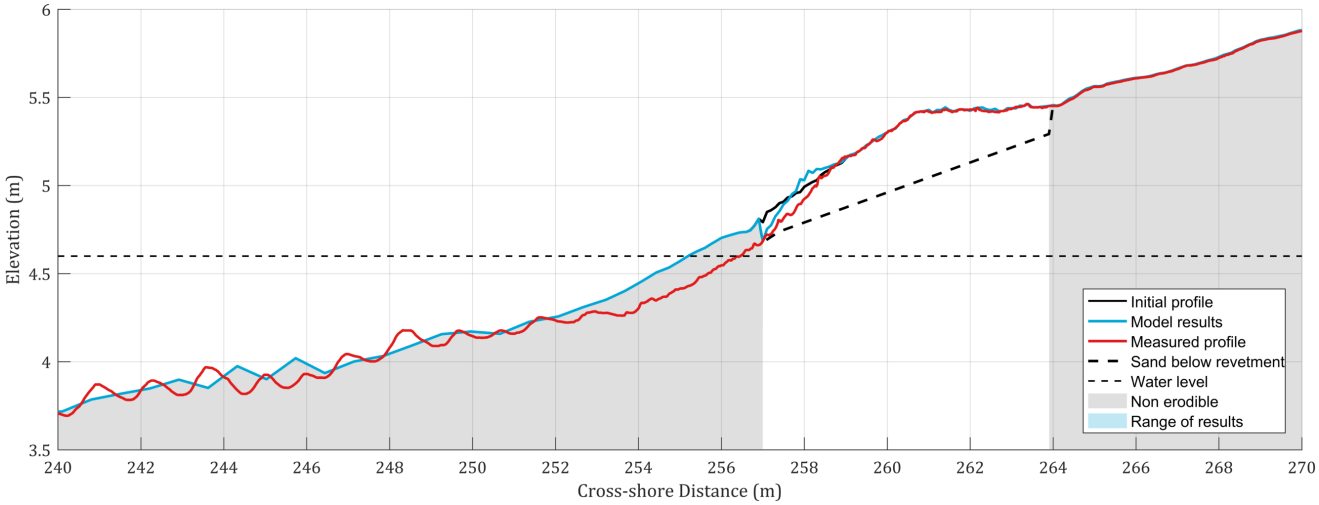

(b) Test G2 - Van Rijn - Only revetment erosion

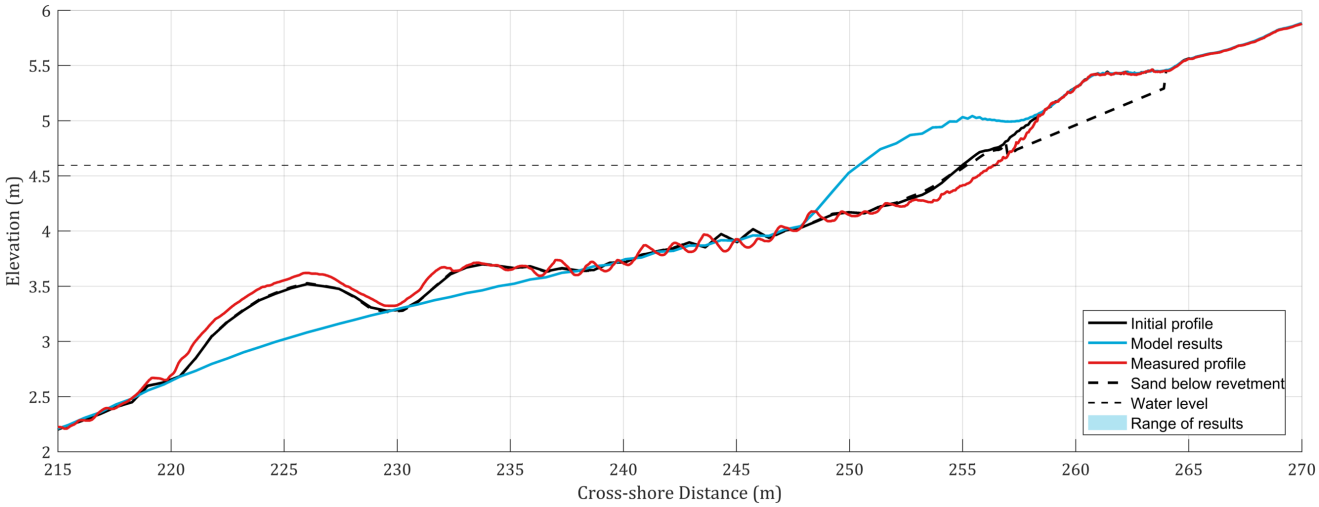

(c) Test G3 - Van Rijn - Erosion over entire cross section

Figure 5.3: XBeach-G performances on DR1

5.4.2. MODEL PERFORMANCES OF DR4 - G4 – G6

The performance of XBeach-G on wave set DR4 is shown the cases G4 and G5 with revetment erosion in figure 5.4a and 5.4b. The bottom of the revetment that has been used for these models is the same for the groundwater flow analysis in section 5.2.2. Here it was concluded that for the hydrodynamics the revetment depth was of less importance than the hydraulic conductivity.

From both performance tests G4 and G5 one can see how XBeach-G model the gravel to build up a crest. This was something that was also expected to occur during the DynaRev experiment, but was not observed during DR4. During other wave sets this building of a crest was observed, see figure 4.4b. A possible explanation for the fact that the model does show the crest building is that erosion of sand below from the revetment is missing. Test G6 is not discussed as it has similar results as test G3, see figure C.10.

The influence of the hydraulic conductivity K is not significant, but this does not mean that groundwater flow is negligible. Without groundwater flow the morphodynamic changes would be more significant, as infiltration in the swash helps to reduce erosion of the upper beach (McCall, 2015).

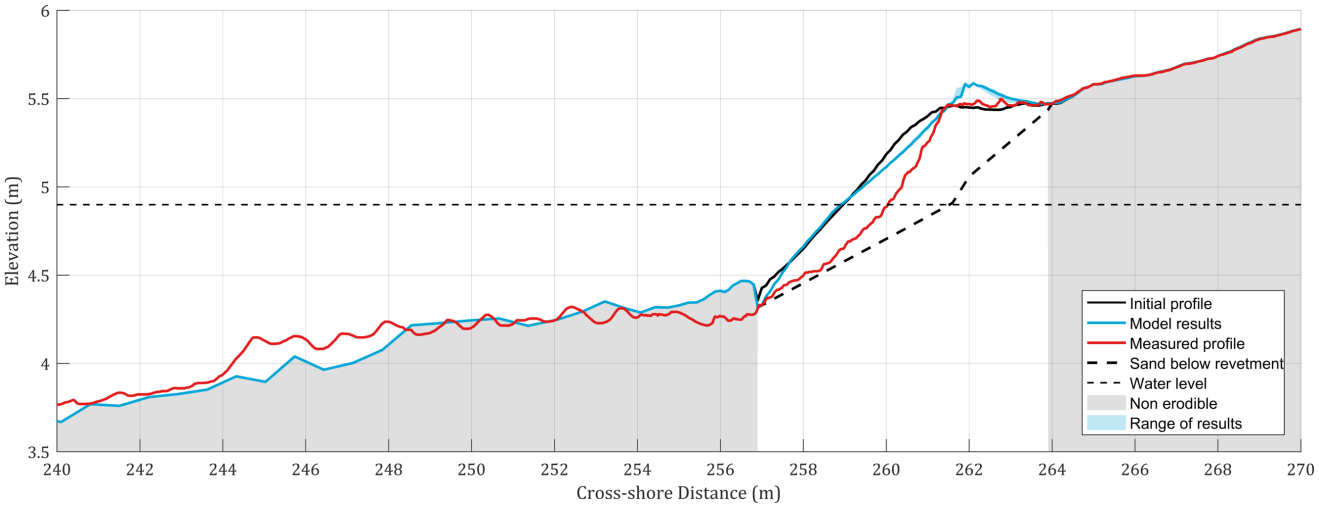

(a) Test G4 - Nielsen ($\varphi = 25°$) - Only revetment erosion

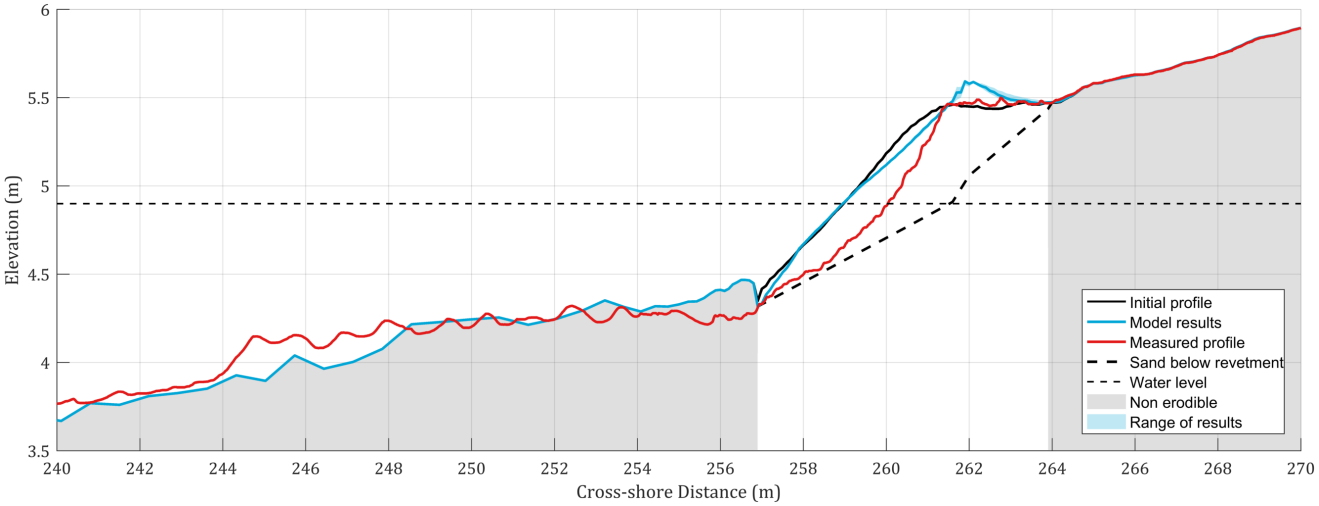

(b) Test G5 - Van Rijn - Only revetment erosion

Figure 5.4: XBeach-G performances on DR4

5.5. CONCLUSIONS

It can be concluded from the performance tests that the XBeach and XBeach-G model are currently not able to model composite beaches. First of all, neither of the models were able to get morphological changes close to that of the measured changes. This was not achieved for the sandy beach section of the profile and neither for the revetment section of the profile. Furthermore quite some assumptions had to be made in order to get a sufficient representation of real conditions of the profile. These assumptions, such as the assumption that only one fraction was present or that certain areas of the profile were non erodible, seem to undermine characteristics of the neglected processes.

Still some details of the model results show to be promising. First of all it was found in the XBeach performances that XBeach was able to model the erosion in front of the revetment relatively well for DR1, given that there is no up slope erosion of sand (see figure 5.2a). Both the slope and elevation of the model results come close that those of the observations. Furthermore the XBeach-G models show steepening of the slope, which is a development of the revetment that was also observed during the experiments. It can be argued whether the steepening of the slope could also be accounted to erosion of sand underneath the revetment. Lastly it has also been found that the uncertainty of the hydraulic conductivity K did not show any big difference in the morphological developments.

6

PROCESS IDENTIFICATION

Which processes are missing?

In Chapters 2 and 3 background information was provided on processes on composite beaches from the literature and on the processes as modelled by XBeach and XBeach-G. Chapter 4 provided information about observations made during flume experiments and Chapter 5 showed the performances of XBeach and XBeach-G. This chapter gives an overview of missing processes in the models and an approach to include these missing processes is proposed.

Section 6.1 discusses the hydrodynamic processes, section 6.2 the morphodynamic processes and section 6.3 the groundwater processes. In section 6.4 the most relevant missing processes are identified.

6.1. HYDRODYNAMIC PROCESSES

Even though the hydrodynamic processes and any adaptation to these processes are not in the scope of this thesis, they are still of interest as morphology is of course depending on the flow. As was mentioned in section 3.1 both long and short waves are resolved in XBeach and XBeach-G. Effects of neither of these processes should be missing in either of the models. XBeach solves the hydrodynamics depth-averaged, which simplifies the many of the actual dynamics such as undertow, turbulence and wave breaking.

Long-shore transport is non negligible in real life situations, especially at non-uniform coasts. The hydrodynamics are already in place for XBeach and therefore also for XBeach-G, but coupling to the morphodynamics is missing for XBeach-G. For this thesis all processes regarding this long-shore transport is out of the scope and is assumed to have been of little significance during the DynaRev experiments.

Relevant process	Implemented in XBeach?	... XBeach-G?
Long waves	Yes	Yes
Short waves	Yes	Yes
Undertow	~	~
2DH flow	Yes	No

Table 6.1: Overview of implemented hydrodynamic processes in XBeach(-G)

6.2. MORPHODYNAMIC PROCESSES

Many things can be said about the morphodynamic processes at composite beaches and as implemented in XBeach and XBeach-G. Below these processes are discussed separately. An overview of implemented processes in XBeach and XBeach-G is given in Table 6.2.

Relevant process	Implemented in XBeach?	... XBeach-G?
Sediment transport		
single fraction	Yes	Yes
multiple fractions	~	No
1 sand and 1 gravel fraction	No	No
Sediment transport below bed layers	No	No
Avalanching	Yes	Yes
Bed slope effects	Yes	Yes
Hiding	No	No
Exposure	No	No
Armoring	Yes	No
Longshore transport	Yes	No

Table 6.2: Overview of implemented morphodynamic processes in XBeach(-G)

- First the sediment transport functions of XBeach and XBeach-G are discussed. As was mentioned in section 3.2.2.1 the sediment transport formulation for sand, the Van Thiel-Van Rijn equations, are wave-averaged. This approach works well for the surf-beat mode as energy depended velocities are used in the advection diffusion equation, see Equation 3.9. This equation should not hold for the non-hydrostatic mode as this mode models instantaneous flow. In surfbeat turbulence is calculated using the obtained root-mean-squared velocity from the wave group varying wave energy and a wave breaking turbulence term. Possibly the missing transport is related to this malfunction of the sediment transport formulation in combination to the implementation of the undertow in the non-hydrostatic mode. Research on this question is still going on and is out of the scope of this thesis. For XBeach-G the transport formulation was adapted to a formulation that is valid for instantaneous transport.
- As can be seen in Table 6.2 the implementation of sediment transport of multiple fractions is noted to be neither a yes or a no. This option of modelling in XBeach with multiple fractions has been present in XBeach for quite a while, but little research has been done about its performances. As it is not a commonly used option of XBeach it has not been discussed in Chapter 5. In this chapter though it was concluded that an interaction between gravel and sand was missing. Therefore modelling with multiple sediment fractions is of interest. Modelling with multiple fractions is only implemented for XBeach and its transport functions. It is to be expected that this does not yield the desired results, as in section 5.3 it was found that using the XBeach transport formulation with a gravel grain size does not perform well. Modelling with a both a sand and gravel formulation has not been implemented in XBeach and XBeach-G.
- From literature and from the DynaRev experiments it was found that sediment transport below the revetment is of importance. It was possibly a contributor to the sinking of the revetment during the experiments. From the performance studies it was found that the depth of the revetment was not of large influence on the morphological developments. That does not mean it is negligible, as the possible introduction of sand from underneath the revetment into the water column might influence the down slope morphodynamics.
- Avalanching and bed slope effects are implemented in both XBeach and XBeach-G. Avalanching could possibly to be of importance for interaction between gravel and sand, as it was found in section 5.3 that erosion of sand in front of revetment was modelled. These erosion holes could lead to avalanching.
- Hiding and exposure are not implemented in XBeach or XBeach-G. Hiding of sand between gravel reduces the transport of sand. This very likes occurs, but the erosion rates of sand from the revet-

ment are rather significant. Furthermore hiding and exposure occurs in graded beds, but the DynaRev predominantly consisted of cross-shore and vertical separated fractions. Therefore it is assumed that during DynaRev experiment the large influence of hiding and exposure is negligible.

- Armoring could possibly be of importance for modelling composite beaches. During the experiments in Hannover the gravel was found on top of sand near the toe, where the gravel might have protected sand erosion. On the other hand it was also mentioned that erosion of sand below gravel might be of importance. This is contradicting and one could argue whether armoring occurs in the swash or only for larger depths.
- As was mentioned the longshore transport at composite beaches is out of the scope of this report.

6.3. GROUNDWATER PROCESSES

In the literature it was found that the groundwater flow could be described with either the Darcy or Darcy-Forchheimer equations. McCall (2015) implemented a simplification of the Darcy-Forchheimer equation in order to easily reproduce the decrease of of the hydraulic conductivity K after reaching the critical Reynolds number. This simplification could reduce the accuracy of the hydraulic conductivity, but the certainty of knowing the initial hydraulic conductivity is also an issue. From the performance study it was found that different hydraulic conductivities do not influence the morphodynamics much, but it does have a significant effect on the hydrodynamics (overwash and runup).

Currently only one hydraulic conductivity can be chosen in XBeach(-G), which should represent all the sediments present. This can be sufficient if indeed only one fraction is present, but it might underestimate or overestimate the hydraulic conductivity once multiple fractions are present. Furthermore the hydraulic conductivity could locally become different. As fractions start mixing the conductivity changes. If one wants to perfectly replicate this one needs a model that has a space and time varying hydraulic conductivity K and therefore possibly also a space and time varying Re_{crit}.

Relevant process	Implemented in XBeach?	... XBeach-G?
Groundwater flow		
for a single fraction	Yes	Yes
for multiple fractions	~	No

Table 6.3: Overview of implemented groundwater processes in XBeach(-G)

6.4. IDENTIFICATION OF RELEVANT PROCESSES

Two different processes are found to be missing in the current models from which it is expected to contribute to more accurate results: the inclusion of gravel transport in XBeach and sand transport in the gravel revetment. Adding other processes such as hiding and exposure might also contribute to model, but is out of the scope of this model as they are assumed to be of less importance. Below the two processes are discussed.

6.4.1. PROCESS 1: INCLUSION OF GRAVEL TRANSPORT IN XBEACH

From the performance test is was concluded that XBeach had issues with the modelling of the beach because it regarded the beach having only a single fraction of sand. Figure 6.1 shows what the XBeach loop looks like when multiple fractions are present. XBeach stores information about the bed composition in all layers of the soil through $pbbed$, as was discussed in section 3.2.6.

The loop in Figure 6.1 is for the case of two sand fractions, which means no gravel fractions. Should the transport formulations of XBeach-G be implemented in XBeach, in a way that both gravel as sand can be modelled, the loop would look like Figure 6.2. Once more it can be seen that the sediment transport formulation is different for XBeach-G and it can be seen that XBeach-G does not have suspended sediment formulations.

Introducing multiple sediments becomes complicated when using groundwater flow. The groundwater flow is dependent on the depth of the revetment and the hydraulic conductivity. When sand and gravel start mixing the hydraulic conductivity at different location of the profile will change. One can decide to do a few things in order to overcome this obstacle, which is discussed in section 7.2.1.

The following steps are undertaken in order to gradually include modelling with a gravel transport in XBeach:

Process 1: inclusion of gravel transport in XBeach

(a) Two D_{50} with XBeach transport formulations
XBeach is used to model with two D_{50}'s using the transport formulation of XBeach.

(b) Two D_{50} with additional XBeach-G transport formulations
XBeach is used to model with two D_{50}'s using the transport formulation of XBeach and that of XBeach-G.

(c) Two D_{50} with additional XBeach-G transport formulations and groundwater flow
The model is tested to run with multiple fractions including groundwater flow.

These steps are all undertaken in Chapter 7.

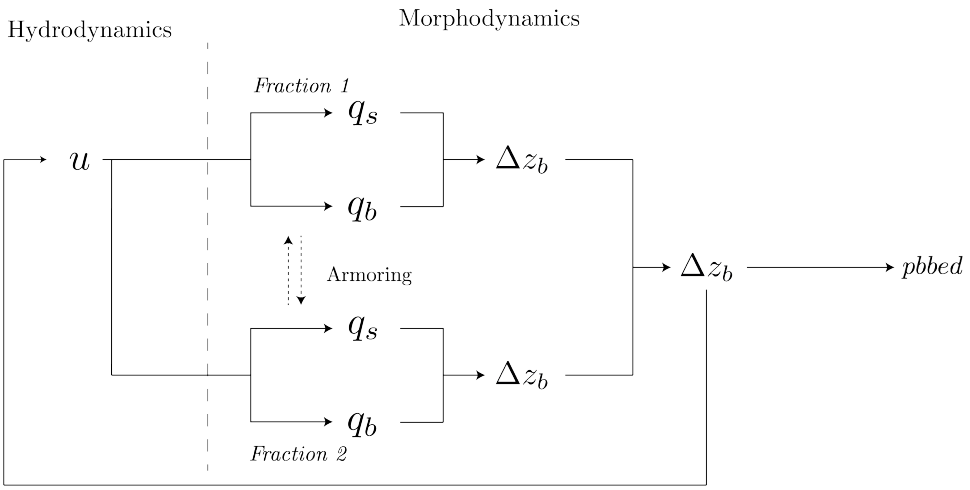

Figure 6.1: Model simplification of XBeach with 2 fractions

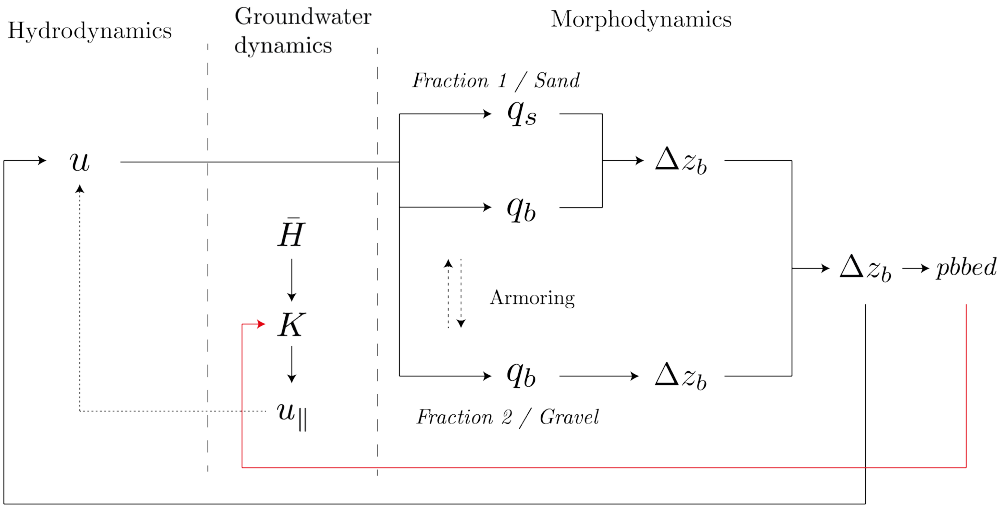

Figure 6.2: Model simplification of XBeach with a sand and gravel fraction

6.4.2. PROCESS 2: SAND TRANSPORT IN THE GRAVEL REVETMENT

The process of sand transport in the gravel revetment is a complex process. In the literature study the research by Jacobsen et al. (2017) was discussed. A transport equation was described and from correspondence with Jacobsen it was concluded that this transport equation could indeed be tested for the case study of DynaRev within the XBeach model. Figure 6.3 visualises the processes and transport modes occurring in the case of the addition of the transport equation of Jacobsen et al. (2017).

In Figure 6.4 the transport flux due to sand transport inside the gravel is shown as q_{ss}. The groundwater flow introduces a sediment transport flux when it reaches a certain threshold. The sediment transport influences the bed level update with settling where erosion occurs and an increase of sand between the gravel pores.

This erosion introduces complications that have also been identified for the first process. The groundwater flow becomes complicated as sand is eroded from the bottom of the revetment. The bottom of the revetment changes and therefore the groundwater dynamics also change. Currently it is not possible to have a time varying aquifer bottom. Furthermore a varying aquifer bottom would also complicate the bed composition *pbbed* and the mass balance.

The following steps can be undertaken in order to gradually model this type of erosion:

Process 2: Sand transport inside the revetment

(a) San transport flux calculations with groundwater velocities, which is discussed in Chapter 8.

(b) Bed level update with a two-line model, which is discussed in Chapter 9.

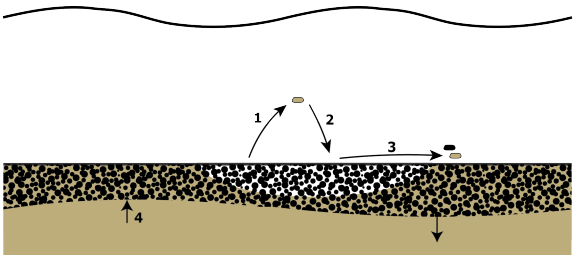

Figure 6.3: Addition of erosion in revetment - Here (1) and (2) describe the transport of suspended sediment of sand, (3) describes the bed-load transport gravel and/or sand and finally (4) describes the interaction between sand and gravel.

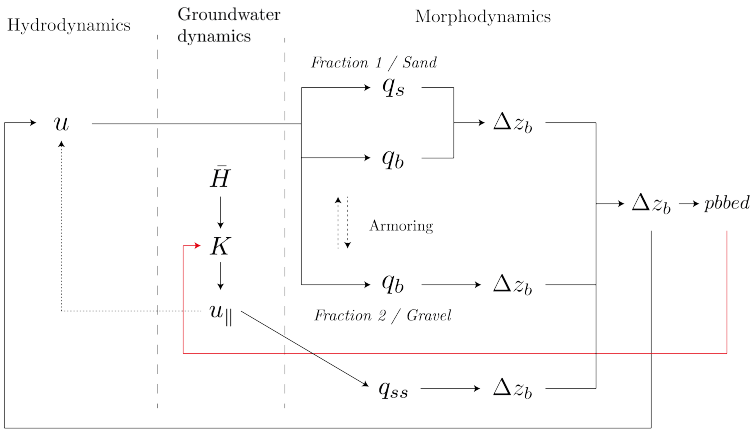

Figure 6.4: Model simplification of XBeach with a sand and gravel fraction plus sand transport inside the gravel revetment

7

MULTI-FRACTION MODELLING

From Chapter 6 it was concluded that modelling with multiple fractions was lacking in the current models. This chapter explores the introduction of the gravel transport formulation to XBeach. Before this transport is included into XBeach, the modelling with multiple fractions in the current XBeach model is analysed in order to see how the model performs. Thereafter the gravel transport was added to form an adapted XBeach model.

In section 7.1 multi-fraction modelling with the current XBeach model is examined and in section 7.2 the adapted model of XBeach with a gravel transport formulation is elaborated and tested. Section 7.3 provides some conclusions.

7.1. XBEACH MULTI-FRACTION MODELLING

As was already mentioned the multi-fraction modelling was already in place for the XBeach model, but has not been investigated much yet. Therefore it is dealt with as if it is a new option in XBeach. First the model setup is discussed and a test overview is given, after which the results are presented.

7.1.1. MODEL SETUP AND TEST OVERVIEW

An overview of the models that are run is given in Table 7.1. In order to specify multiple fractions in XBeach one must define where these fractions are situated in the model. As was discussed in section 3.2.6 on the bed composition of XBeach, multiple layers are defined in the vertical. Each layer has the same initial layer thickness. For the setup the vertical of the initial DynaRev profile, including the revetment, has been split up into layers of 0.1 m. For the sandy beach only a sand fraction was set to be present and for the revetment only gravel. An example of such an setup is visualised in Figure 7.1. Yellow corresponds to sand and dark blue to gravel. Colors in between yellow and blue indicate a mixture of sand and gravel. This occurs at the edges of the revetment, as interpolation between the grid size and vertical layers is inevitable without changing the shape of the revetment.

The D_{50}'s used in the basic model MF1 correspond to the actual sand and gravel fractions present, respectively 0.3 mm and 50 mm. A model has been run in order to see the effect of avalanching. This is done with model run MF2 with a larger D_{50} for gravel of 1000 m, details are provided in section 7.1.2. The boundary conditions are the same as for the performance studies, as well as the grid size and duration of the model. For the multi-fraction modelling of this section the groundwater flow is turned off.

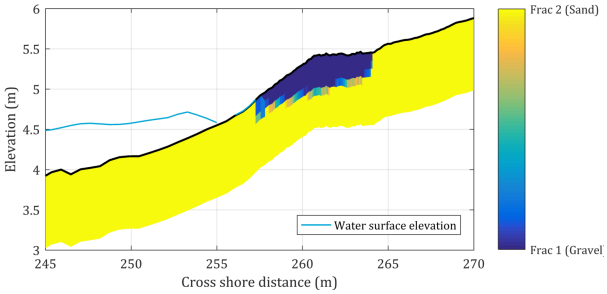

Figure 7.1: Model setup for modelling with multiple fractions

Test	Model	Reference wave set	Transport formulation	D_{50}'s (mm)	Comment
MF1	XBeach	DR1	VT-VR	0.3 & 50	Basic case
MF2	XBeach	DR1	VT-VR	0.3 & $1000 \cdot 10^3$	Increased D_{50} for gravel
MF4	XBeach	DR4	VT-VR	0.3 & 50	Basic case
MF5	XBeach	DR4	VT-VR	0.3 & $1000 \cdot 10^3$	Increased D_{50} for gravel

Table 7.1: XBeach multiple sediment runs - VT-VR stands for the Van Thiel-Van Rijn transport equation

7.1.2. RESULTS CASE DR1 - MF1 – MF2

The first tested model is the multi-fraction model MF1, with the actual D_{50}'s that were present during the DynaRev experiments. From Figure 7.2 it can be seen that the model does not get close to the results found in the experiments. Both the elevation and slopes do not match the measurements, but this is not unexpected. This result looks similar to the results found in the section of the XBeach performances, see section 5.4. What does differ from these XBeach performance runs is the fact that the two fractions were able to mix over the cross-section. In model MF1 revetment erosion is possible and the gravel is now eroded down slope and mixes with the sand. As was mentioned the transport formulation used in XBeach is faulty for gravel, such that one can expect this faulty transport of gravel. To prevent the gravel from transporting down slope and therefore get the erosion in front of the revetment similar to test S1, one can increase the D_{50} of the gravel. This prevents suspended and bed-load transport of gravel, while avalanching and mixing of the fractions is still possible.

Test MF2 is a model run where the latter has been modelled. The D_{50} of the gravel has been increased to 1000 m and the result is shown in Figure 7.3. One can clearly see the improvement. The deposition rates down slope are lower than for MF1 and the slope of the revetment matches quite well with the measured profile. Avalanching is now the only process that acts as a enabler of erosion/accretion for gravel to the locations where mixing did occur in model MF2. Appendix D provides additional figures where these MF1 and MF2 can be compared with vertical mixing differences (see Figures D.1 and D.2).

7.1.3. RESULTS CASE DR4 - MF4 – MF5

The multi-fraction model performs about the same for DR4 as it did for DR1 regarding the modelling with the actual D_{50}'s. Therefore MF4 is not discussed in detail, but its results are shown in Appendix D Figure D.4. Test MF5 did show different results and is discussed below.

Where modelling with an increased D_{50} was relatively successful for case DR1 with test MF2, this was not the case for modelling DR4 with test MF5. As can be seen in Figure 7.4 there is a mismatch between the model results and measured final profile. Onshore the gravel slope has not changed and barely any erosion or accretion is found. This is not necessary a bad result, as the slope of the revetment in the model look similar to that of the measured profile. Once more it is visible that a significant volume loss at the revetment area seems to be missing for which the missing process is most probably erosion of sand underneath the revetment.

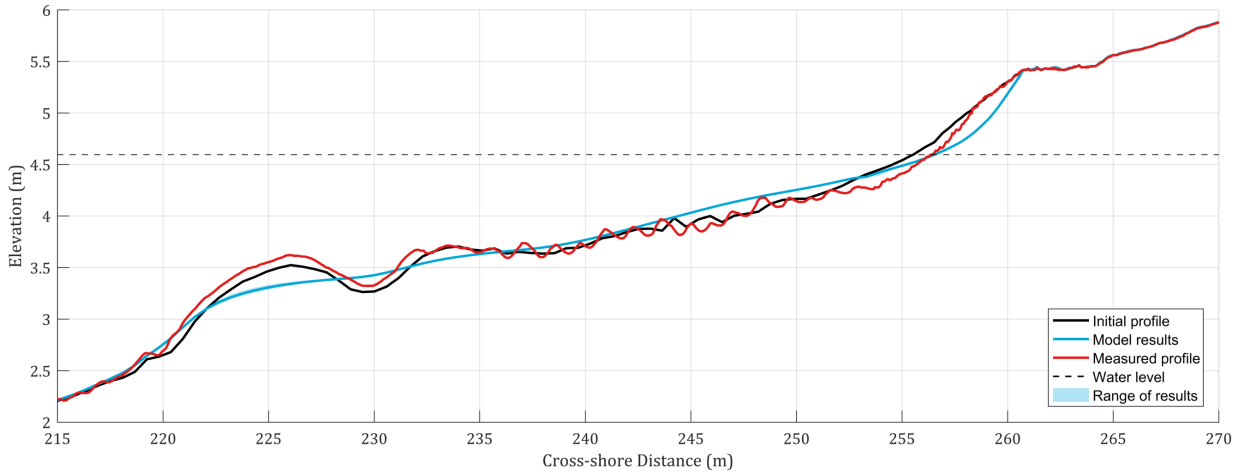

Figure 7.2: XBeach multi-fraction result MF1

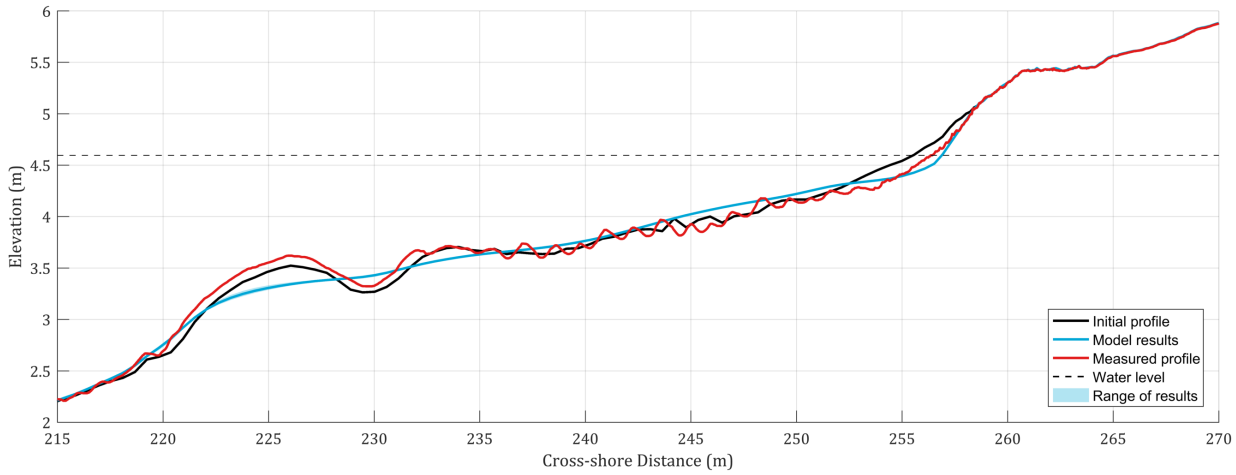

Figure 7.3: XBeach multi-fraction result MF2

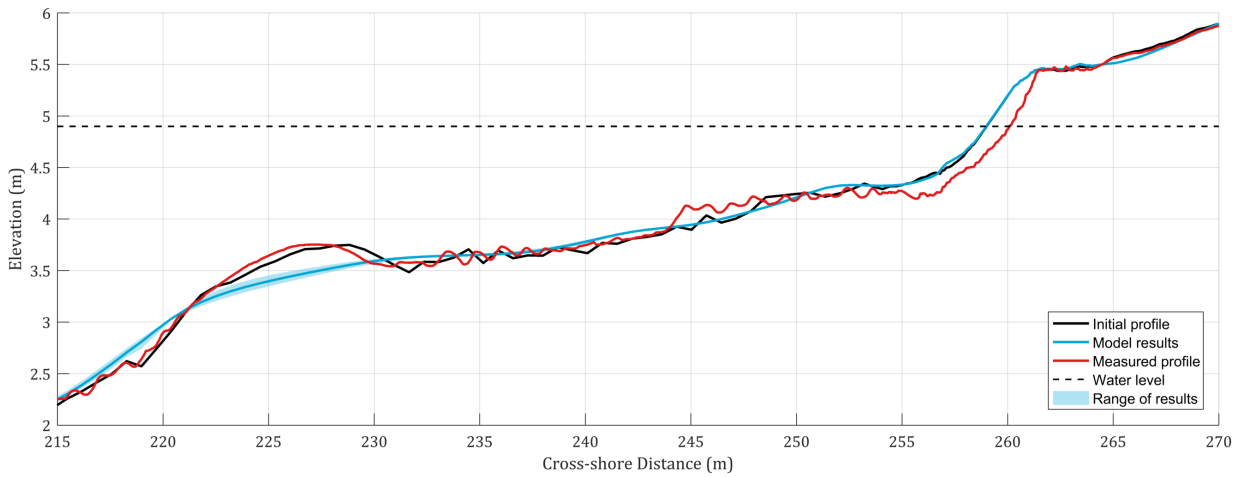

Figure 7.4: XBeach multi-fraction result MF5

7.2. XBEACH(-G) MULTI-FRACTION MODELLING

From the results from multi-fraction modelling it was found that the gravel transport equation of XBeach-G could potentially contribute to improving the model results, especially for wave set DR1. A few adaptations have been made to the last release of the XBeach model named XBeachX in order to incorporate the gravel transport formulation of XBeach-G in the XBeachX model. This is shortly explained in section 7.2.1.

7.2.1. MODEL SETUP AND TEST OVERVIEW

In essence the model adaptation is a forced combination between XBeach and XBeach-G. Two transport formulations have been forced for two separate fractions. Fraction 1 is modelled with the XBeach assigned formulation and fraction 2 is modelled with the XBeach-G assigned formulation.

The hydrodynamics are the same as for the normal multi-fraction modelling with XBeach and are therefore not discussed. Groundwater flow however was not enabled for the normal multi-fraction models of section 7.1. McCall (2015) noted however that the groundwater flow is of importance for modelling gravel and has therefore also been tested. It was mentioned in section 6.4.1 that modelling groundwater flow could get difficult when multiple fractions are modelled. The mixing of sediments give locally different hydraulic conductivities and therefore change the dynamics of the groundwater flow. To solve this issue one can do several things. The ideal solution to this issue, but also the most complicated and computing expensive, would be introducing some new dynamics to the model. One should introduce a time and space variable hydraulic conductivity K, a time and space variable critical Reynolds number Re_{crit} and a varying groundwater depth file. Furthermore one should know how much K and Re_{crit} vary under certain compositions of fractions. For the scope of this thesis it has been chosen to take a more crude and simplified approach. Under the assumption that mixing of sediments occurs only near the toe of the revetment where the groundwater flow is not of large influence, a single value for K and Re_{crit} (of gravel) has been chosen. It is assumed that groundwater flow only occurs at the revetment, where the revetment is the same as for the performance tests of XBeach-G for wave set DR1 and DR4.

An overview of the performed tests is given in Table 7.2. For both wave sets DR1 and DR4 three model runs have been performed. The adapted model showed to have difficulty with suspended transport, therefore the first two runs only take into account bed-load transport of sand. The third run includes both suspended and bed-load transport of sand and this is where the model has difficulties, which are clarified in the following sections.

		Transport formulation				
Test	Reference wave set	XBeach	XBeach-G	Groundwater flow?	D_{50}'s (mm)	Comment
MFG1	DR1	VTVR	McCall-Van Rijn	No	0.3 & 50	Only bed-load transport
MFG2	DR1	VTVR	McCall-Van Rijn	Yes	0.3 & 50	Only bed-load transport
MFG3	DR1	VTVR	McCall-Van Rijn	Yes	0.3 & 50	Both bed-load and suspended transport
MFG4	DR4	VTVR	McCall-Van Rijn	No	0.3 & 50	Only bed-load transport
MFG5	DR4	VTVR	McCall-Van Rijn	Yes	0.3 & 50	Only bed-load transport
MFG6	DR4	VTVR	McCall-Van Rijn	Yes	0.3 & 50	Both bed-load and suspended transport

Table 7.2: Test overview for adapted XBeachX model

7.2.2. RESULTS CASE DR1 - MFG1 – MFG3

The results from the adapted model tests MFG1, MFG2 and MFG3 for wave set DR1 are shown in Figures D.6, 7.5 and 7.6. Only MFG2 and MFG3 are discussed, as the model results without groundwater flow MFG1 showed similar results to the model results with groundwater flow MFG2.

The results of the adapted model are promising for wave set DR1. Onshore the model matches the measured profile pretty well, both in elevations and slope. These results look a bit similar to the multi-fraction model tests where the D_{50} was very high. For a high D_{50} the gravel fraction would not be mobilised and this looks also to be the case for the adapted model results. Apparently the combination of water level and wave height is not sufficient enough to really mobilise the gravel stones and therefore avalanching seems to be the dominating process of the model to influence morphological changes onshore. This would also explain why the results for the adapted model with groundwater flow are almost identical to that without groundwater flow. When gravel is not mobilised in the model without groundwater flow, the gravel definitely won't get mobilised with groundwater flow. This is because groundwater flow actually helps stabilise the gravel and reduces transport.

Furthermore there are little differences to be seen near the revetment between the model runs with and without suspended sediment transport of sand. Slightly more erosion can be seen in front of the revetment with suspended sediment transport, therefore better matching the measured profile. A short look at the fraction distribution shows that sand has mixed with gravel at the toe of the revetment, see Figure D.7.

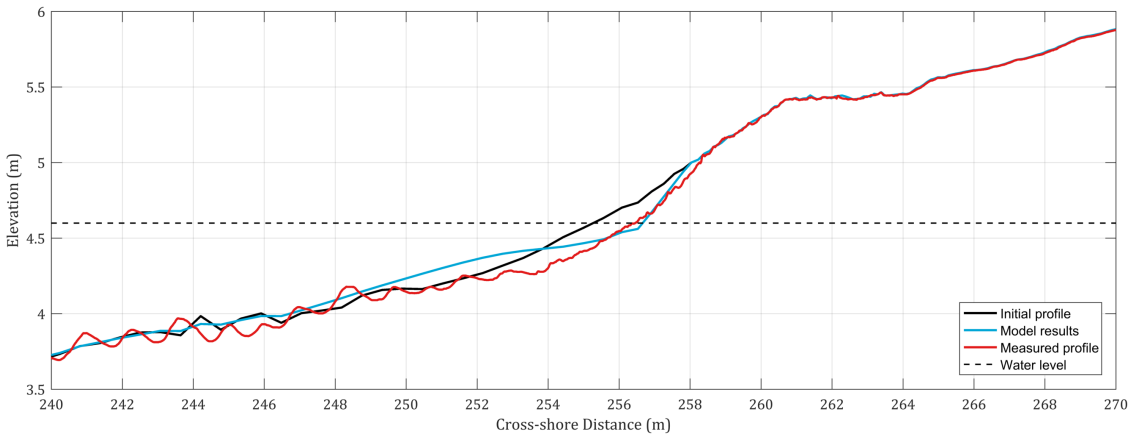

Figure 7.5: XBeach multi-fraction result MFG2

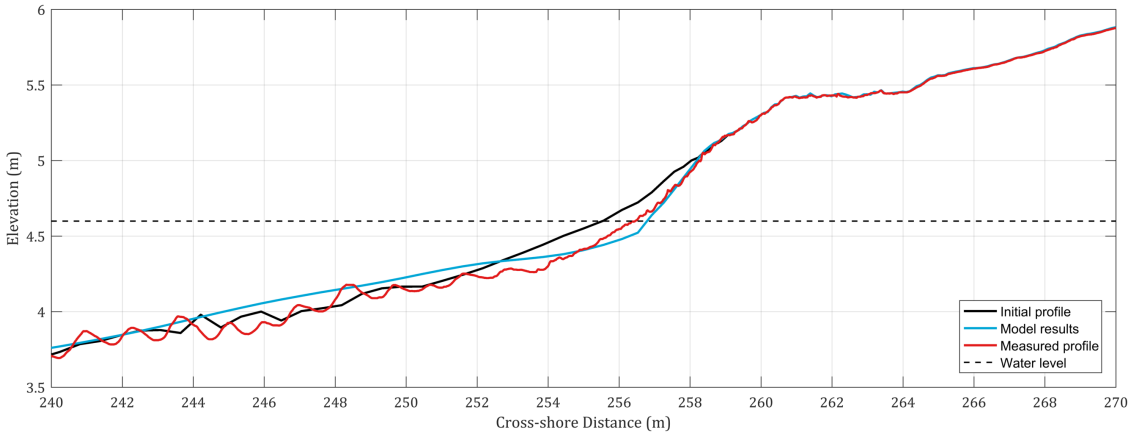

Figure 7.6: XBeach multi-fraction result MFG3

7.2.3. RESULTS CASE DR4 - MFG4 – MFG6

Different results with the adapted model have been found for wave set DR4. The result without groundwater flow is shown in Figure D.8, with groundwater flow in Figure 7.7 and with suspended sediment transport in Figure 7.8.

Wave set DR4 has a higher water surface elevation than DR1 and therefore much more impact of waves is located on the revetment. This was evident from the results without groundwater flow MFG4, where the revetment slope has formed into a slight S-curve. The results from MFG5 with groundwater flow show no change in slope, see Figure 7.7. This shows that groundwater flow is of large influence on the morphological development. The slope of the revetment is somewhat similar to that of the measured profile, but the elevations do not match. The mismatch of the measured profile of the revetment and the model results is most probably due to erosion of sand beneath the revetment. Lastly in the XBeach-G performance tests crest building was found, but this is not the case for the adapted model.

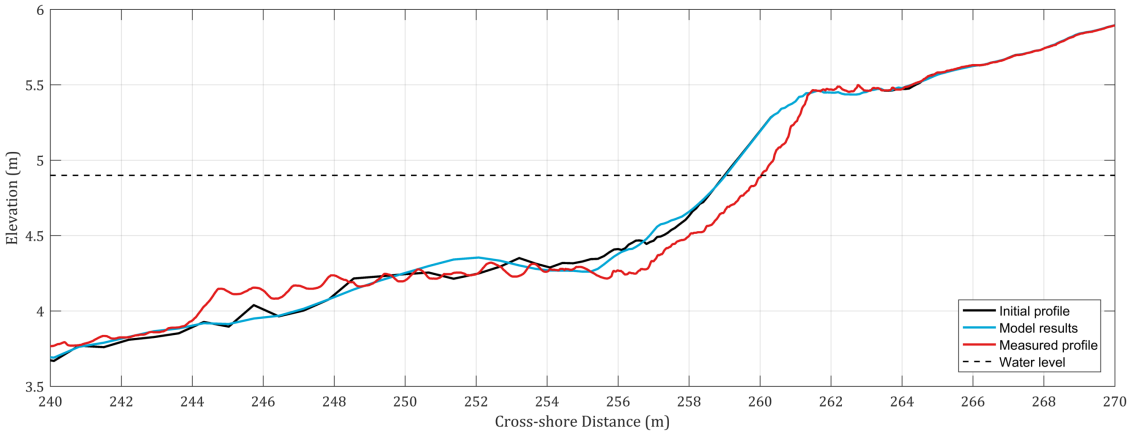

Figure 7.7: XBeach multi-fraction result MFG5

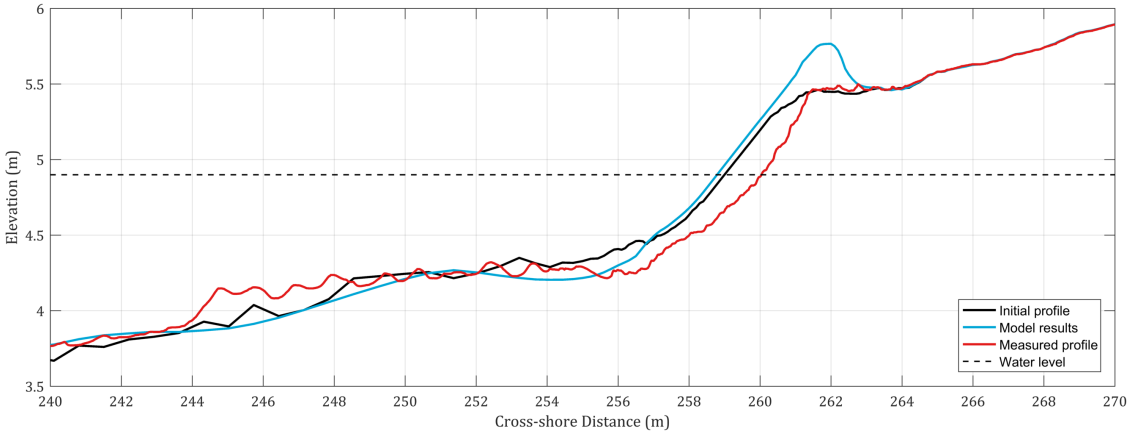

Figure 7.8: XBeach multi-fraction result MFG6

With the introduction of suspended transport of sand in MFG6 severe changes in the model results can be seen. A big crest has been formed and this crest consists entirely of sand, see Figure 7.9. Apparently something in the model occurs which causes sand to travel up the slope of the beach. Some reference models have been run and it was concluded that the cause of these results most probably originates from a combination of groundwater flow, the hydraulic conductivity K and the general accounting system used in XBeach for multiple fractions. In the development of XBeach-G it was found that the addition of the groundwater module affected the morphodynamics. As mentioned by McCall (2015) for the development of XBeach-G, the morphodynamic effect of the inclusion of groundwater

processes is primarily caused by the by modification of the surface water dynamics through the exchange of mass between the surface water and groundwater, leading to higher onshore-directed and lower offshore-directed bed shear stress and bed-load transport rates in the swash (first-order groundwater processes). With the presence of groundwater processes in XBeach this now also leads higher onshore-directed and lower offshore-directed suspended transport rates. Figure D.10 shows a comparison of the mean velocities in the water column between a model with and without groundwater velocity. As it can be seen the velocity is rather different and is more onshore directed for the model with groundwater velocities.

In Figure 7.10 a visualisation is given what type of velocities are present in the model with and without groundwater flow. Flow velocities are also present inside the revetment. This means water can flow up the gravel, infiltrate the revetment and then exits the revetment after travelling through the gravel revetment. Therefore less offshore-directed flow is present in the water column and the (suspended) transports are also less offshore-directed. Furthermore the suspended sediment can not travel through the gravel in similar manner as water: it is deposited in the top layer, which acts like a sieve.

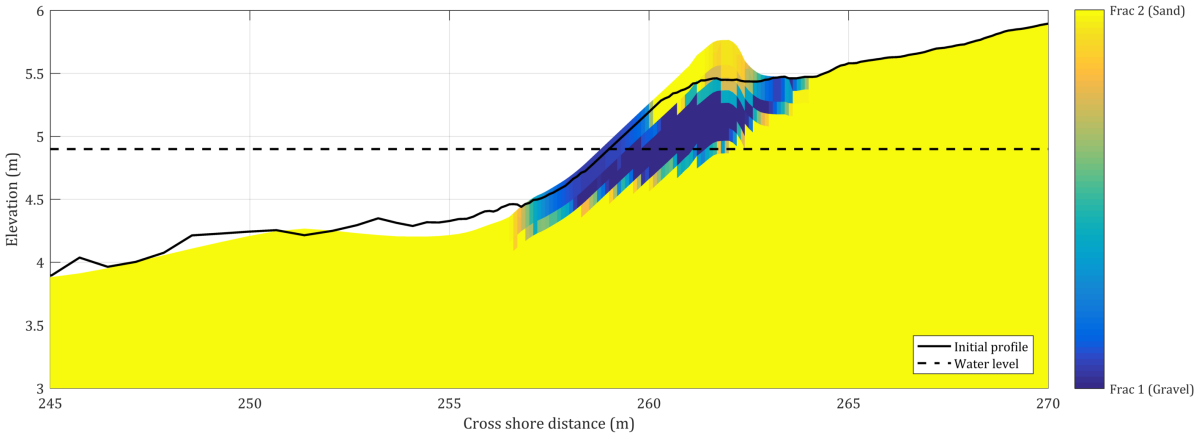

Figure 7.9: Deposition of sand on top of revetment during MFG6

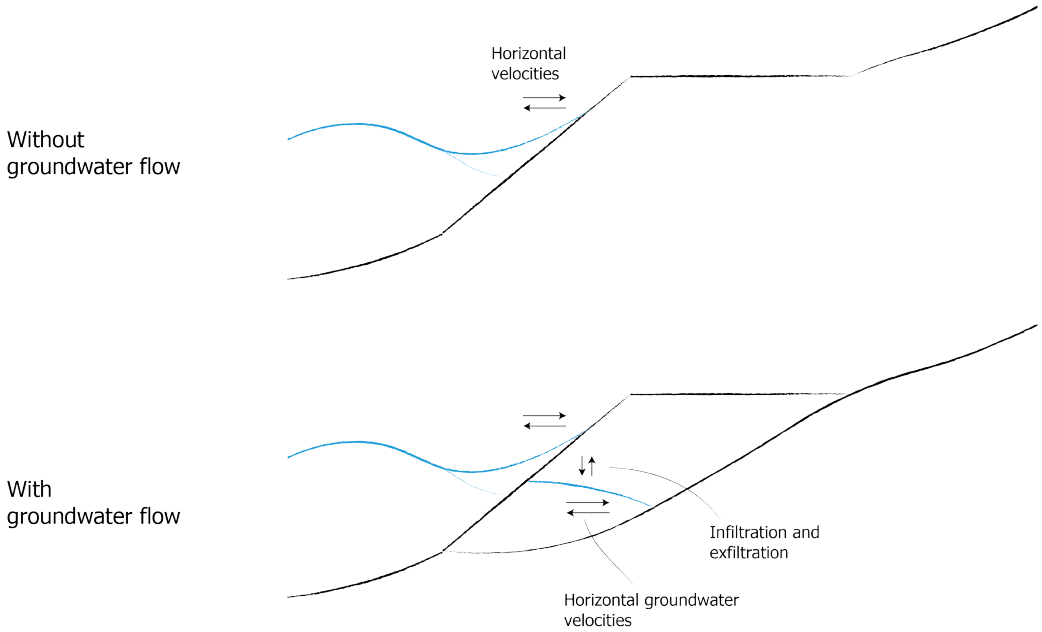

Figure 7.10: Impression of the hydrodynamic differences at the revetment with and without groundwater flow

7.3. CONCLUSIONS

In this chapter the current multi-fraction option of XBeach was studied and an adaptation to this model was made to include both sand and gravel transport formulations. The models were tested for two reference cases, one where erosion of sand in front of the revetment seemed to be of larger importance (DR1) and one where erosion of sand underneath the revetment seemed to be of importance (DR4).

The adapted model performs well in replicating the results of DR1 onshore, both elevation and slopes from the model results matched the observations. In front of the toe of the revetment sand is eroded and gravel almost only deposits in this eroded location due to avalanching. It can be argued though whether this is just a coincidence or not. It could be possible that the avalanching is just a good approximation of the observed changes. Modelling with or without groundwater flow showed to be of little influence as the hydrodynamic forcing was too little to influence morphological development on the revetment itself. This can most probably be related to the amount of wave breaking on top of the revetment, which was low for DR1. Furthermore suspended sediment transport showed to be of little influence on the onshore model results.

For case DR4 the model did not perform very well, especially when looking at the elevation. The model does not perform accordingly when suspended sediment transport is included. This is most probably caused by the coupling between the suspended sand transport and the hydrodynamics that include groundwater dynamics. For the results without suspended sediment transport a mismatch between the model results and measured profile was found, most probably due to the missing process of erosion underneath the revetment. For case DR4 modelling with groundwater flow was found to be of importance for modelling of gravel transport, as it decreases the deformation the revetment slope.

8

SAND TRANSPORT MODELLING IN THE GRAVEL REVETMENT

With the groundwater module from XBeach velocities are calculated within the gravel revetment. These velocities represent flow within the revetment that could transport sand within this revetment. The erosion of sand inside the revetment was shown from Chapters 4, 5 and 6 to be of importance for modelling the artificial composite beach. This chapter discusses the coupling of the groundwater dynamics with two transport formulations with which it is possible to estimate the initial transport rates of sand within the revetment and see if erosion is indeed expected to occur. From the transport estimates several remarks are made about bed level updates within the revetment.

Section 8.1 introduces the transport formulations, section 8.2 discusses the results with these transport formulations and section 8.3 provided a reflection of the results.

8.1. TRANSPORTS RELATIVE TO GROUNDWATER VELOCITIES

The groundwater module from XBeach-G calculates the horizontal groundwater velocities inside the revetment. With these velocities is it possible to calculate sediment transport fluxes. Model runs have been done with XBeach-G without any morphological developments and run with the same boundary conditions as the performance tests. The horizontal groundwater velocity is set as a time-series output for every 0.5 seconds.

The first transport equation that is discussed has already been discussed in section 2.2.4.1, namely the transport equation by Jacobsen et al. (2017). This equation has been designed to describe sand transport through a filter layer, which is the reason it is of interest for this report. The second equation considers a transport equation that is a slightly adapted version of the transport equation for gravel by McCall (2015). This equation is of interest as it was used for instantaneous bed-load transport and is based on a report by Van Rijn (2007a) and provides a comparison to the transport equation by Jacobsen et al. (2017).

The transport equation by Jacobsen et al. (2017), from now on referred to as *Jacobsen*, was described to be:

$$q_b = C_1 \left(\Psi - \Psi_{cr}\right)^{1.5} \frac{u_{\parallel}}{||u_{\parallel}||_2} \tag{8.1}$$

Section 2.2.4.1 has discussed the details of the parameters. The calibrated values by Jacobsen et al. (2017) have been used in the report. Therefore $C_1 = 1 \cdot 10^{-5}$ $m^3 m^{-1} s^{-1}$ and $\Psi_{cr,0} = 0.115$ (-). The parallel

filter velocity $u_{\|}$ has been replaced by the horizontal groundwater velocity as found from the groundwater dynamics. This groundwater velocity is also used to calculate the mobility number Ψ.

The adapted transport equation from McCall (2015), from now on referred to as *McCall-Van Rijn*, is defined as:

$$q_b = C_{qb}\gamma D_{50} D_*^{-0.3} \sqrt{\frac{\tau_b}{\rho}} \frac{\theta' - \theta_{cr}}{\theta_{cr}} \frac{\tau_b}{|\tau_b|} \tag{8.2}$$

The variables in this equation are discussed in detail in section 3.2.3. In the McCall-Van Rijn the physical velocity is used, not the filter velocity. Therefore the velocity used in this transport equation is divided by the porosity of the medium. Thus $u = \frac{u_{gw}}{n_{p,g}}$. Additionally a calibration parameter C_{qb} has been added in order to allow calibration of the transport fluxes. Ideally this parameter is left out of the equation, but it has been implemented to allow future calibration. The dimensionless friction factor c_f is assumed to be about 0.0059 (-), see section E.1.

8.2. RESULTS

Figure 8.1 gives an overview of the sediment transports of sand when using the horizontal groundwater velocity for case DR4. In this report the horizontal groundwater velocity is named gwu. The left panels show the results with Jacobsen and right with McCall-Van Rijn. For both Jacobsen and McCall-Van Rijn it can be seen that the mean transport at the toe of the revetment is positive (onshore-directed). Around 258 m the directions of the transport becomes negative (offshore-directed). For both formulations the mean of the onshore-directed transport is rather large compared with the average horizontal groundwater velocities. The shape of the velocities and transports resemble the results as found by Jacobsen et al. (2017). Figure E.10 reveals that the groundwater velocities can get very large compared to the mean velocities. These velocities are the filter velocities, not the velocities in between the gravel stones. Those velocities would be even larger. Large velocities give large transport volumes that dominate the mean transport volumes. These large velocities can most probably be related to breaking waves, which occurs mainly between 256 m and 260 m, see Figure E.11.

Jacobsen and McCall-Van Rijn both show offshore-directed transport fluxes (around 259 m) as well as onshore-directed transport fluxes. The magnitudes of the fluxes is larger for the Jacobsen transport equation. The mean transport gradients for each cell are shown in the bottom panels. Firstly large fluctuations at the edges of the revetment are seen, here constant transport gradients are present due to a sudden change in the bed transport which goes to zero. Within the revetment the mean gradients fluctuate from positive to negative, which is caused by local fluctuations between the transport fluxes. A zoomed view of the transport gradients revealed values of about $2 \cdot 10^{-6}$ $m^2 s^{-1}$. For 3 hours of wave impact and a porosity n_p of 0.4 this corresponds to a bed level change of:

$$\Delta z = \frac{2 \cdot 10^{-6} \cdot 10800}{0.4} = 0.054 m$$

The same calculations as for DR4 with Jacobsen and McCall-Van Rijn have been done with DR1. Figure E.2 of Appendix F shows these results. A distinct difference from the results with DR4 is that the groundwater velocities are on average negative. This leads to offshore transport gradients for Jacobsen. For McCall-Van Rijn this is not the case and only onshore (positive) transports are found. This can be contributed to the fact that the negative groundwater velocities for DR1 are not large enough to reach the critical shear stress for McCall, i.e. transports were smaller than the critical transport.

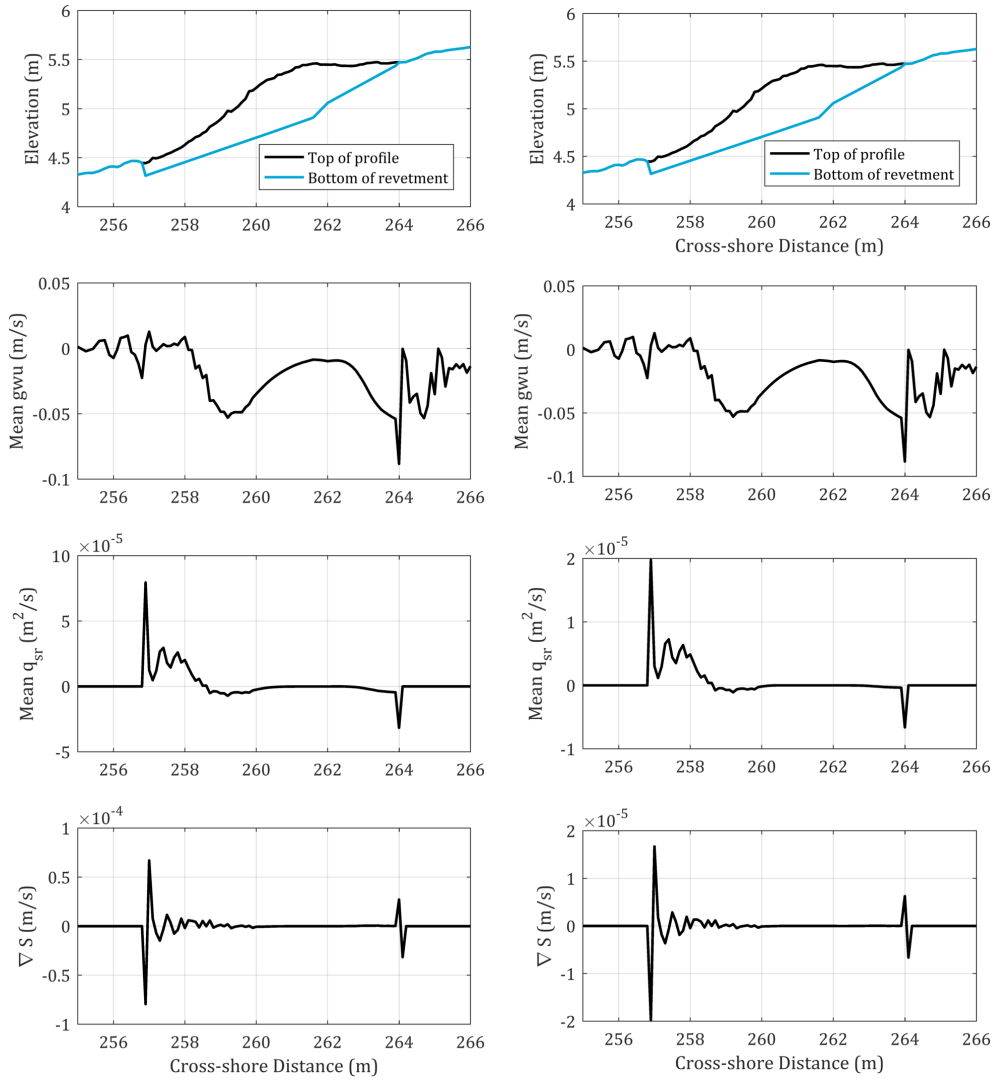

(a) Jacobsen (b) McCall-Van Rijn

Figure 8.1: Overview of results with transport equations (DR4) - Left shows results with Jacobsen and right with McCall-Van Rijn. Top panel shows the revetment, second panel shows average horizontal groundwater velocity in each cell gwu (negative is offshore-directed, positive is onshore-directed), the one to last shows the bed transport fluxes at cell interfaces q_{sr} and bottom panel shows the transport gradients ∇S. At the landward side of the revetment where barely any groundwater flow should be present a negative gwu is found. This is due to the conditions of the groundwater level in the groundwater module, where groundwater head difference are used to calculate velocities.

8.3. REFLECTION

The transport formulations Jacobsen and McCall-Van Rijn have been used without interfering with any of the settings in the context of modelling sand transport inside a gravel revetment. The results should therefore be handled with care. This section reflects on these results by comparing them with visual observations form the DynaRev experiments and by looking at possible sensitivities of the transport equations. The focus of this section is on DR4, as erosion was more significant for this wave set. Results from DR1 are discussed and results are presented in Appendix E.

8.3.1. EXPECTED EROSION AND DEPOSITION RATES IN REVETMENT

With the shapes of the mean transports at the revetment retrieved from the results one can evaluate what is likely to occur inside the revetment. Figure 8.2 shows a sketch of the expected sedimentation and erosion in the revetment for DR4. As can be seen one can expect sedimentation inside the revetment with the current transport fluxes. In a similar manner one can represent where erosion and de-

position occurs with the results with the McCall-Van Rijn formulation. As only positive transport fluxes are found it will most probably lead to erosion at the toe of the revetment and deposition in the center of the transport active area.

Whatever the shape of the transport fluxes, if erosion occurs it will deposit somewhere in the revetment. The deposition will most likely occur in between the gravel particles (mixing). From the DynaRev experiments no significant mixing of sand and gravel within the revetment was found. Deposition of sand is therefore expected to in combination of erosion of sand out of the revetment. Chapter 9 discussed some details regarding this deposition and whether these patterns actually make sense.

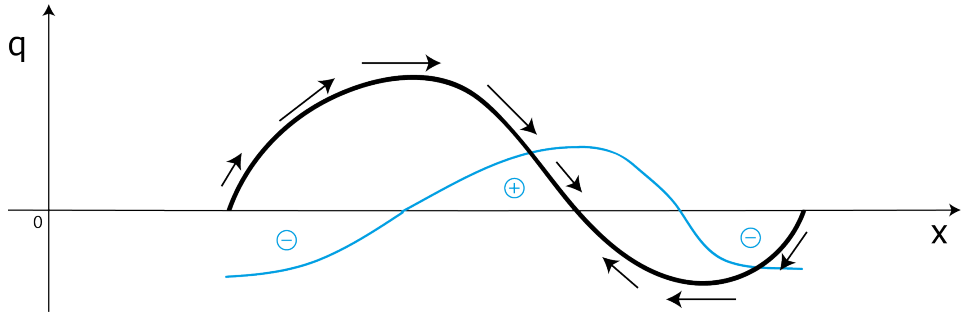

Figure 8.2: Expected erosion and deposition - Black line shows a hypothetical curve of the transport inside the revetment. Blue line expresses the expected erosion and deposition patterns inside the revetment.

8.3.2. SENSITIVITY ANALYSIS OF TRANSPORTS EQUATIONS

Sensitivities of the transport equations can affect how the transports behave and therefore affect what the erosion and deposition look like. Several of these sensitivities have been addressed below.

Hydraulic conductivity K

The hydraulic conductivity influences the velocities in the groundwater module. Six XBeach-G models are run with three values for the hydraulic conductivity as assessed in the performance study (0.2, 0.3 and 0.4 ms^{-1} for both DR1 and DR4). The groundwater velocities retrieved from these models are used to identify the effect of different hydraulic conductivities to the transport fluxes.

The results for DR4 show that the mean groundwater velocities are larger for larger K's, see Figure 8.3. This is as to be expected following Darcy's law. From the figure it can be seen that the hydraulic conductivity is of large influence on the transport fluxes. This shows that the magnitudes of the transport equations are very sensitive to a change in the groundwater velocities, while the pattern of transports stays the same.

Defining a gwu_{max}

All results show the mean of the transport fluxes. As was mentioned it is possible that extreme transport fluxes due to wave breaking influence this mean transport. In order to see what the transports look like without these extreme transports a maximum velocity has been assigned to the groundwater flow (filter velocity). Values of gwu_{max} = 0.05, 0.1 and 0.2 ms^{-1} have been assessed and the results are shown in Figure 8.4. These values have been based on the gwu_{rms} found in revetment, namely to be $1 \cdot gwu_{rms}$, $2 \cdot gwu_{rms}$ and $4 \cdot gwu_{rms}$, see Figure E.12.

Distinct differences can be seen for the different transport formulations, different maximum groundwater velocities and for DR1 and DR4. First Jacobsen is discussed. With the large maximum velocity of 0.2 ms^{-1} one can see that the transports look different compared to the results from the original results, see Figure 8.1a. The main difference is that the original transport peak at the toe has decreased and the magnitudes of the onshore transports have decreased. For the two other maximum velocities 0.05 and

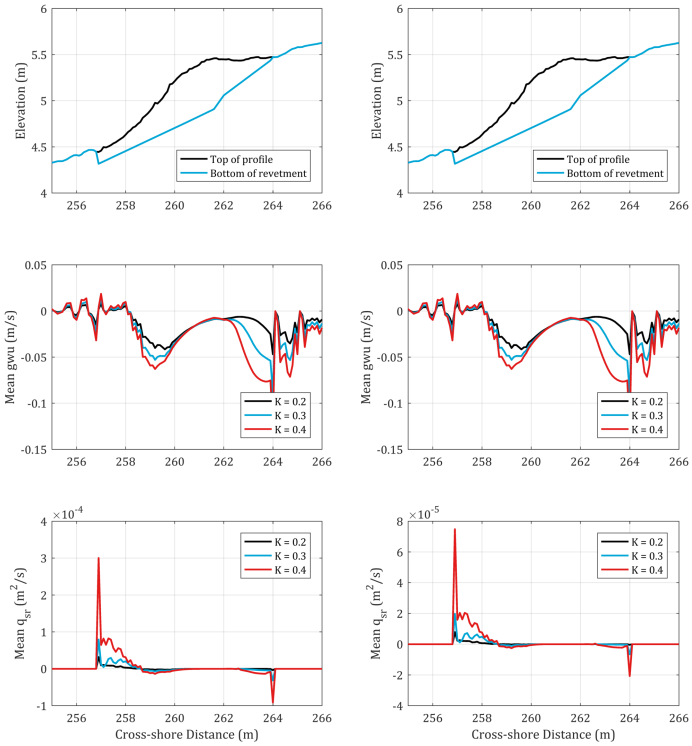

(a) Jacobsen (b) McCall-Van Rijn

Figure 8.3: Sensitivity to hydraulic conductivity K for DR4

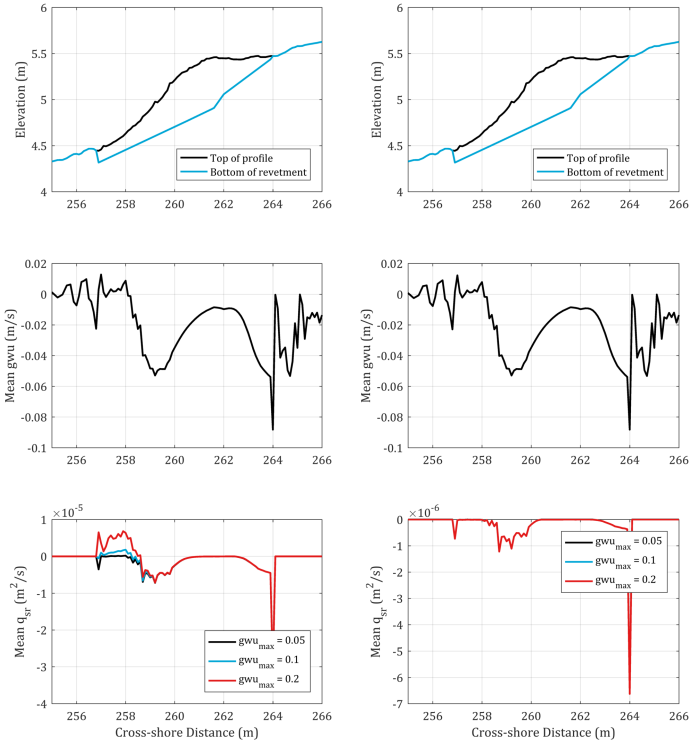

(a) Jacobsen (b) McCall-Van Rijn

Figure 8.4: Sensitivity to gwu_{max} for DR4

0.1 ms^{-1} the onshore transports near the toe of the revetment are even lower, approaching zero. Apparently at the toe of the revetment the transport is dominated by large groundwater velocities.

For McCall-Van Rijn the results look rather different. Compared with the original transports (Figure 8.1b) the onshore transports are no longer present (on average). Apparently the larger velocities that are filtered all contributed to onshore transports. Some offshore transport is still found and this is exact same for the smaller maximum velocities.

The results for DR1 were rather similar as for DR4. For Jacobsen the transport peak due to wave breaking disappeared and now only offshore transport is present. The results with McCall-Van Rijn show only negative transports just as for the results with DR4. With only negative transports the deposition of the eroded sand occurs at the toe of the revetment.

8.4. CONCLUSIONS

The transport formulations show that it is expected that erosion will occur in the revetment, especially for DR4, but also for DR1. Both positive and negative transports are found and there are indications that deposition of sand inside gravel would likely occur. It has been found that the transports are sensitive to the hydraulic conductivity and would change in magnitudes if a maximum groundwater velocity would be defined. Essentially every sensitivity of the transports leads back to the groundwater velocities. It is evident that the impact of wave breaking impact is large. Where wave breaking occurs is then again depending on the water level at the revetment.

In order to model deposition and erosion a coupling to a bed level change must be made in the model. To do so an entire new accounting system must be put in place for XBeach, as this type of erosion is not possible with the current model. This is discussed in the next chapter.

9

TWO-LINE MODELLING IN XBEACH

This chapter introduces a different system for accounting with sediment fractions in XBeach. From the chapters on modelling with multiple fractions and on sand transport in the revetment it was found that the current XBeach model is not able to account for modelling with multiple fractions and erosion/deposition in the revetment. Therefore an experimental model has been proposed and elaborated named the two-line model.

Section 9.1 provides a model introduction and section 9.2 gives an overview of the model runs. The two-line model results for modelling multiple fractions is discussed in section 9.3 and the results for modelling sand transport in the revetment is discussed in section 9.4. Conclusions are made in section 9.5.

9.1. MODEL INTRODUCTION

As has been discussed the current XBeach model defines the bed to consist of multiple layers when modelling multiple fractions. Each layer has a certain thickness and stores information about which fractions are present in these layers, which is expressed in percentages. It has been established that inside the revetment transports occur. This happens inside the model bed, which would be located in the second or third layer (depending on layer thickness) of the vertical composition of the current XBeach model. Applying transport formulations (and therefore transport fluxes) at these layers is not possible. Implementation of these transports would conflict with the current accounting system regarding mass balances and numerical mixing. Adapting it would become unnecessary complex, which is why it has been decided to develop of a fully new accounting system.

The development of the new accounting system was focussed on enabling transport of sand inside the revetment. The model preferably has the following capabilities (which are based on the restrictions XBeach, but also its current capabilities):

- Current sediment transports as implemented in XBeach are still possible
- The XBeach-G transport is introduced
- Allow transports of sand inside revetment (inside gravel)
- Bed levels are updated for sand, gravel, sand underneath gravel and sand inside gravel

A two-line model has been established to allow for all these capabilities to exist. An impression of the two-line model is given in Figure 9.1. The model defines a certain line that describes the elevation of the sand z_s. On top of the sand a layer of gravel that can have a certain thickness z_g. Sand is able to grow through this gravel layer. When this does occur the model registers that a certain $overlap$ between the sand and gravel has occurred. In the model it is also possible that sand fully fills the gravel

and sand is deposited on top of a gravel layer. In that case a certain $counter$ is registered by the model to locally memorise that a buried gravel layer is present.

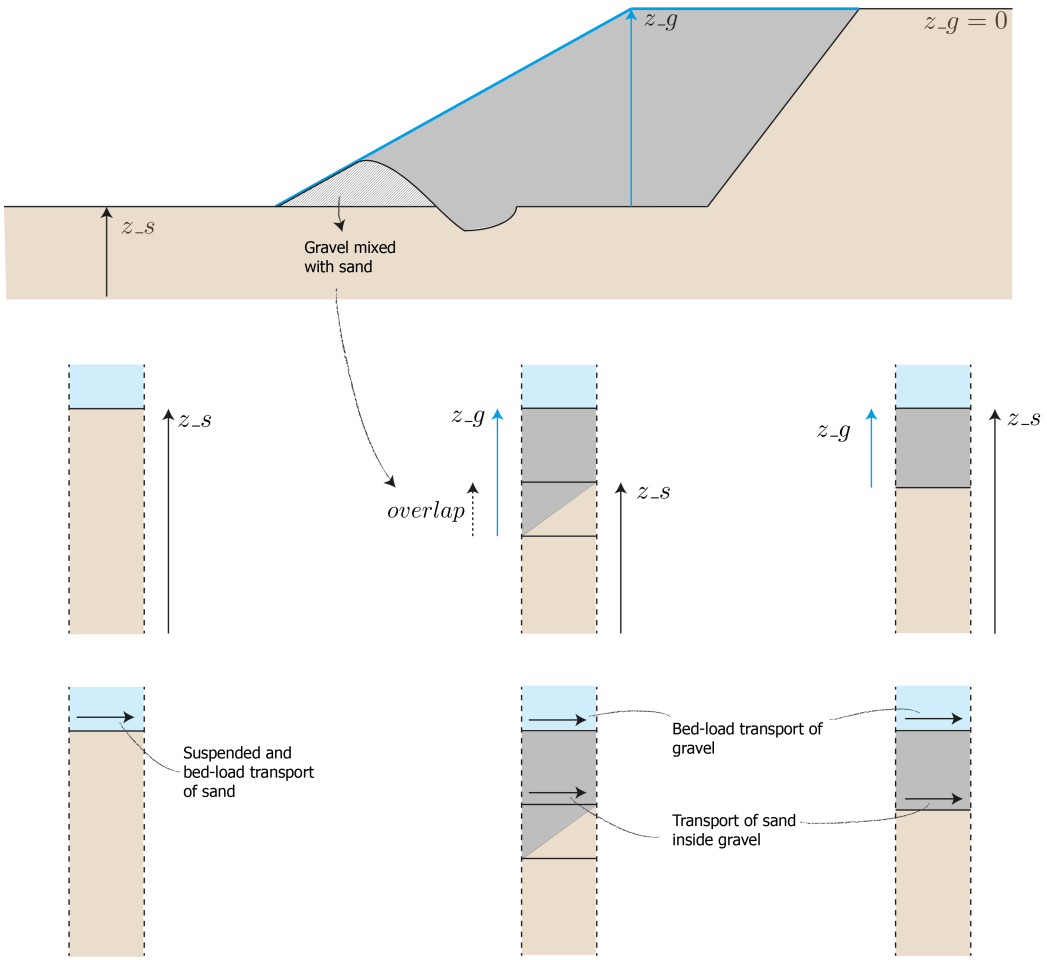

Figure 9.1: Two-line model - Top picture shows a sketch of a gravel revetment on top of sand. In the center the different lines can be seen. At the bottom it can be seen where the transports are imposed.

This model is implemented into XBeach, which enables the model to use the hydrodynamics and groundwater dynamics of XBeach. Furthermore current transport equations from XBeach can theoretically still be used. Because the transition of sand to gravel to sand-filled gravel can easily be defined in the model, transport equations both above gravel and sand as well in gravel can be defined. An additional benefit of the two-line model is that one can use the transition of gravel to sand-filled gravel to define to be the bottom of the groundwater aquifer. This is not possible with the current multi-fractions accounting system of XBeach. The groundwater dynamics of XBeach have been adapted in order to hold the mass continuity.

Figure 9.1 also shows on which interfaces the transports are calculated. It can be seen where normal transport of sand occurs, the bed-load transport of gravel and where the transport of sand occurs within the revetment. From Chapter 8 it was found that the transport of sand inside the revetment was sensitive to high groundwater velocities. Therefore an option has been built into the two-line to give a maximum limit for the horizontal groundwater limit with which the transports are calculated. Both the transport formulations *Jacobsen* and *McCall-Van Rijn* are implemented in the two-line model.

9.1.1. BED LEVEL UPDATES

Two types of bed level updates are used in the two-line model. In the case sand is eroded/accreted in a sandy environment or gravel is eroded/accreted in a gravel environment the basic Exner equation is used (with the respective porosity of sand or gravel):

$$\frac{\partial z}{\partial t} = -\frac{\nabla S}{(1-n_p)} \tag{9.1}$$

Something else occurs when sand is eroded from or is deposited in gravel. It is assumed that the sand fully fills the void between the gravel particles. The sand bed level than following the Exner$^+$ equation:

$$\frac{\partial z_s}{\partial t} = -\frac{\nabla S}{(1-n_{p,sand})} / n_{p,gravel} \tag{9.2}$$

9.1.2. MODEL IMPLEMENTATION

It is of importance to know when different types of transport and therefore different types of bed level updates are used in the model cells. This is done by checking which fractions are located in the top of the bed. If only sand is present, bed-load transport of gravel and bed-load transport of sand in gravel will not be calculated in the model. If gravel is present on top of sand, then bed-load transport of gravel and bed-load transport of sand in gravel are calculated in the model. Additionally no bed-load transport and suspended transport of sand is possible from such a cell. Lastly a transition is possible, where all the transports are calculated. This occurs in cells where gravel is present, but where it is assumed that is too thin to prevent suspended and bed-load transport of sand.

On every grid interface the flux of sand, gravel and sand in gravel is calculated. This is followed by the calculation of the transport gradients in each cell. Here the fluxes of sand and of sand in the gravel are combined in one gradient ∇S_s. The transport gradient of gravel is noted as ∇S_g.

With the transport gradients calculated the bed level updates can be carried out. The first bed level update that is undertaken is that of gravel, followed by that of sand. These steps are quite extensive and are discussed in detail in Appendix F, where other details that are undertaken each time step, such as gradient calculations and identification of types of transport, in the model are discussed.

9.2. MODEL RUNS

As was mentioned in the introduction of this chapter it is in theory possible to run the two-line model with the three different forms of transport. The model is currently not able to run with all these forms of transport turned on without the model exploding. The combination of transport of sand in gravel and sand transport in the water column (bed-load and suspended load) shows to be sensitive. For this thesis it has been decided to split the use of the model into two parts: one for modelling with multiple fractions and one with erosion in the revetment. In the latter the model runs where all the transports turned on is shortly discussed.

All model runs have been executed with the McCall-Van Rijn transport formulation for gravel. Groundwater flow is turned on in the model and all the other settings are the same for as the model runs from previous performance tests.For suspended and bed-load transport of sand and the Van Thiel-Van Rijn equation are used and the McCall-Van Rijn equation for gravel. The model runs had a hydraulic conductivity of 0.3 ms^{-1}.

9.3. RESULTS - MODELLING MULTIPLE FRACTIONS

This section discusses the model results with every type of transport turned on, except the erosion of sand inside the revetment. Two model runs have been done, one for DR1 and one for DR4.

For DR1 the model exploded quite early as can be seen in Figure 9.2. At the location where the model exploded the transition between gravel to sand is present. This location is slightly above the waterline, therefore could experience negative velocities and thus negative transport fluxes. As no sand is entering the cell coming from the gravel cell a large negative transport gradient will likely to occur. This leads to large erosion in a single cell which causes the model to explode. The exact same occurs for model runs with DR4, see Figure 9.3.

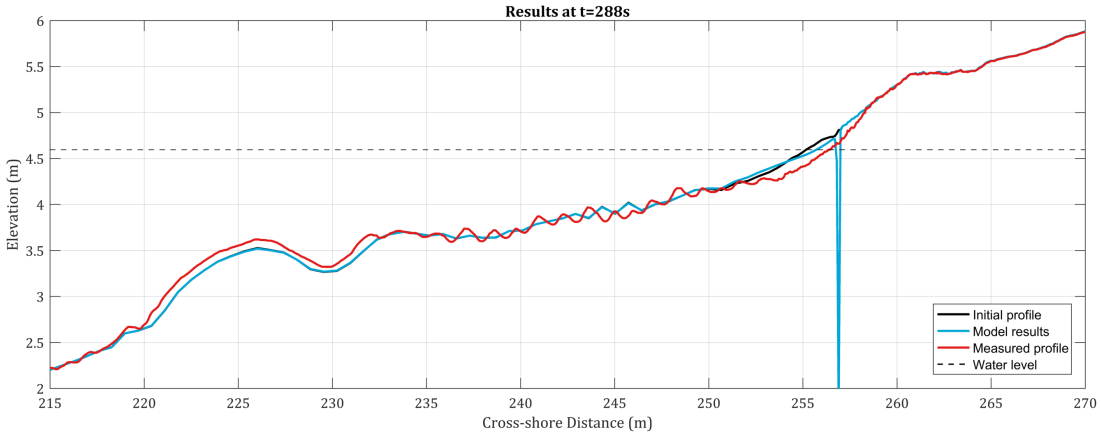

Figure 9.2: Two-line model run DR1 - All types of transport, except erosion in revetment

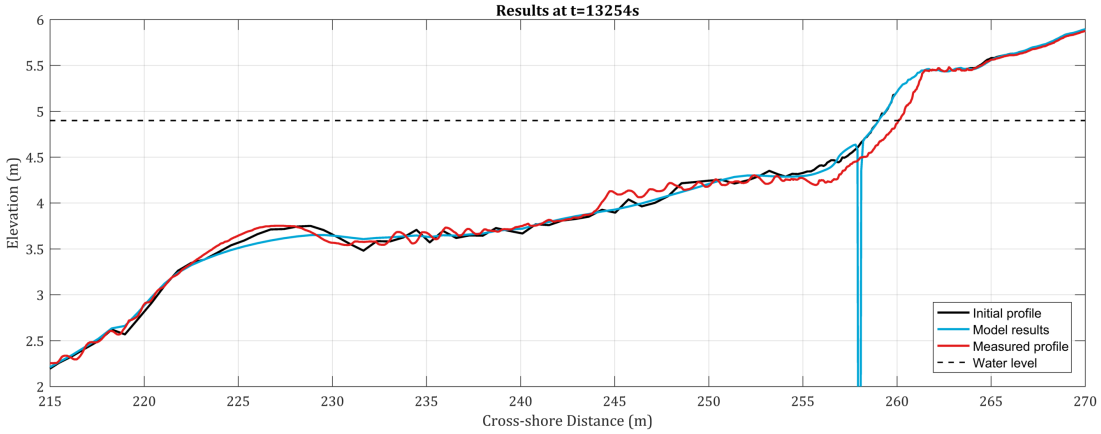

Figure 9.3: Two-line model run DR4 - All types of transport, except erosion in revetment

9.4. RESULTS - EROSION IN REVETMENT

Several models have been run in order to see how the model performs regarding modelling of erosion in the revetment. It was found from Chapter 8 that the hydraulic conductivity and maximum groundwater velocity have a large influence on the transports in the revetment. Therefore model runs for Jacobsen and McCall-Van Rijn with different K's and gwu_{max}'s have been done. This section only discusses the most relevant results, see Table 9.1. An overview of all the model runs is shown in Table F.1 together with the corresponding results. Before the model DR4 crashed it could be observed that sand was filling the toe of the revetment. What causes this accretion is discussed in further detail in section 9.4.3 where this model run has been run including erosion in the revetment.

Test	Reference wave set	Transport equation	K (ms^{-1})	gwu_{max} (ms^{-1})	Comment	Figure
C2	DR1	Jacobsen	0.3	100	-	9.4
C3	DR1	Jacobsen	0.4	100	-	9.5
C8	DR4	Jacobsen	0.3	100	- Failed	9.6
C10	DR4	Jacobsen	0.3	0.05	-	9.7
C19	DR4	McCall-Van Rijn	0.2	100	-	9.8

Table 9.1: Model runs with Jacobsen and McCall-Van Rijn for DR1 and DR4

9.4.1. JACOBSEN

The first model runs to be discussed are the results for Jacobsen for DR1, without a restriction on the maximum groundwater velocity, test C2. In Figure 9.4 one can see in the left panel that the top of the profile has only slightly been lowered. The right panel shows the specifications inside the revetment. Here it can be seen that some sand below the toe of the revetment has been eroded and has mainly deposited in the center op the revetment. A model run with a K of 0.4 ms^{-1} shows that more erosion occurs with higher groundwater velocities, see Figure 9.5 test C3. For the larger K it was also found that more deposition was found at the most outer point of the toe of the revetment. The results confirm the expected deposition of sand in the revetment as was predicted from the chapter on erosion in the revetment. The results with $K = 0.4$ ms^{-1} actually predict the erosion rates quite well, if compared with the measured results. If the erosion of sand in front of the toe would occur and the deposed sand in the toe of revetment would also be able to erode, the results would come close to the results found in the experiment. This also hints that at DR1 erosion might be a cause of lowering of the slope, but also in combination with avalanching due to erosion in front of the revetment.

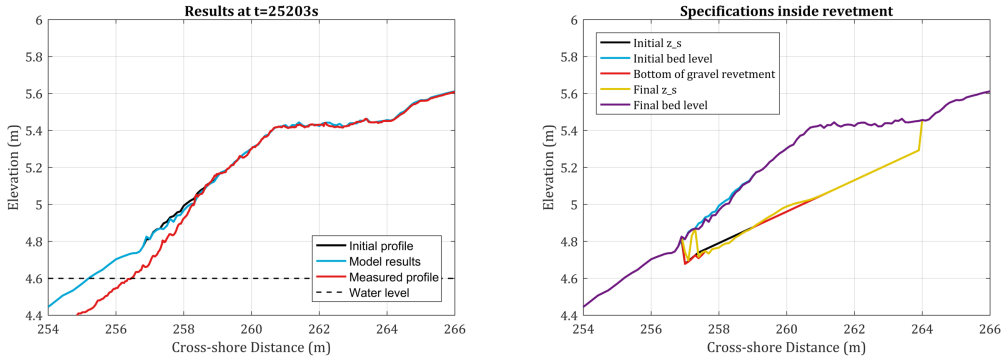

Figure 9.4: Model run C2

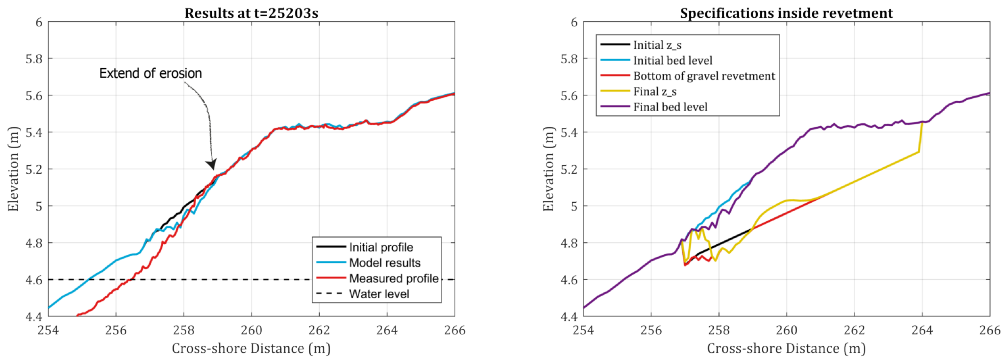

Figure 9.5: Model run C3

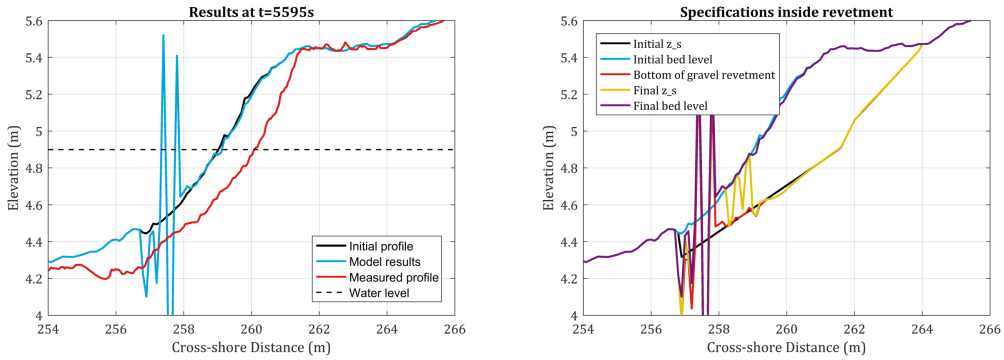

Figure 9.6: Model run C8

Figure 9.6 shows the results for DR4 with Jacobsen with a K of 0.3 ms^{-1} (test C8). The model run failed due to model instabilities, but some interesting developments are seen within the specifications of revetment: erosion of the bottom of the revetment occurs in the center and deposits in between the center and the toe of the revetment. This is also expected to be one of the causes of the model instability: sudden changes in water depth and revetment depths can lead to large surface water variations. This leads to large groundwater velocities which then cause large transports gradient. This is a positive feedback loop. These instabilities also occurred with a smaller or larger hydraulic conductivity.

It is expected that the model instabilities are caused by large groundwater velocities. Therefore a maximum groundwater velocity has been analysed to see how the model reacts while being bound to this maximum velocity. Figure 9.7 shows the results with a maximum groundwater velocity of 0.05 ms^{-1}, for which the model did not explode. At first glance the model results seem to be bad: there is no lowering of the top of the revetment to be seen and the results look a bit shaky. When looking into the results inside the revetment one can observe that almost half of the revetment is now filled with peaks of sand. This sand originates from the bottom of the revetment. It is expected that these peaks are caused by the continuous change of direction of the groundwater velocity at these locations. Furthermore the horizontal groundwater velocities from the groundwater module are dependent on the surface water pressure where cells are wet. This does not lead to smearing of the bed in the revetment, see Appendix F.3 for details.

Also it was expected from Chapter 8 that deposition would occur at this location. On the bright side though the location at which the erosion of the bottom is almost zero corresponds well with the location for which no lowering of the revetment has been found in the experiments, see arrow showing the extend of erosion. Also the sand is deposited up to the top of the gravel where it could easily be mobilised as suspended sediment in the model.

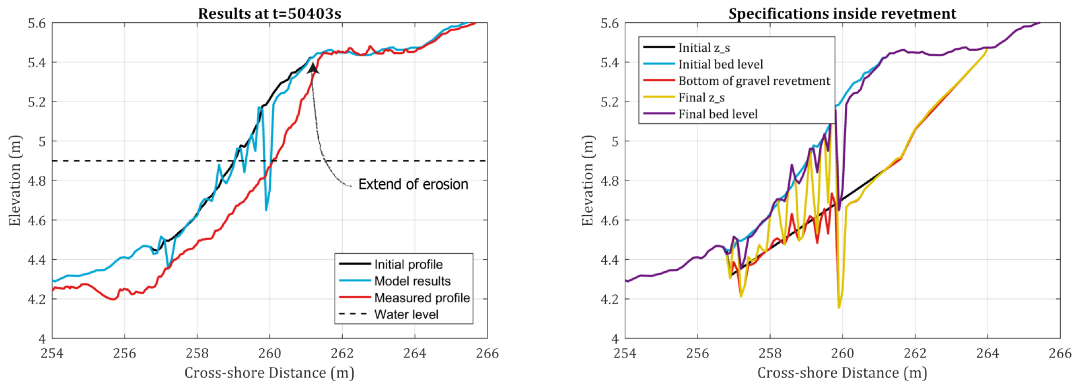

Figure 9.7: Model run C10

9.4.2. MCCALL-VAN RIJN

The results with the McCall-Van Rijn formulation were quite different from those of Jacobsen. For DR1 it has been found that the groundwater velocities were not large enough to mobilise any sand in the revetment. Therefore barely any to no changes in the revetment were observed. For DR4 the model runs did show changes in the revetment, see Figure 9.8. Sand is eroded at the toe and deposited at onshore of the toe inside the revetment. It is suspected that this is due to the absence of significant offshore-directed transports.

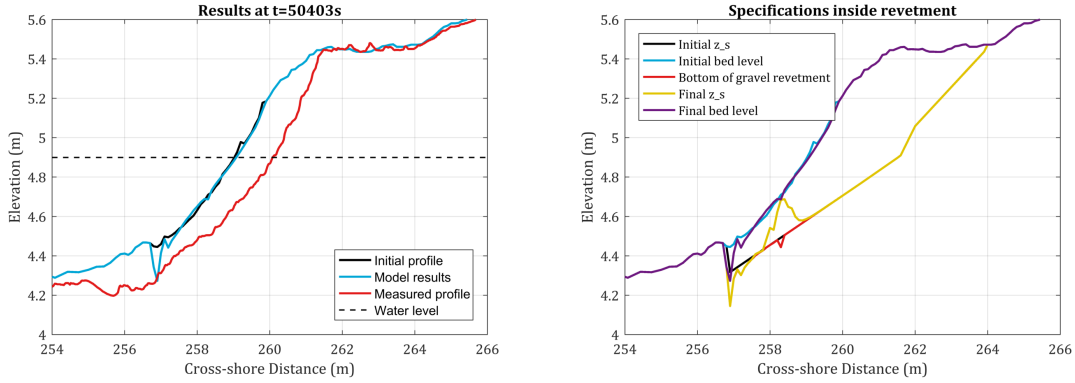

Figure 9.8: Model run C19

9.4.3. RESULTS WITH INCLUDING ALL OTHER TRANSPORTS

Lastly a model run was attempted that included all the possible types of transport: suspended transport of sand, bed-load transport of sand, bed-load transport of gravel and transport of sand inside the revetment. This model run was done with the Jacobsen formulation (as this showed erosion patterns), a K of 0.3 ms^{-1} and a $g w u_{max}$ of 0.05 ms^{-1}.

The results are shown in Figures 9.9 and 9.10. Obviously the model run has exploded due to instabilities at the toe. When taking a closer look it is apparent that suspended sand is deposited on top of the revetment, after which it is converted to sand deposition inside the gravel by the model. This causes the toe of the revetment to quickly fill up therefore the groundwater dynamics change. This can be seen in Figure F.25 where it can also be seen that no instabilities were present only 300 seconds earlier than the final result.

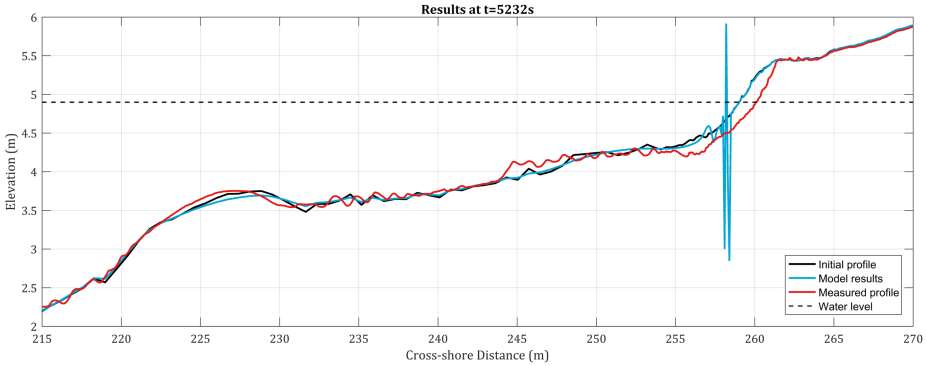

Figure 9.9: Two-line model run DR4 - All types of transport, including erosion in revetment

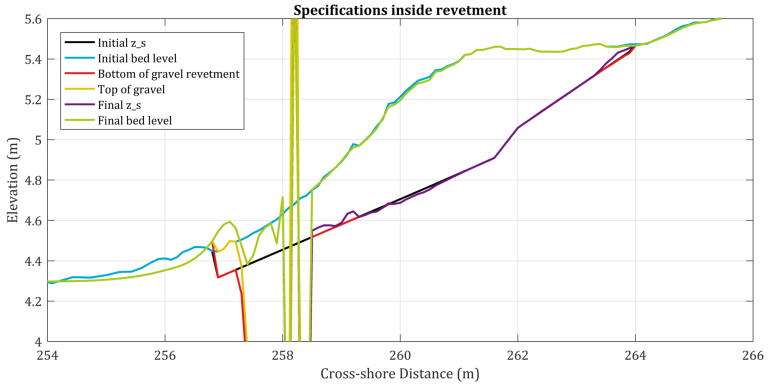

Figure 9.10: Specifications inside revetment - Model runs with all types of transports

9.5. CONCLUSIONS

This chapter introduced a new two-line model that was intended to be able to model with multiple fractions and model erosion of sand inside the revetment. It has been shown that it is (however currently still limited) capable to do so. The sand transports can be modelled within the gravel revetment, allowing erosion and deposition with a new accounting system for XBeach. Sand is able to grow through the gravel and the bottom of the revetment is able to change, allowing groundwater dynamics with a varying bottom. Still several remarks should be made about the current state of the model:

- The two-line model is in its current state not able to correctly model multiple fractions. First of all it currently shows instabilities at the transition of sand to gravel. Furthermore it shows to have the tendency to fill the toe of the revetment with sand, which is not observed in the experiments. It should not be the case that sand is transported towards the revetment. This is most likely due to the exact same problem that caused the problem in Chapter 7 on multi-fraction modelling, namely the coupling of the suspended sediment transport equation to the hydrodynamics. Sand is not expected to be transported onshore near the revetment, but it does in the model. Thirdly, once sand is deposited on top of the gravel it gets sent to interface of sand and gravel, while in reality the sand could very well be deposited on top of the gravel.

- Model runs with all the types of transport turned on were unstable, but the two-line model is a good start for the modelling of multiple fractions. It was already shown in Chapter 7 that the results from modelling with two transport equations came close to the observations, but the elevation changes due to sand erosion from the revetment was a missing piece from the puzzle. This missing piece can now almost be added to the puzzle, but still has some issues. The model shows to be very unstable to erosion volumes and deposition of sand in gravel. Furthermore the deposition does not occur at the expected locations inside the revetment. One can argue whether deposition of sand inside gravel should even occur. It has not been found during the experiments that large volumes of gravel were filled with sand.

10

DISCUSSION

This chapter provides a reflection on the results and models developed in this thesis.

10.1. LIMITATIONS OF THE SAND TRANSPORT EQUATIONS IN GRAVEL AND THE TWO-LINE MODEL

Limitations of transport equation for sand transport under gravel

- The transport equation by Jacobsen et al. (2017) for sand transport in the revetment was intended for use of transport of sand under rocky open filters. This transport formulation has been validated against several data sets. These data sets considered a filter with a D_{n50} of about 0.038 m for the filter material, which is smaller than the gravel stones in the DynaRev experiment. The D_{n50} for the sand core was 0.18 mm. It is unknown to what extent the transport formulation holds for different grain sizes such as the grain sizes used in this thesis.
- The transport equation was implemented in OpenFoam and the flow was solved by means of solving free surface flows with the volume of fluid method (VOF). For solving the groundwater dynamics the Darcy-Forchheimer equations were used, but these dynamics have several uncertainties due to the absence of data to calibrate velocities inside the filter, see Jacobsen et al. (2017). The groundwater dynamics are solved with multiple layers within these filters, whereas this thesis used groundwater dynamics that were solved with a depth-averaged groundwater module.
- In correspondence with an author of the paper (Jacobsen et al., 2017) which published this transport equation it was concluded that the suspended sediment transport should not be neglected for reasons explained in the section on the two-line model. The current bed-load transport formulation is validated to account for transports in reality caused by suspended sediment transports. When introducing a suspended sediment transport within the gravel this means the *Jacobsen* bed-load transport should also be recalibrated (only if bed-load transport inside the revetment is not neglected).
- The McCall-Van Rijn transport equation was investigated to provide an alternative to the Jacobsen equation, but it is intended to be a formulation for sand at the interface between sand and water. Mobilisation of sand is based on the bed shear stress present. This bed shear stress is calculated with the dimensionless friction factor c_f, which is based on the velocity profile present. Normally this c_f is based on a logarithmic velocity profile and in this thesis it has been assumed that between two gravel particles the velocity profile is also logarithmic. This is a rough approximation and can be questioned. Furthermore this transport equation also does not account for suspended transport inside the revetment.

Limitations of two-line model

- The two-line model is currently a very restricted model, thus some remarks can be made about its limitations. First of all the model neglects processes that could be of influence inside the revetment. For sake of simplicity these processes have been neglected for this report, since what goes on such a revetment (or open filter) is highly complex: the transport formulations do not consider different transports for different porosities and no significant relation to turbulence in the revetment is considered (only in the form of a decline in K in the groundwater module). Turbulence was excluded for modelling inside the gravel by Jacobsen et al. (2017), because the velocity profile was found to practically uniform over depth (Stevanato et al., 2010). Still this approach can be questioned, because visual observations at the DynaRev experiments clearly showed that turbulence is very much present at the revetment and simplification to a uniform velocity profile might be an oversimplification. Another missing process is the avalanching of sand inside the revetment. As was mentioned earlier the transport of suspended sediment inside the revetment is also missing. Vertical groundwater velocities are not used or considered in the two-line model, which could contribute to transports of sand from inside the revetment to out of the revetment. In chapter 7 it was mentioned that the adapted model has issues with the suspended sediment transport in combination with the hydrodynamics at the revetment. If suspended sediment transport inside the revetment would be added to the two-line model and the deposited suspended sediment on revetment would be included in the revetment as suspended sediment inside the revetment, the difficulties found in this chapter could be solved. Figure 10.1 gives an impression of how sand could flow through the revetment could flow.
- Currently the Darcy-Forchheimer equation does not take into account inertia as it is assumed to be relatively small compared to the laminar and turbulent terms of the equation. With large velocity gradients the inertia term $\left(\frac{\partial U}{\partial t}\right)$ possibly becomes of more significance and could decrease the large horizontal groundwater velocities. See McCall (2015) for an overview of the extended Darcy-Forchheimer equation.
- The instabilities in the model are caused by a positive feedback loop in the model due to large erosions. These large erosion are caused by large velocities from the groundwater module. The groundwater module is validated by McCall (2015) using a dataset with groundwater head differences retrieved from pressure transmitters. The velocities in the groundwater module due to wave breaking are not validated and their values should therefore be considered with care. Additionally it must be mentioned that the groundwater module works restricted for modelling transports where cells are wet. The groundwater head is depended on the surface water elevation at wet cells and this causes little differences in horizontal groundwater velocities where a revetment depth difference is indeed found. Such a depth difference would in reality cause velocities differences that would lead to smearing of the sand deposition in the revetment.
- The bed level updating system in the two-line model assumes that sand can only leave the revetment by travelling through the gravel towards the water column. In order to do so sand must first be deposited in between the gravel. In reality no significant amounts of sand was found to be buried in between gravel. Thus the sand has left the revetment without significant deposition between gravel and one can argue that the entire deposition in the two-line model is done in a wrong way. Possible this is affiliated with the absence of suspended sediment in the revetment.
- Lastly it must be mentioned that avalanching as implemented in XBeach is turned off in the two-line model. This has also been done because of its complexity regarding implementation with regard to bed updating. It is expected though that avalanching prevents erosion holes in front of the revetment, which is of importance for modelling the DynaRev experiments.

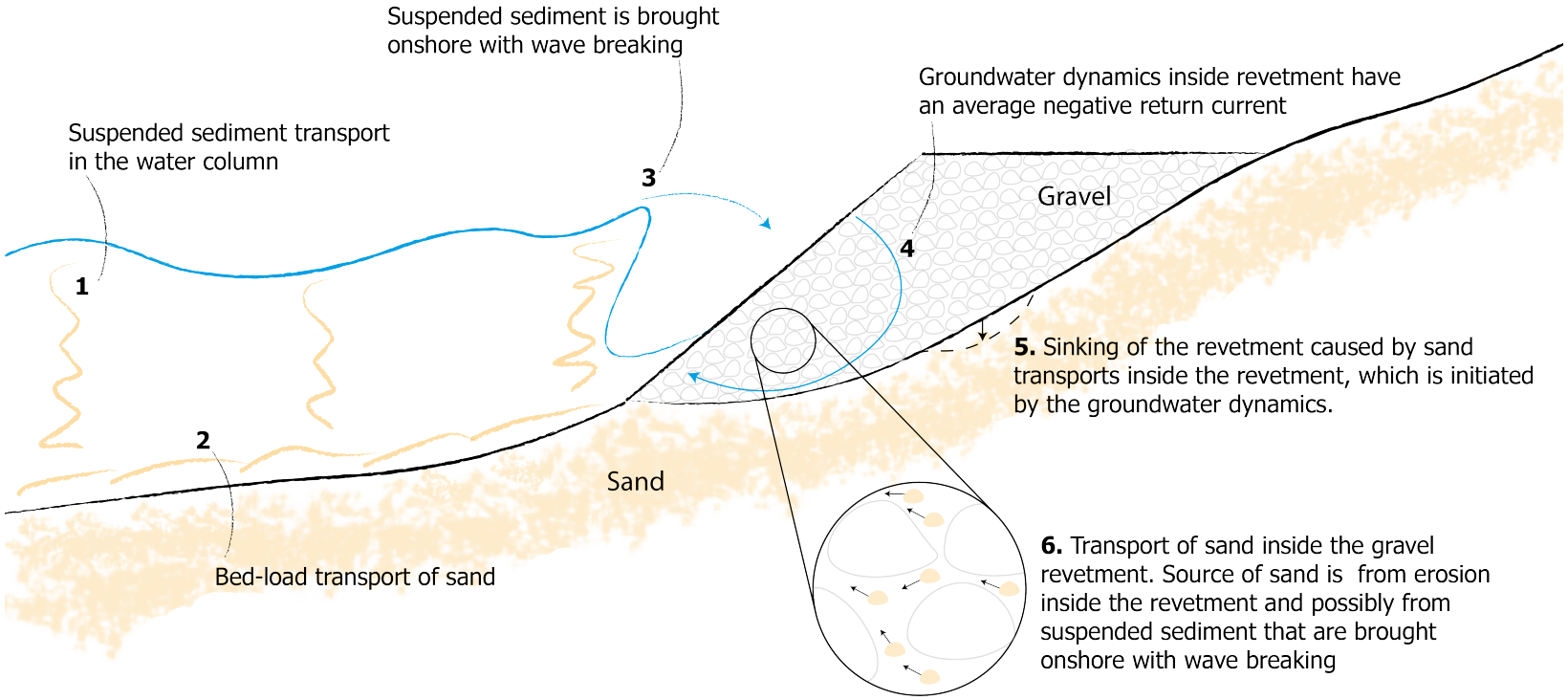

Figure 10.1: Interactions of sand inside the gravel in combination with the hydrodynamics and groundwater dynamics present - The figure does not indicate many other processes/interactions, such as gravel transport, deposition of sand inside the revetment or infiltration/exfiltration.

10.2. DYNAREV AND PRACTICAL IMPLICATIONS OF (ARTIFICIAL) COMPOSITE BEACHES

Research objectives of the DynaRev experiments

The results from all the model tests are compared with the DynaRev experimental results. From the model tests it was found that sand transport inside the revetment is of importance for modelling (artificial) composite beaches. This was concluded because it was observed to be of importance for the DynaRev experiments. During these experiments it was seen that once the water level was increased it triggered erosion in the revetment. The beach (and sand below the revetment) is constantly adapting to these new imposed conditions. The question remains however what happens to the erosion rates once the water level is lowered after some time being high. Possibly erosion in the revetment is not that significant once it has already been eroded for a certain water level. This has not been tested during the DynaRev experiments as these experiments focussed on the influence of sea-level rise on composite beaches. If indeed the erosion rates decrease after a high water level was imposed, one can argue whether erosion of sand in the revetment is only relevant for (extreme) water levels. It would mean that the modelling of multiple fractions would be more important than modelling sand transport inside the revetment for natural composite beaches and well developed artificial composite beaches.

Modelling performances

The performances of the model are partly dependent on the imposed boundary conditions. The imposed boundary conditions for this report are based on the conditions at the wave paddle in the flume and a short validation. More data on the hydrodynamics will become available as the analysis of the DynaRev data by other parties progresses. This could allow for a better validation of the boundary conditions and possible change the results of the performance study. This is not expected to change, as the performance tests showed that the profile development was not very sensitive to differences in wave heights. Still it would contribute to the foundation of the performance study and would allow a good assessment of the runup and overwash events on artificial composite beaches.

Practical implementation of artificial composite beaches

The practical implementation of artificial composite beaches is out of the scope of this research, but some comments are worth mentioning. A first comment to be made is that gravel could easily be buried by sand. Imagine a gravel revetment with a distinct interface between gravel and sand. In storm conditions it could occur that sand is eroded from underneath the revetment. This causes sinking of the revetment. In mild conditions it could occur that sand brought onshore and deposits on the revetment. When this occurs sand will most likely mix with gravel. It is very unlikely that sand is deposited under the revetment and pushes the revetment back up. This process of erosion and deposition could in time affect the functionality of the revetment. The revetment is functional because of its ability to dissipate energy through groundwater processes. This is undermined if sand mixes with gravel, reducing the dissipation. This does show how important it is to be able to give an estimation of when erosion of sand from the revetment occurs as this could re-introduce groundwater flow once the sand is separated from the gravel.

A similar process could occur due to aeolian transport of sand. It has been found at cobble beaches that sand can infiltrate the cobbles. This also undermines the ability of the revetment to dissipate wave energy through groundwater processes.

10.3. USE OF MODEL IN FUTURE RESEARCHES

This section discusses two cases that are of interest with respect to future researches. It was mentioned in the introduction of this thesis that this study also had the intent of gaining knowledge into sand-gravel interactions. The following cases are practical examples that could show what type of interactions might be of interest for future studies in combination with what was found in this thesis.

Case 1: Gravel pockets on a composite/sandy tidal beach

This case is on the placement of gravel pockets on sandy or composite tidal beaches. It has occurred that a vessel had to beach on the sandy slope of the beach due to tidal fluctuations. This vessel was a cable-laying vessel, for which it needs to be close to land. On a sand slope this beaching would normally be possible, but in this occasion large boulders were present on the beach. These boulders could harm the hull of the vessel. The placement of large gravel pockets on the sandy beach was proposed as a beaching location for the vessel. These pockets should maintain their position for a few months after which they would not be of any more use. A tool that could predict how large the fraction size of these gravel stones would have to be and how long the pockets stay stable is desired and is not present at the moment.

With the results of the current study one can say several things about the use of the two-line model for such a case. The two-line model is in theory able to model with multiple sediments and even transport of sand under gravel. Still modelling with multiple sediments and of sand transport in gravel has been done with the focus on the swash for this thesis. At tidal beaches these gravel pockets will experience deeper water. XBeach itself is already known to have issues with larger water depths. Therefore it can be expected that modelling of multiple fractions and of erosion in gravel will encounter difficulties.

For this case the following aspects should also be considered:

- *Influence of different gravel fractions*:
  For the case it is of importance to know what grain size of gravel is needed to create stable beach pockets. Therefore effect of different grain sizes on the stability of these pockets could be of interest. Additionally the gravel transport equations should ideally be validated for a wide range of gravel grain sizes.
- *Maximum grain size of gravel for which the gravel transport formulations are valid*:
  Possibly cobbles could be used for these pockets instead of gravel stones. The gravel transport formulation is not developed for cobble stones, but possibly it could perform well.

Case 2: Temporary scour protection with use of gravel

Consider the placement of a temporary bund inside a harbour which protects an excavated area behind the bund from flooding. This bund can be created using sand or if possible using the excavated material. The bund should be able to withstand erosion from wind waves, waves generated by vessels and sea waves penetrating the harbour. An easy erosion mitigation measure is simple placing more sand, but it could be beneficial to place gravel on top of sand. This reduces the amount of material needed to build the bund and therefore reduce costs.

A case like this has resemblance to the scope of this thesis, as placing gravel on a sandy slope can be considered to be an artificial composite beach. From the DynaRev experiments it was found that a sandy beach does erode quicker than a beach with a gravel revetment, thus such a beach for prevention of erosion has potential. The question remains however how different grain sizes of gravel perform, as was also the question for the first case. Additionally for this case one can wonder how great the influence of grading differences between are gravel and sand. If excavated material containing gravel is placed it is likely to also contain sand. Mixed-sand-gravel acts different from sand and gravel. Hiding and exposure become more important and groundwater dynamics change. Therefore it must be identified when a medium can be considered to be a mixed medium.

11

CONCLUSIONS

The main research question to be answered in this thesis was to what extent the morphological developments of the artificial beach of the DynaRev experiments could be modelled with a numerical model. This chapter is dedicated to answering this research question. First the four sub-questions are discussed after which a general conclusion can be made regarding the main research question.

Current performance of modelling artificial composite beaches

The current models XBeach and XBeach-G that are used to respectively model sand and gravel beaches have been tested in chapter 5 for their performances regarding the modelling of composite beaches. The model runs were simplified in order to replicate the existing profiles of the DynaRev experiments. Simplifications included assumptions that gravel was immobile in XBeach and sand was immobile in XBeach-G. These simplifications and general limitations of XBeach and XBeach-G have shown that both XBeach and XBeach-G are not able to provide model results similar to those observed during the DynaRev experiments.

Current limitations of XBeach and XBeach-G regarding modelling of composite beaches and processes to be added and adapted in XBeach

In chapter 6 the current limitations of the numerical models regarding composite beaches have been discussed. Information gathered from the literature study, an analysis of the DynaRev experiments and the performance tests identified two main processes missing in the current models.

- A differentiation between gravel and sand transport formulations is lacking in the models. In storm conditions it is expected that sand is transported offshore, while gravel transport is expected to be directed onshore. This is not possible with the current models. Only a single type of transport formulation can be used in XBeach and XBeach-G, which prohibits a combination of a transport formulation for sand and a transport formulation for gravel.
- The second process that is missing in the current models is the transport of sand inside the revetment. From observations during the DynaRev experiments it was seen that the revetment sinks, while it does not lose mass of gravel stones indicating that sand is leaving the revetment. Furthermore profile measurements showed that the bottom of the revetment had indeed been eroded. This transport of sand inside the revetment is not implemented in XBeach or XBeach-G. From the experimental results it is unsure whether sand transport inside the revetment is always present during wave action or if it is only significant until the sand profile below the revetment has reached a certain equilibrium. It is clear though that this transport is very likely to occur when placing gravel on a sandy slope, as is the case when constructing artificial composite beaches.
- Several other limitations of the current models were identified. Armoring, hiding and exposure are processes that could be of influence for modelling of composite beaches. These processes

are all typical for beach profiles containing multiple fractions, but are not considered in the report as they are assumed negligible compared to the two identified missing processes. These two identified processes (modelling of multiple fractions and sand transport inside the revetment) significantly influence the morphological changes in the profile.

Contribution of additional processes to performances of the model

The addition of two processes to the model and their performances have been assessed, namely the inclusion of gravel transport to XBeach and addition of transport of sand inside the revetment. Lastly a two-line model has been established that introduces a new accounting system for fractions in XBeach.

- Introducing the first process to XBeach showed to be rather promising. It was able to model with two transport formulations and some morphological developments match well, such as the elevation and slope of the sand in front of the revetment and the slope of the revetment for DR1. The adapted model encountered difficulties with coupling between the hydrodynamics with the groundwater module and transport of suspended sand.
- The second process of transport of sand inside the revetment was investigated by coupling transport to retrieved time series of groundwater velocities. When introduced, the transport equations showed that transport inside the revetment is indeed to be expected. The transport equations are still sensitive to the groundwater velocities of the model, which can get very large due to wave breaking.
- A two-line model was introduced that could model suspended and bed-load transport of sand, bed-load transport of gravel and bed-load transport of sand inside the revetment. This two-line model replaced the old accounting system of XBeach, which was not able to model transports of sand inside the revetment, whereas the two-line model can. Even though the two-line model is only just in development is has shown promising results: sand transport inside the revetment is modelled and these transports are translated into erosion and deposition in the revetment, which is done with a different bed level updating system. The two-line model does show some forms of instabilities. For modelling with multiple fractions it shows instabilities on the sudden transition from sand to gravel. Inside the revetment the model is sensitive to the accumulation of sand which changes the groundwater dynamics. This causes large velocities and thus large erosion magnitudes leading to the model instabilities. When combining multi-fraction modelling and erosion in the revetment the same instabilities were present. Once the instabilities are resolved it is expected to perform better than the current XBeach model, but the current form of bed level updating and types of transport inside the revetment are questioned: suspended transport of sand inside the revetment is not present in the model, but might physically occur inside the revetment. Furthermore no vertical groundwater velocities are used in transports and could possibly influence the transport flux directions.

Modelling the morphological developments of the artificial beach of the DynaRev experiment

The focus for modelling the morphological developments of the artificial beach of the DynaRev was on the development of the revetment and in front of the revetment. Developments in slopes and elevation were assessed throughout this thesis. Current models performed well in what they were designed to do: XBeach showed to perform well in modelling the sandy developments in front of the revetment and XBeach-G showed to correctly model the slope of the revetment. However, the models did not perform well regarding modelling of the developments in front of revetment and at the revetment at the same time. Furthermore the models are not able to model sand transport inside the revetment. The addition of the gravel transport formulation to XBeach showed better results, but still the modelling with sand transport inside the revetment was missing. A new two-line model was introduced with a new accounting system for fractions in XBeach. This was shown to be able to model sand transport inside the revetment. It has opened opportunities for modelling with sand and gravel and introduced new perspectives regarding the complexity of modelling with sand and gravel. Currently the two-line model is still development and does show instabilities. Even when these instabilities would be resolved, it could be argued whether a realistic coupling between transport of sand inside gravel and the hydrodynamics is missing.

12

RECOMMENDATIONS

This chapter discusses the recommendations that follow from the research. First some recommendations are provided that could contribute to increase the knowledge on what happens at artificial composite beaches, with the focus on the revetment. Thereafter some more general recommendations are made.

- Adding suspended sediment to the two-line model could contribute to understanding what happens within the revetment. This would also imply recalibration of the bed-load transport formulation for sand in the revetment. It is recommended to first introduce simple suspended sediment transports in order to analyse what happens when coupled to groundwater velocities.
- It is recommended to explore the use of the vertical groundwater velocity in transport formulations. Possibly it could be used in combination with the horizontal groundwater velocity as the absolute velocity. This could enable the exfiltration of sand out of the gravel. It would also imply a recalibration of the Jacobsen transport equation. Additionally it could be of interest to introduce multiple layers for modelling the groundwater dynamics within the revetment, which could contribute to more accurate groundwater dynamics.
- Apparently sand does not necessary leave an open filter, which was evident from the results as shown by Jacobsen et al. (2017). Possibly this is due to the fact that the filter stones are not large enough for sand to easily be transported through its pores by any form of transport other than bed-load transport. There will most probably be a certain range of a grading ratio for which this holds, Mutlu Sumer et al. (2001) provided some interesting insights regarding this ratio. Small scale experiments with different fraction ratios could be conducted in order to establish with which ratios erosion out of the filter is significant. This could then also show whether artificial beach can possibly be expected to exhibit significant sinking due to erosion.
- For these open filters the two-line model could to be able to show erosion and deposition. Data sets are present (van Gent and Wolters, 2015) that could validate the newly added accounting system of the two-line model and the *Jacobsen* transport equation for XBeach. These data sets have been used to establish the *Jacobsen* transport formulation. For these data sets it is known that sand does not leave the gravel matrix, whereas this is observed for the DynaRev experiment.
- It was found that XBeachX with the addition of the gravel transport formulation worked well, with the exception of modelling suspended sediment transport. This was caused due to the change in hydrodynamics with the groundwater module. It is unknown what happens to the sand particles that are deposited on top of the gravel. Experiments with coloured sand particles could potentially indicate where they settle. Furthermore it would be of interest what the velocities are inside and on top of the revetment and whether model can be validated with these velocities. A technology that allow measuring these velocities is currently not present. Measuring velocities is a complicated practice, especially within gravel (which is why (McCall, 2015) validated the groundwater dynamics with pressure transmitters).

- A study on the development of the sand bottom below the revetment could increase the knowledge on artificial composite beaches. In an experiment one could impose the same revetment to different water levels. This should ideally be done with a long run period, such that a equilibrium profile below the gravel could possibly develop. This would give insight into how long artificial composite beaches show significant erosion of sand from under the gravel. Experiments are costly and time intensive, thus before new experiments are conducted it is of importance to assess which conditions are of highest interest to be studied. Possibly small-scale experiments like the experiments by van Gent and Wolters (2015) are sufficient enough to demonstrate these developments. Once more it should here be considered that grading differences between the sand and gravel could be of influence as small-scale experiments involve the scaling of the sediments.

Additional recommendations that could improve the current results are:

- The non-hydrostatic mode of XBeach has not yet been fully validated for the transport of sand, as has been mentioned in this report. Future work on validation of this mode contributes to getting the developments just below the swash correct.
- As was mentioned in the discussion more data on the hydrodynamics will become available as the analysis of the DynaRev data by other parties progresses. It is recommended to re-validate the hydrodynamics of this thesis to assure that the morphological results of the models performances are not affected by setup errors in the hydrodynamics.

Lastly some recommendations are provided that are of interest regarding research on sand, gravel or sand-gravel interactions:

- The composite beaches as described by Allan et al. (2005) had gravel stones with varying grain sizes from 30 mm to 128 mm. The largest classified grain size of gravel is 64 mm. Values between 64 and 128 mm are considered cobbles. The transport formulation of gravel is not designed for cobbles and therefore XBeach(-G) can not be used for cobble beaches. However the limits of the gravel transport formulation are not known, possible they hold for small cobbles. A functioning transport formulation for cobbles in XBeach could be valuable as soft to hard transitions are common in practise. It is therefore advised to investigate the limits of the gravel transport equation.
- The DynaRev experiments consisted of a comparison of the performance of a sandy beach and an artificial composite beach with respect to sea-level rise. It has been observed that the erosion rates for the artificial beach were lower compared to the sandy beach. It would be of interest to look into these different erosion rates. Does the artificial beach also perform well compared to the sandy beach despite the erosion of sand from the revetment? How well does it prevent run-up compared to sandy beaches? Potentially it could show once more that artificial composite beaches are excellent alternatives to sandy beaches. Lastly if artificial beaches are shown to perform well, an assessment of feasibility of the construction of such a beach could be made (availability of gravel, costs of placement and maintenance).
- Possibly the erosion of sand from the revetment can be prevented by adding a filter layer between the revetment and sandy beach. This filter layer could prevent the escape of sand and therefore the sinking of the revetment. An assessment can be made with filter rules whether prevention of erosion could be possible. This would make the construction of such an artificial composite beach complexer and less interesting as a shore protection measure as one of its advantages was easy placement and maintenance of the structure.

A

LITERATURE

A.1. BEACH CHARACTERISTIC PROCESSES

This section shortly introduces some of the main characteristics that are present near and at coastal regions. Some terminology of beaches is provided and several types of gravel beaches that are of importance are classified.

A.1.1. BEACH TERMINOLOGY

Some typical features from a beach profile are visualised in figure A.1 which is established by US Army Corps of Engineers (2002) and adapted by De Vet (2014).

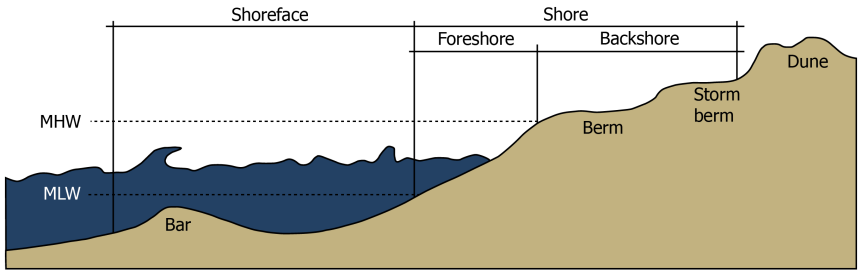

Figure A.1: Terminology coastal region ((De Vet, 2014),(US Army Corps of Engineers, 2002))

In section 2.1.1 some coastal profiles are introduced that differ from the one depicted above, but the definitions of these beaches are still the same. The tidal water levels are shown as *MHW* and *MLW*, respectively mean high water and mean low water. The *shoreface* reaches from the MLW to the offshore, the *foreshore* is the area of the profile between MHW and MLW where all the intertidal wave action takes place and the *backshore* is extends from the dune to the MHW level.

A.1.2. HYDRO- AND MORPHODYNAMICS

The hydrodynamics describe, as the word itself already suggests, the dynamics of water. Near the coasts the so called non-linear shallow water equations (NLSW) are used to calculate the movement of water. These equations are discussed in section 3.1. The hydrodynamics include many different types of waves. In section A.1.1 these waves are described by the way they break on beaches, but the waves themselves can be characterised by their period or wave length. The longest waves considered in this thesis are the infra-gravity waves. These long waves are formed by groups of wind-generated waves (Holthuijsen, 2007). Shorter waves discussed in this thesis are the wind-generated waves, which have

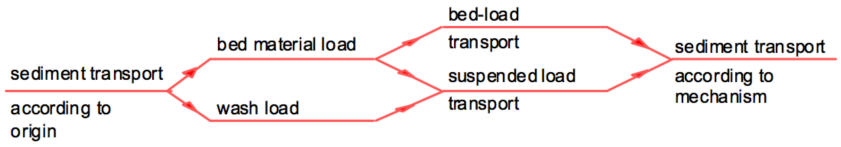

Figure A.2: Classification of sediment transport (Zanen et al., 1994) - The scope of this thesis is on both suspended and bed-load transport. Wash load is not included in the suspended transport as it is not of significance and is not included in the used process-based models.

wave period shorter than 30 seconds. Many different other types of waves exist, such as tides, swells or seiches. Information about these waves is well described by Holthuijsen (2007).

The morphodynamics are the descriptions of the dynamics of the sediments. The transportation of sediment is highly complex. This is caused by the nature of flow, which is a two-phase flow (liquid and solid phase), and the interaction between both phases: flow → transport of bed material → development of bed forms (ripples, dunes, depth changes) → influence on water motion and sediment transport (Vriend et al., 2011). Several sediment transport modes are classified and are specified in figure A.2. Whether a certain particle exhibits bed load transport or suspended transport depends largely on the flow it is exerted to, but also on density and grain size. The transport modes are further elaborated in section 2.2.4.1.

Silt, sand and gravel behave differently from one another. The classification for different types of grains can be done with the so called Wentworth scale, see figure A.6. Here gravel is named *pebbles* and has a grain size between 2 to 64 mm. In transport formulations these grain sizes can be formulated in different ways. With a sieve a median sieve size D_{50} can be found. The 50 stands for the fact that cumulatively 50% of the total grains have passed through the sieve. Another formulation typically used for grain size is the median nominal grain size D_{n50}. This variable assumes the grain to be a cube and can be calculated from its mass and density. D_{50} is found to be about 20% larger than D_{n50} for the same grain (Schiereck, 2001).

A.1.3. GRAVEL BEACH CLASSIFICATIONS

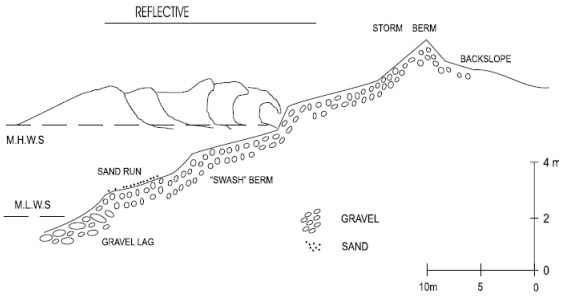

Figure A.3: Representation of a pure gravel beach (Jennings and Shulmeister, 2002)

A.2. BEACH CHARACTERISTICS

A.2.1. IRIBARREN NUMBER

Different kind of beach slopes have effect on the breaking of waves on the beaches. Most often the Iribarren number is used to identify different breaker types, which Battjes (1974) defined to be:

$$\xi = \frac{\tan\beta}{\sqrt{\frac{H_0}{L_0}}} \tag{A.1}$$

In which $\tan\beta$ describes the slope of the beach, H_0 is the deep water wave height and L_0 is the deep water wave length.

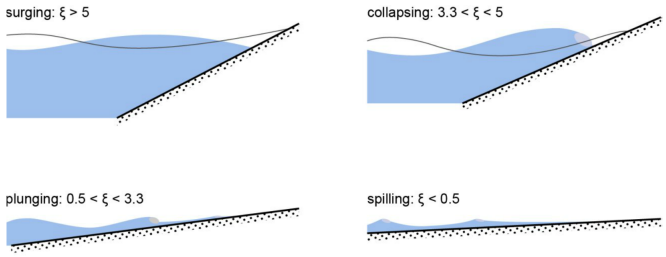

Figure A.5: Breaker types (Bosboom and Stive, 2015)

As can be seen in figure A.5 steep and reflective beaches often have high Iribarren numbers, while mild and dissipative beaches often have low Iribarren numbers. It must be noted that this is all relative. For waves with a large wave length a mild slope could be experienced to be rather steep. A beach that has a ξ of 0.05 for wind waves could have a large ξ for tidal waves (Bosboom and Stive, 2015).

A.2.2. HYDRAULIC CONDUCTIVITY OF SEDIMENTS

She et al. (2006) have done research on the porosity and hydraulic conductivity of mixed-sand-gravel sediments and have used the definitions *under-filled*, *fully-filled* and *over-filled*. A sediment mix is over-filled when there is more sand required to fill up the gravel pore space, under-filled when the sand fraction is not enough to fill the pore space between the gravel particles and fully-filled is a transitional zone between the under-filled and fully-filled stages. The fully-filled stage is called the critical point as for this stage the bulk volume of the sand is equal to that of the gravel pore space (She et al., 2006).

$$\begin{cases} K = K_g(1-\xi)^2 + K_s n_g \xi & \text{for } \lambda \le \lambda_c \\ K = \frac{K_s \lambda}{\lambda + (1-n_s)(1-\lambda)} & \text{for } \lambda \ge \lambda_c \end{cases} \tag{A.2}$$

In which K_g is the hydraulic conductivity of pure gravel, K_s is the hydraulic conductivity of pure sand, n_g is the porosity of pure gravel and n_s is the porosity of pure sand. Furthermore λ is the percentage of sand by weight and its critical value λ_c is defined to be:

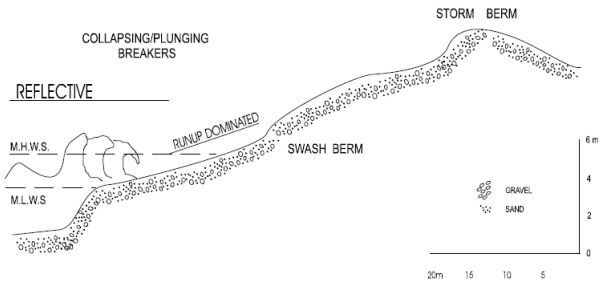

Figure A.4: Representation of a MSG beach (Jennings and Shulmeister, 2002)

$$\frac{n_g(1-n_s)}{1-n_g n_s} \tag{A.3}$$

Lastly ξ is derived by She et al. (2006)1 to be:

$$\xi = \frac{(1-n_g)\lambda}{n_g(1-n_s)(1-\lambda)} \tag{A.4}$$

Mason et al. (1997) discussed that the modelling of the groundwater table was successful using a single value for the hydraulic conductivity for medium sand. This suggests that the main impact of gravel upper beach in combination with a sandy lower beach is not the groundwater behaviour, but that the beach gradient is larger importance.

A.3. PROCESS-BASED MODELLING

A.3.1. NON-LINEAR SHALLOW WATER EQUATIONS

The depth-averaged dynamic pressure term that is used in XBeach is described by McCall (2015) and the application of $\bar{q}$ is validated for the model. Values are found by computing the mean of the dynamic pressure at the surface and the bottom. The dynamic pressures at these locations follow from changes of bed elevation and subsequently vertical current velocities. The equations that enable the computation of $\bar{q}$ are:

$$\frac{\partial w_s}{\partial t} = 2\frac{q_b}{h} - \frac{\partial w_b}{\partial t} \tag{A.5}$$

$$\frac{\partial u}{\partial x} + \frac{w_s - w_b}{h} = 0 \tag{A.6}$$

Equation A.5 describes the vertical momentum balance at the surface and Equation A.6 describes the local continuity equation.

A.3.2. EULERIAN AND LANGRANGIAN VELOCITIES

Two frames of references can be distinguished for flow, namely *Eulerian* and *Lagrangian* flow. Eulerian flow is flow measured from a fixed point in space as time passes. An example is the velocity as derived from a pressure meter fixed on the bottom of the ocean. Lagrangian flow is the flow as measured while following a particle as it moves through space and time.

In surfbeat mode of XBeach mode the Lagrangian flow velocity u^L is found by adding the Stokes drift to the Eulerian flow velocity found on the grid:

$$u^L = u^E + u^S \tag{A.7}$$

u^S can be retrieved from a simple equation using the wave-action balance, namely:

$$u^S = \frac{E_w}{\rho h c} \tag{A.8}$$

For the advection-diffusion equation the Eulerian flow velocity is used in order to account for a strong undertow. Because the non-hydrostatic mode does not solve the wave-action balance the Stokes drift

is not resolved (the non-hydrostatic mode includes this drift in the intra-wave velocity). Therefore the Lagrangian flow velocity is stored as the Eulerian flow velocity in the model and in case the Eulerian flow velocity is used this velocity is the same of the Lagrangian flow velocity. This means only one flow velocity is present in the non-hydrostatic mode.

A.4. FIGURES

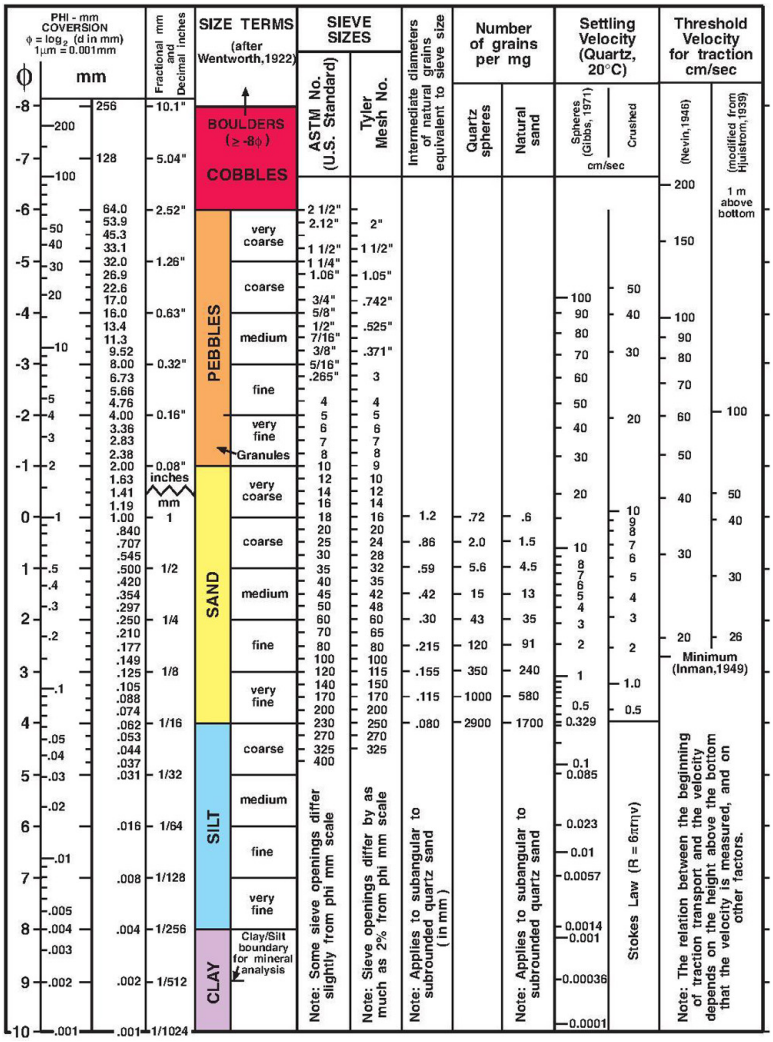

Figure A.6: Wentworth grade scale (USGS, 2006)

B

DynaRev Observations

B.1. Overview and observations DynaRev - Sand

The imposed sets of waves on the sandy beach vary in intensity and have different wave heights, see Table B.1. From set SB0 to set SB4 the water level rose by 0.1 m per set in order to study the effects of sea level rise. After raising the water level some resilience tests have been performed, see wave set SBE1 and SBE2. Initially it was planned to increase the wave height up to 1.3 meters, but this overheated the wave paddle. Therefore only two resilience tests were performed. Lastly a set of waves used to stimulate accretion was imposed on the beach, namely set SBA1.

Wave set	Profiles	H_s (m)	T_p (s)	Water level (m)	Duration (s)
SB0	SB0_1 - SB0_15	0.8	6	4.5	72000
SB1	SB1_1 - SB1_9	0.8	6	4.6	25200
SB2	SB2_1 - SB2_9	0.8	6	4.7	25200
SB3	SB3_1 - SB3_9	0.8	6	4.8	25200
SB4	SB4_1 - SB4_9	0.8	6	4.9	61200
SBE1	SBE1_1 - SBE1_3	1.0	7	4.9	7200
SBE2	SBE2_1 - SBE2_5	1.2	8	4.9	14400
SBA1	SBA1_1 - SBA1_8	0.6	12	4.9	21600

Table B.1: *DynaRev - Sand* wave sets - During each set multiple profiles have been measured in order to evaluate the dynamics of the profile

The observations made during the experiments are shown in figure B.1a and B.1b. The first figure shows the development of the profiles from wave sets SB0 to SB4 and the second figure are the profile developments of the erosion/accretion wave sets SBE1 to SBA1.

After the first wave set it can be seen that the planar beach reformed quite severely. An offshore bar had developed and onshore erosion had occurred. During the first wave set the offshore bar slowly retreated offshore and the shore erosion seemed to reach an equilibrium. Detailed figures of offshore retreating bar and shore erosion can be found in Appendix B. After the first wave set SB0 the water level was raised for each new wave set. Figure B.1a shows that the shore erosion increased with the rising of the water level. The offshore bar had grown in size, but stayed more or less at the same location. In between the shore and bar it can be seen that the beach slope had flattened in comparison with the original slope of 1 : 15.

With the resilience testing (SBE1 and SBE2) the onshore erosion continued, as can be seen in figure B.1b. The offshore bar seemed to decrease in size and move a bit further offshore. The last wave set SBA1 was intended to stimulate accretion, which seems to have worked. The offshore bar seems to

have been eroded and the sediments seem to have deposited in between the shore and bar. In a zoomed view of the shore in figure B.1c it can be seen that accretion above the water level had occurred.

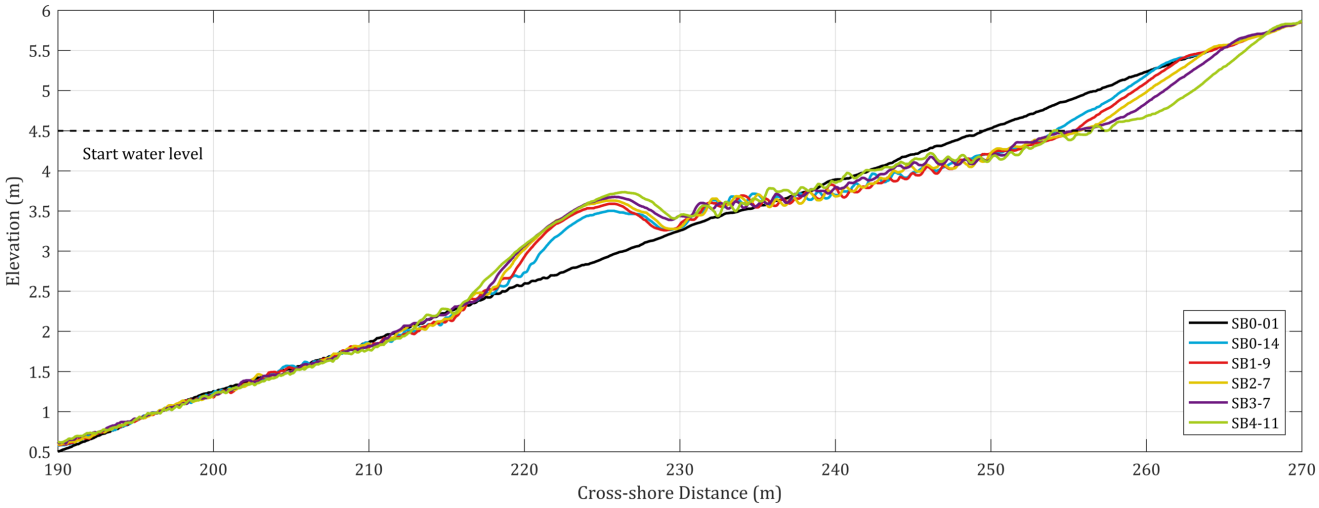

(a) Observed changes between SB0 and SB4

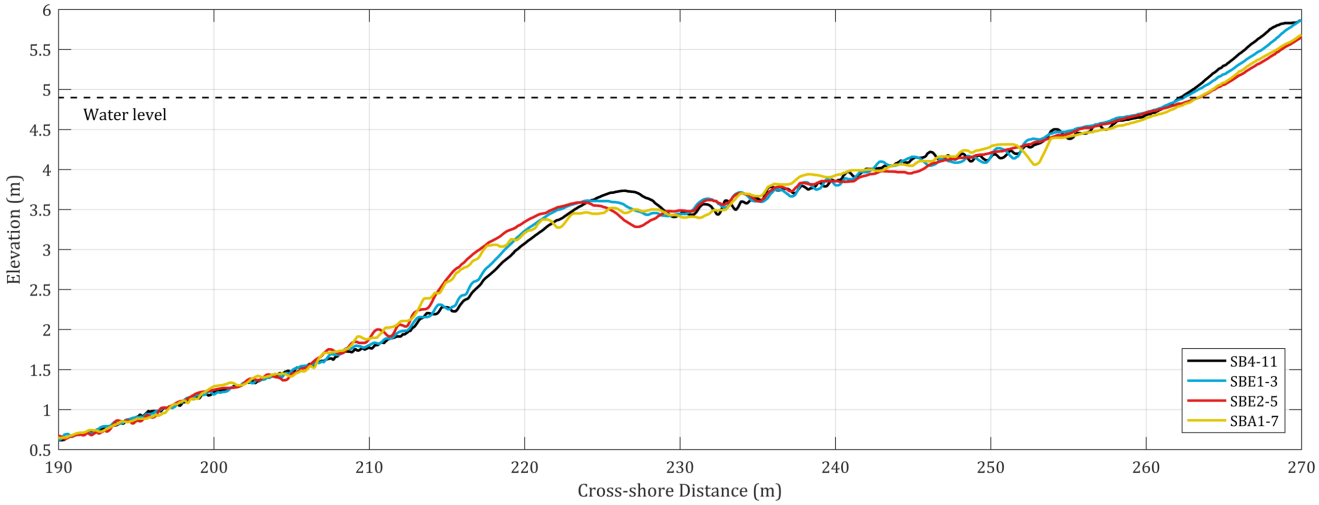

(b) Observed changes between SB4 and SBA

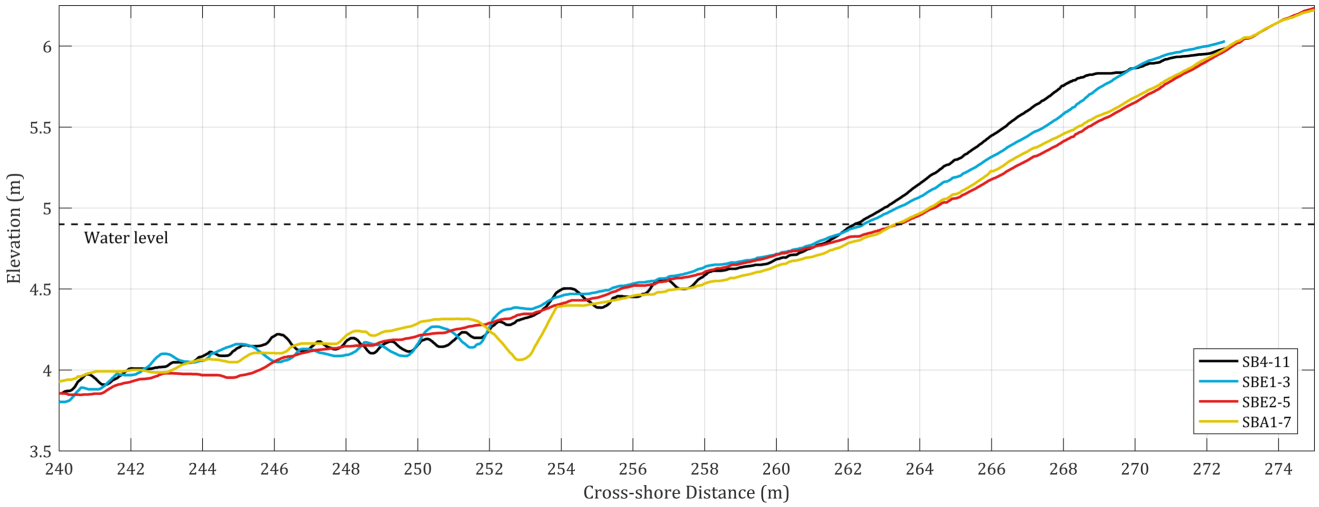

(c) Zoom of observed changes between SB0 and SB4

Figure B.1: Observations from DynaRev - Sand

B.2. Figures

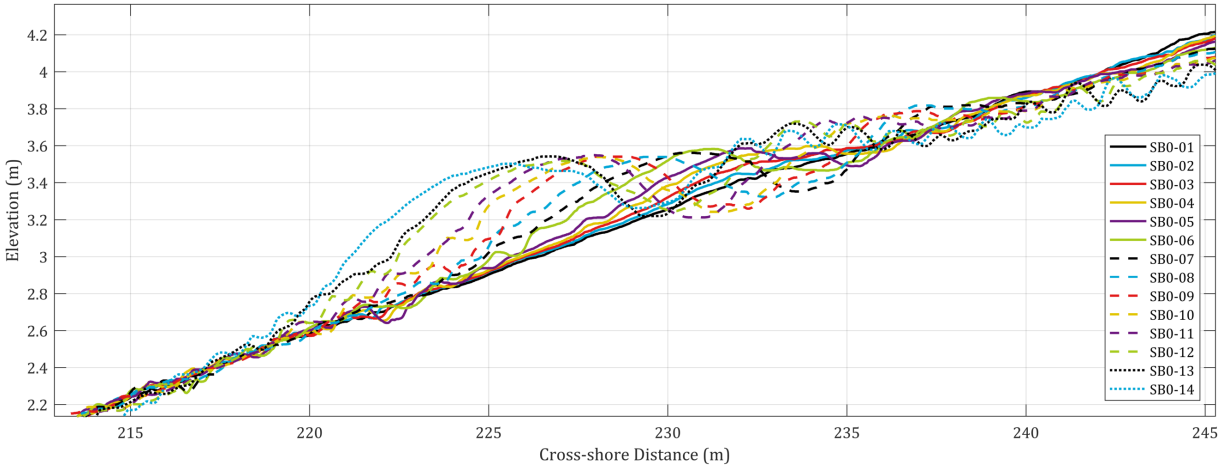

Figure B.2: Offshore retreat of bar during SB0

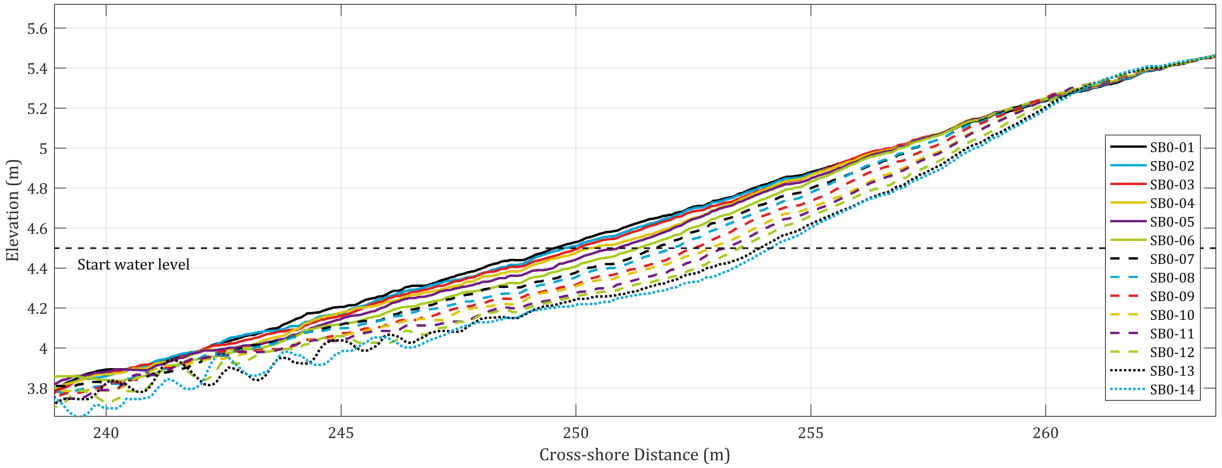

Figure B.3: Shore erosion during SB0

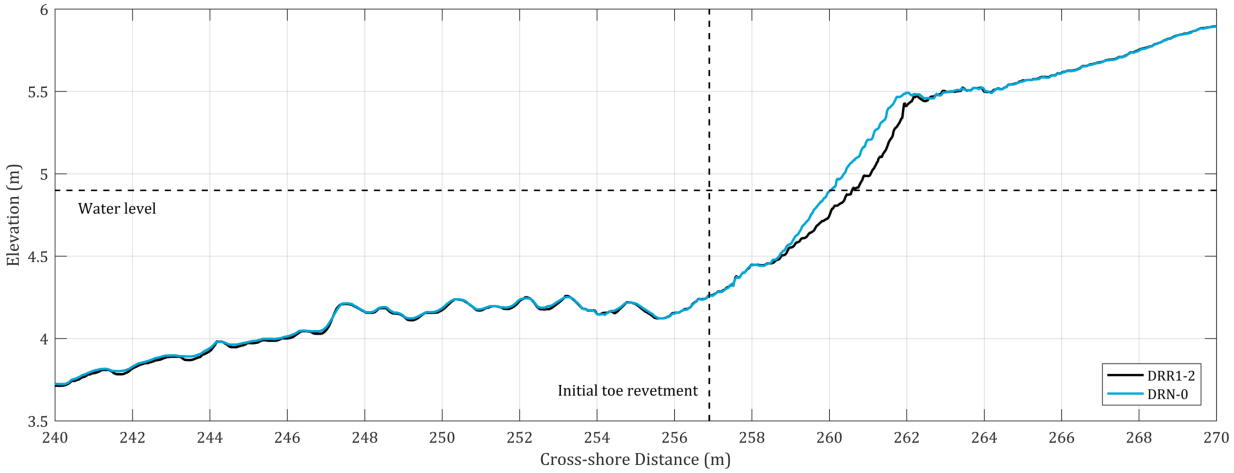

Figure B.4: Profile before and after placement of gravel

Figure B.5: Toe observation after set DR4

Figure B.6: Pictures of sand bed before placement of gravel revetment - Pictures by Paul Maxime Bayle

Figure B.7: Picture of bottom of revetment with the gravel stones removed - Picture by Paul Maxime Bayle

Section		Total volume change (m^2) of wave set: DR1	DR2	DR3	DR4
Offshore - Offshore side sand bar	from 185m to 220m	-0.0472	+0.0482	+0.0728	-0.0522
Sand bar	from 220m to 235m	+1.1968	+0.3074	+0.3708	+0.2480
Onshore side sand bar - Toe revetment	from 235m to 256.9m	-0.7056	-0.2607	+0.0784	+0.4562
Revetment	from 256.9m to 264m	-0.1490	-0.2177	-0.4560	-0.5385
Landward side revetment - Landward side	from 264m to 275m	-0.0570	-0.0086	+0.0132	+0.0650
Total cross section		+0.2379	-0.1311	+0.0791	+0.1784
Loss/m		+0.0026	-0.0014	+0.0009	+0.0020

Table B.2: Total volume changes during wave sets - Positive values correspond to volume increase and negative to volume decrease of results

Section		Mass loss/inaccuracy (-) DR1	DR2	DR3	DR4
Offshore - Offshore side sand bar	from 185m to 220m	-0.5100	+0.9432	+2.3636	-0.7520
Sand bar	from 220m to 235m	+30.1714	+14.0365	+28.0909	+8.3361
Onshore side sand bar - Toe revetment	from 235m to 256.9m	-12.1837	-8.1535	+4.0681	+10.5031
Revetment	from 256.9m to 264m	-7.9359	-21.0014	-72.9834	-38.2412
Landward side revetment - Landward side	from 264m to 275m	-1.9595	-0.5355	+1.3636	+2.9794

Table B.3: Relative total volume changes during wave sets - Positive values correspond to volume increase and negative to volume decrease of results

C

PERFORMANCES

C.1. VALIDATION OF BOUNDARY CONDITIONS

C.1.1. WAVE SPECTRUM

A comparison is made between the hydrodynamic model output and some data retrieved from the DynaRev experiments. During the DynaRev experiments the surface water elevation has been measured at 180 m from the wave paddle, see figure C.1. From the surface water elevation from both the model and the data the wave spectrum can be calculated. For the model the surface water elevation has been retrieved at 190 m from the wave paddle. The wave spectra are shown in figure C.2.

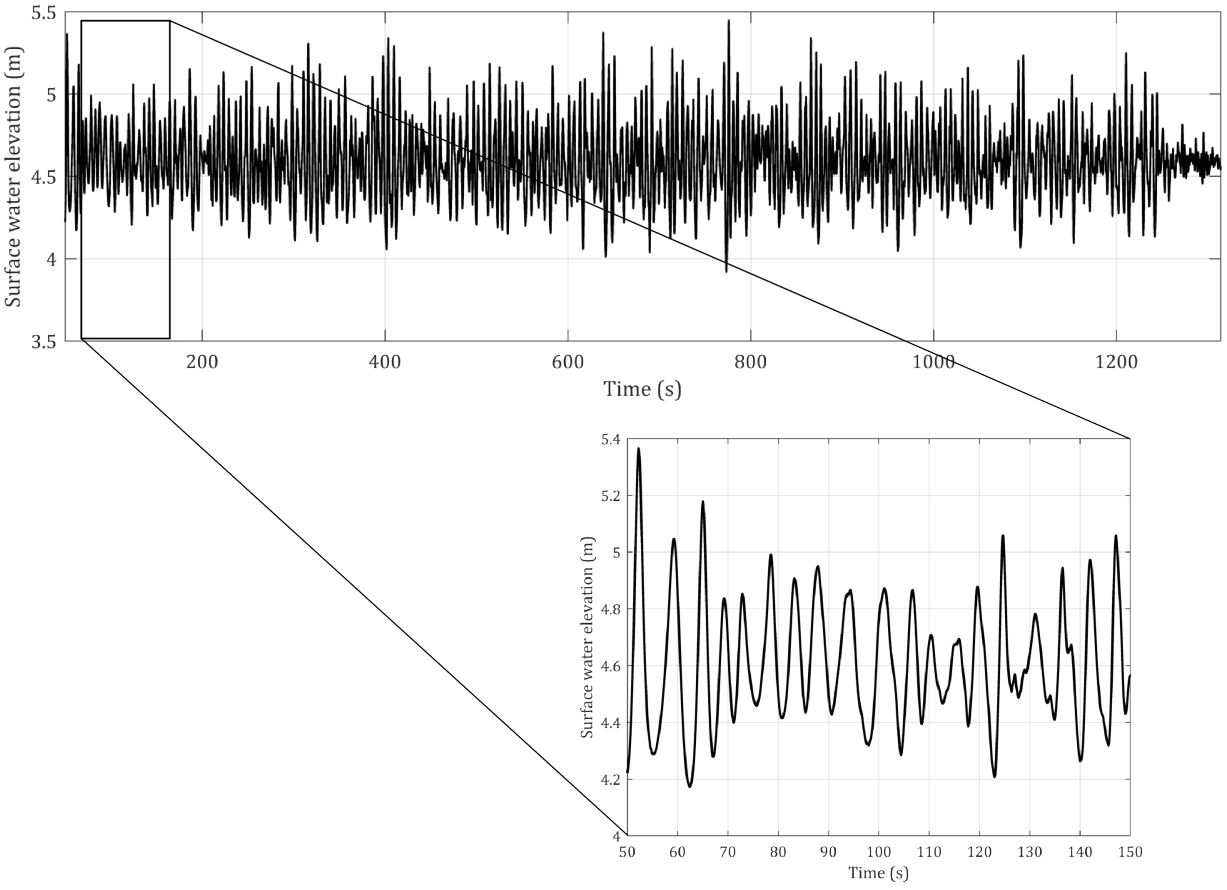

Figure C.1: Surface water elevation from data

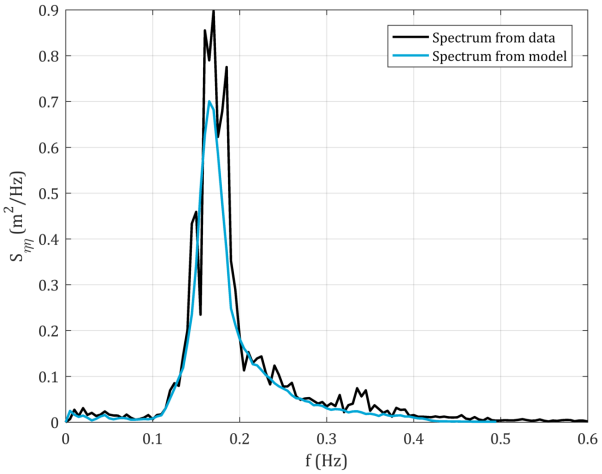

Figure C.2: Wave spectrum comparison

As can be seen from figure C.2 the spectra are quite similar. The shape of the spectra match and the peak of the spectra are located on the same location. The spectrum from the data is large in volume. In other words more energy is present at 180 m as retrieved from the data than at 190 m from the model. The 10 meters of wave propagation is not enough to explain this energy difference from wave breaking, mainly because the water depth is relatively large at this location. It is expected that the main cause for the energy difference can be contributed to wave reflection.

From the data the H_{rms} at 180 meters is found to be 0.6336 m. This gives a H_{m0} of 0.8960 meters. The model gives a H_{rms} of 0.5642 m and a H_{m0} of 0.7979 m at 190 m, which corresponds to the H_s that is given as input to the model. The input of the model corresponds to the wave spectrum as imitated by the wave paddle, with a H_s of 0.8 m. The increased wave height as found from the data can be caused by either wave reflection or shoaling of waves. As was mentioned shoaling is expected not to be of significance around 190 m, where a water depth is present of about 4.6 meters. In order to still consider a wave height of about 0.9 meters it has been considered during the performance studies.

C.1.2. GROUNDWATER FLOW

In table C.1 an overview is given of hydraulic conductivity values and critical Reynolds number (if known) used for different researches. As is evident from this table the values for the hydraulic conductivities vary quite a bit depended on the research and grain size. Using a basic formulation that only needs a D_{50} a K was found of 11 ms^{-1}, which is unrealistically large. It is clear though that it can be expected that K will most probably be larger than 0.2. Furthermore little is known about the critical Reynold number. Therefore a short model is run to vary which set of parameters fits best with the amount of overwash events measured during wave set DR4-7. This wave set is chosen over wave set DR3-7, because some information about the sand bed below the revetment was known for DR4-7, see section 4.2.2.1. One hour of wave impact was modelled without sediment transport. Groundwater flow was only allowed near the revetment, where the sand bed below the revetment was based on interpolation between the data points found during the experiment.

Nine values for K (0, 0.1, 0.2, 0.3, 0.4, 0.5, 0.75, 1.0 and 1.5), seven values for Re_{crit} (1, 10, 20, 30, 40, 50, 75, 150, 225 and 400) and three values for H_s were modelled, a total of 270 model runs. In post-processing the amount of overwash events were calculated by counting the amount times the water elevation surpassed a critical threshold. This threshold of the model represents the crest level of the revetment. Quickly it was noticed that the amount of overwash events found in post-processing was sensitive to this threshold value. Therefore it was investigated what the threshold values should be for 270 separate model runs to agree with the observed 150 overwash events. The result is shown in figure C.3.

Some interesting things can be seen in this 4D plot. As can be seen the hydraulic conductivity K mainly

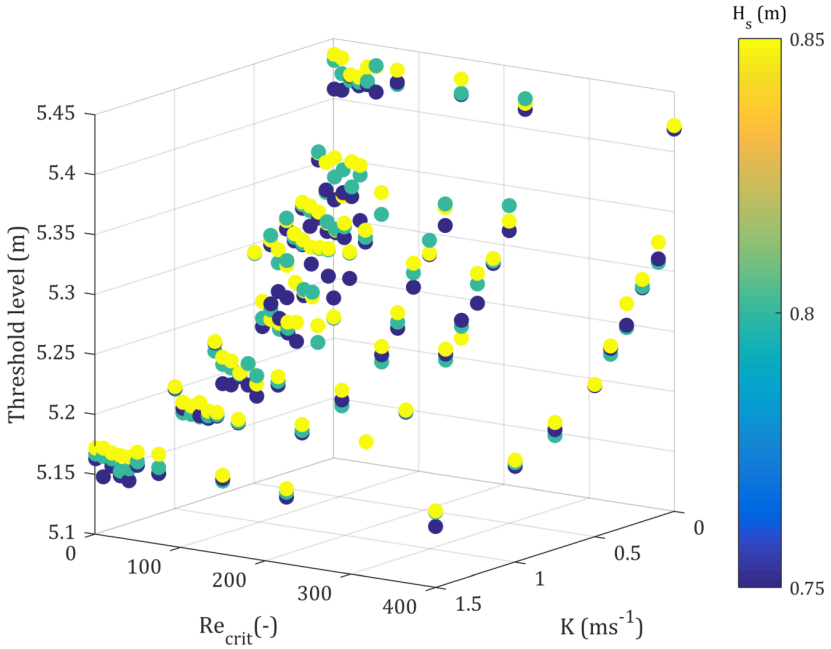

Figure C.3: Threshold values of model runs that correspond to 150 overwash events

dictates the amount of overwash events and therefore the threshold level. High values of K, which correspond to very porous soils, give low threshold values. The opposite applies to low values of K, which corresponds to low porous soils such as sand. The critical Reynolds number is not as influential as K, but not negligible. This Re_{crit} can be seen to be mainly of importance for K's between 1 and 0. Lastly the wave height does not seem the have a large influence on the threshold level. Additional plots that show these influences are located in Appendix C.

As can be expected the amount of overwash events (and therefore the threshold level) decreases with a higher hydraulic conductivity. Surprisingly though the threshold levels are on the low side compared to the expected crest level. Only values of K close to 0 ms^{-1} seemed to correspond to 5.4 m. This difference can be explained with the fact that the amount of overwash events was noted during the experiments by visual observation. The crest level was hard to observe, making it difficult to correctly confirm whether

	D_{50} (mm)	K (ms^{-1})	Re_{crit} (-)	Comment
BARDEX (McCall, 2015)	11	0.155	225	McCall (2015) calibrated the model and varied K between 0.1 and 0.24 and Re_{crit} between 0 and 300.
(Mulqueen, 2005)	~ 23	~ 0.2 – 1.0	-	Hydraulic gradient was measured under different hydraulic gradients. The larger the gradient, the lower the conductivity.
(Ruiz de Alegria-Arzaburu et al., 2011)	6	0.05	-	The was the best fit for XBeach compared with morphological measurements.
(Mason et al., 1997)	4	(0.1 to 0.0001)	-	The values for K were used to fit a model to measured groundwater data. The best fit found for K was 0.01.2
Formulation - (Masselink and Li, 2001) & (Hazen, 1911)	50	11	-	This adapted formulation gets quite rough as the sediment size increases.

Table C.1: Values for hydraulic conductivities and critical Reynold numbers

a wave reached a elevation of 5.3 or 5.4 meters. Furthermore a real wave is very turbulent as it breaks on the revetment, causing local splashes of water overtopping the revetment. These can potentially have been noted as an overtopping event, whereas the model does only models an approximation of a breaking wave.

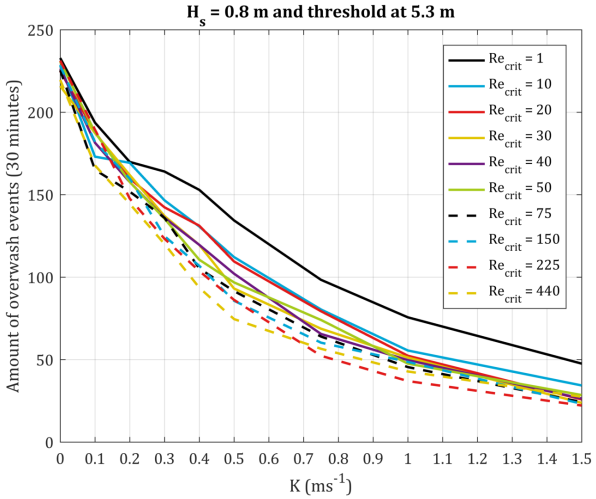

Figure C.4: Amount of overwash events

Figure C.4 shows the amount of overwash events for a threshold level of 5.3 meters and the different K's and Re_{crit}'s. Once more it can be seen from this figure that the hydraulic conductivity mainly influences the amount of overwash events. The different values for Re_{crit} all lie close to each other, which the exception of a critical Reynolds number of 1. A very low critical Reynolds number makes the groundwater flow turbulent for low flow velocities. It is difficult to measure or visually observe where the groundwater flow is turbulent and where it is not. Therefore assuming that the groundwater flow is almost immediately turbulent might overestimate the amount of turbulence. An explanation for the short range of results for the other critical Reynold numbers might be that the groundwater flow does not reach a sufficient velocity for the groundwater flow to become turbulent.

Looking at the values corresponding to the observed amount of overwash events (150 events each 30 minutes) it is found that a hydraulic conductivity K somewhere around 0.3 ms^{-1} fits best with a critical Reynolds number somewhere around 20. As was mentioned, these different values impact the amount of overwash events which means they influence the hydrodynamics of the model. It is unknown how they morphodynamics are influenced by these different values. In order to monitor the sensitivity of the model to the hydraulic conductivity, a range of values is assessed during the performance study. For K three values are assumed: 0.2, 0.3 and 0.4 ms^{-1}. Here 0.3 corresponds to the value found in figure C.4, 0.2 to a medium that has a lower conductivity (if for example sand is found within gravel) and 0.4 if the gravel has a higher conductivity than was assumed. For Re_{cr} a value of 20 was assumed. This means that for each performance study with groundwater flow 3 model runs are performed with which a range of results can be shown.

Lastly it is of interest for the performance tests if the depth of the sand bed influences the hydrodynamics. As was mentioned in section 4.2.2.1 the sand bed below the revetment is unknown for DR3_7 and DR4_7, only for DR4_7 some data points provided some information about the sand bed. However, in order to gain insight into the effect of different depths of the sand bed, several test cases are performed. As was mentioned, the sand bed below the revetment was approximated by interpolating between the data points that were obtained. For the test cases the sand bed has elevated and lowered 0.05, 0.1, 0.15 and 0.2 m with respect to the interpolated data points. The results of these test cases is shown in figure C.5b. From this figure it can be seen that the amount of overwash events increases for an elevated sand bed, which is to be expected. Moreover the increase of overwash events is little compared with the decrease of revetment surface area, see figure C.5a. The impact of a depth change in the revetment

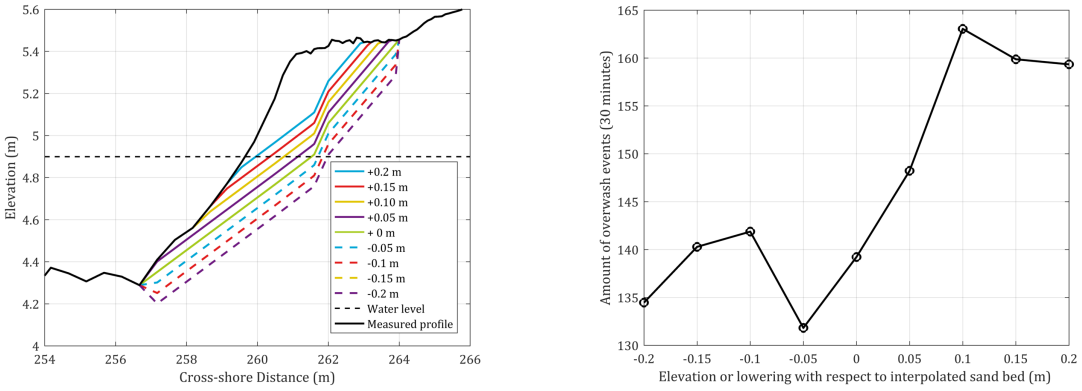

(a) (b)

Figure C.5: Overview and results of test cases with different sand beds below revetment

seems to be of lower importance than the impact that the hydraulic conductivity K has, which can be seen by comparing overwash events changes with a change of depth or K, see figure C.4 and C.5b.

C.2. MODEL INPUT

Settings for DR1_0 with Mcall-Van Rijn formulation of XBeach-G:

%%% Bed composition parameters %%%
D50 = 0.05

%%% Flow boundary condition parameters %%%
front = nonh_1D
back = wall
left = wall
rigth = wall

gwflow = 1
kx = 0.3
gwscheme = turbulent
aquiferbotfile = aqui.grd
gwnonh = 1
gw0 = 4.6
gwReturb = 20

%%% General %%%
nonh = 1
nonhq3d = 0
swave = 0

%%% Defaults from new GUI %%%
Topt = 5
dispc = -1
CFL = 0.9
form = tr2004
bedfriction = white-colebrook-grainsize

%%% Grid parameters %%%
depfile = zgr.grd
posdwn = 0
nx = 301
ny = 0
alfa = 0
vardx = 1
xfile = xgr.grd
xori = 0
yori = 0

%%% Initial conditions %%%
zs0 = 4.6

%%% Model time %%%
tstop = 25200

%%% Morphology parameters %%%
morstart = 0
struct = 1

$ne_layer = ne.grd$

%%% Wave boundary condition parameters %%%
instat = jons

%%% Wave-spectrum boundary condition parameters %%%
bcfile = jonswaplist.txt
rt = 600
dtbc = 1

%%% Output variables %%%
outputformat = netcdf
tintg = 1.0
tintp = 1.0
tstart = 200

%%% Overwash runup gauge %%%
nrugauge = 1
0 0 rug1

nglobalvar = 11
H
zb
zs
u
gwlevel
gwhead
infil
gwu
gwqx
gwheight gwbottom
Kx

nmeanvar = 3
H
zs
u

npoints = 26
190 0
200 0
210 0
220 0
230 0
240 0
242 0
244 0
246 0
248 0
250 0
251 0
252 0
253 0
254 0
255 0

256 0
257 0
258 0
259 0
260 0
261 0
262 0
263 0
264 0
265 0

npointvar = 3
H
zs
u

C.3. VALIDATION OF SAND TRANSPORT - S0

To validate the sand transport of XBeach a model was run that excluded any influence from the gravel revetment. The ideal reference was the DynaRev - Sand tests. In figure C.6 the results from modelling the initial planar beach is shown. As can be seen the onshore erosion is well predicted by the model. The slope and elevation from the model and observation match. The erosion just below the water level is underestimated. This is a known issue of the non-hydrostatic mode of XBeach and is out of the scope of this thesis.

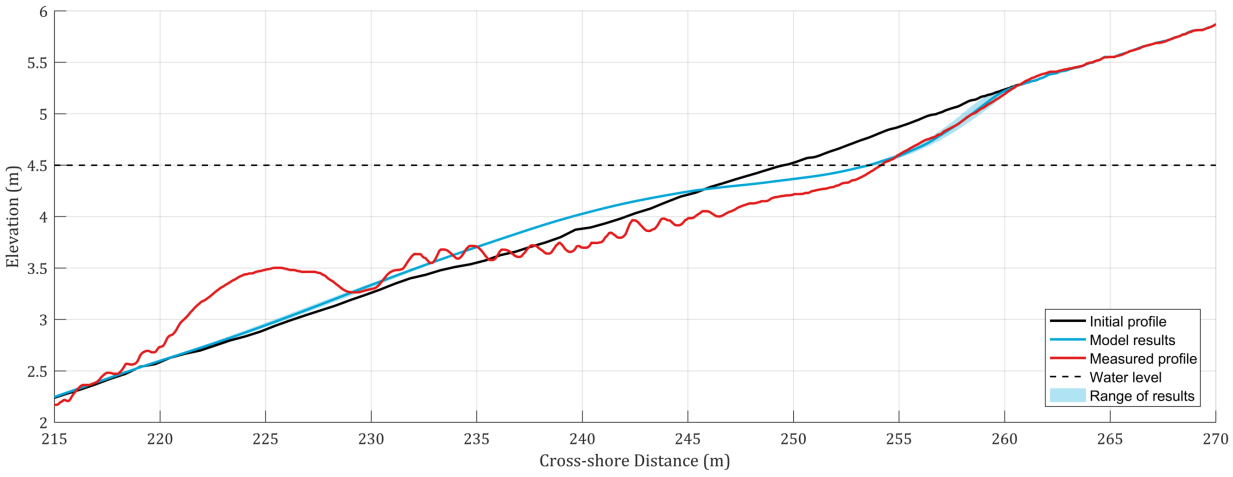

Figure C.6: Test SB0

C.4. FIGURES

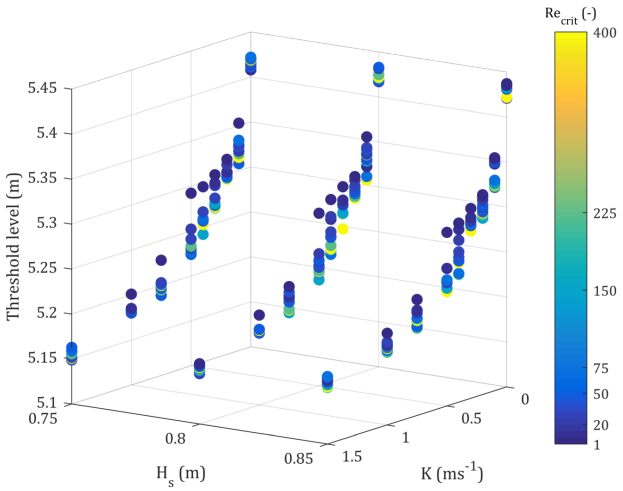

Figure C.7: Threshold values of model runs that correspond to 150 overwash events (2)

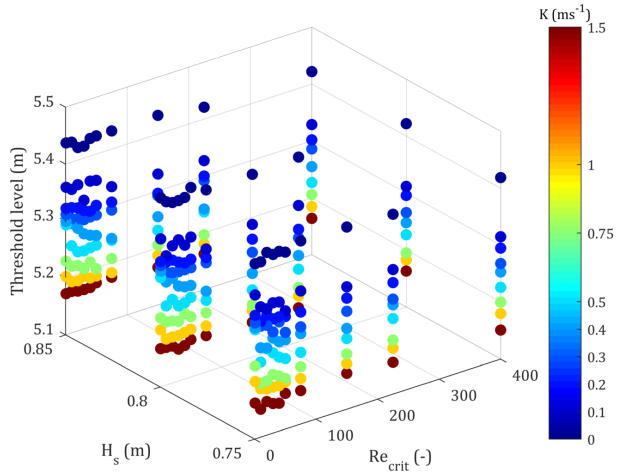

Figure C.8: Threshold values of model runs that correspond to 150 overwash events (3)

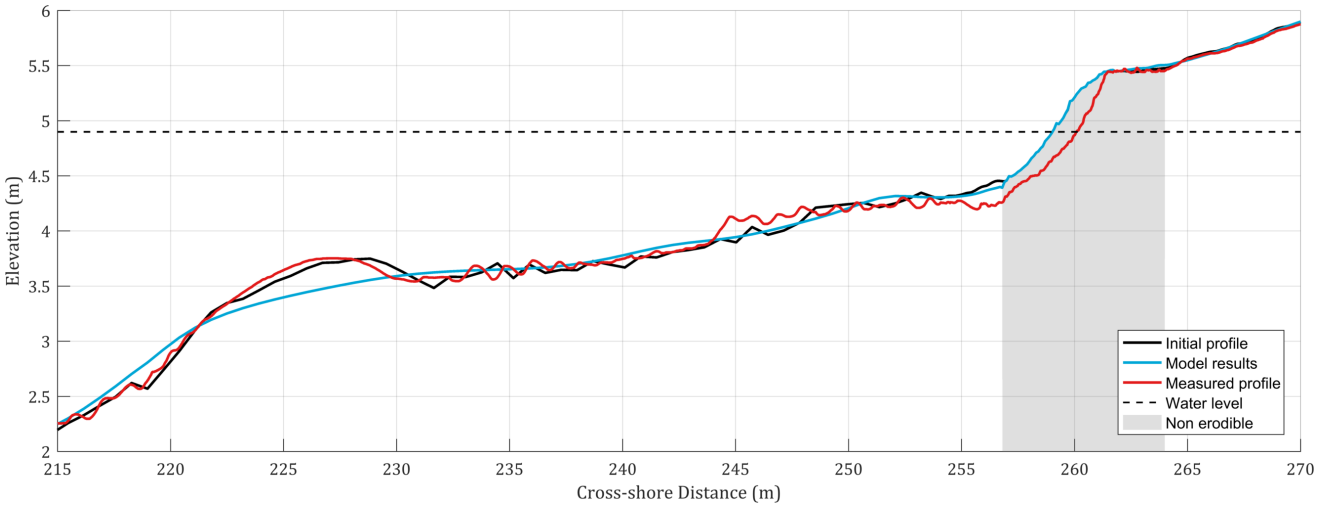

(a) Test S5 - Only beach erosion

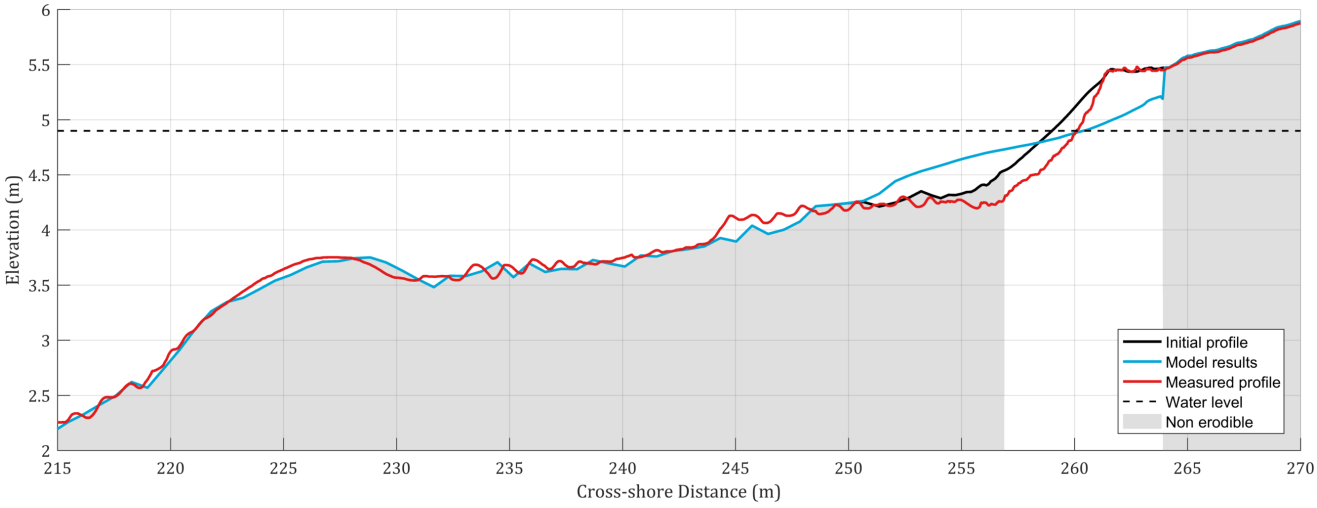

(b) Test S6 - Only revetment erosion

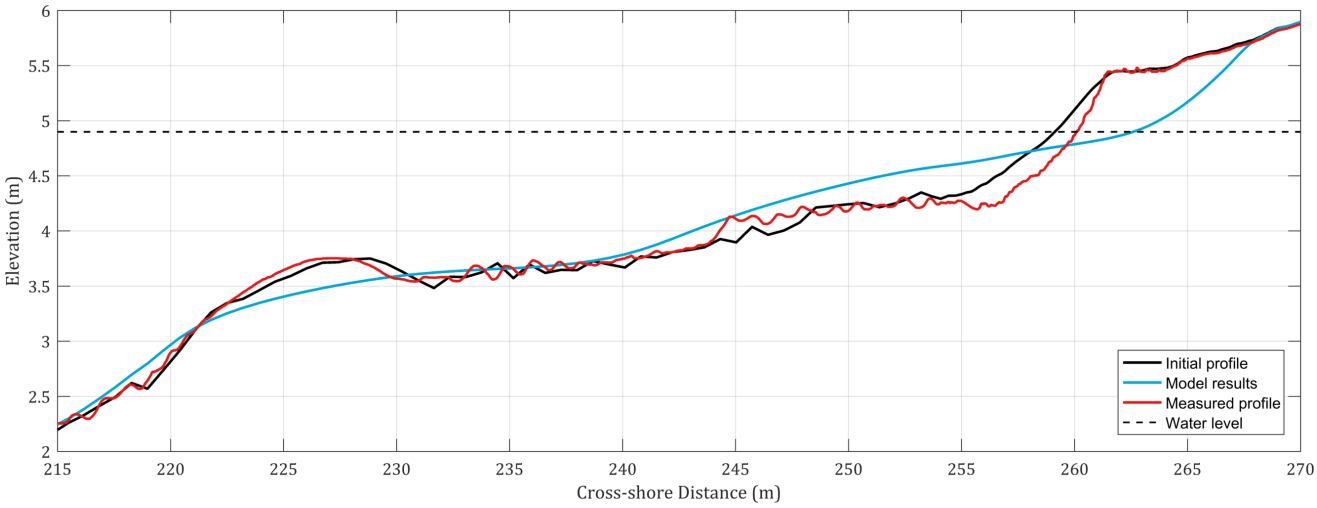

(c) Test S7 - Erosion over entire cross section

Figure C.9: XBeach performances

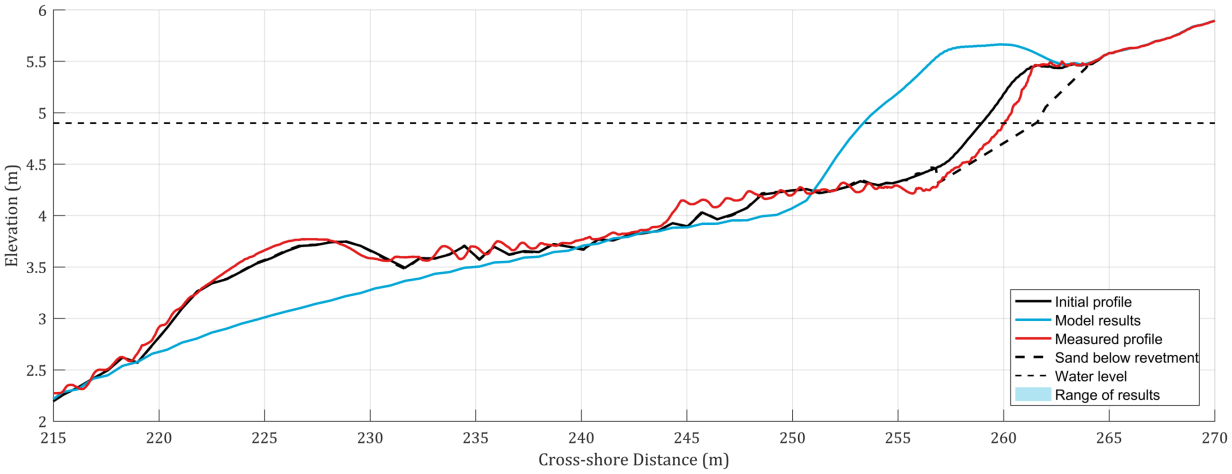

Figure C.10: Test G6 - Van Rijn - Erosion over entire cross section

D

MULTI-FRACTION MODELLING

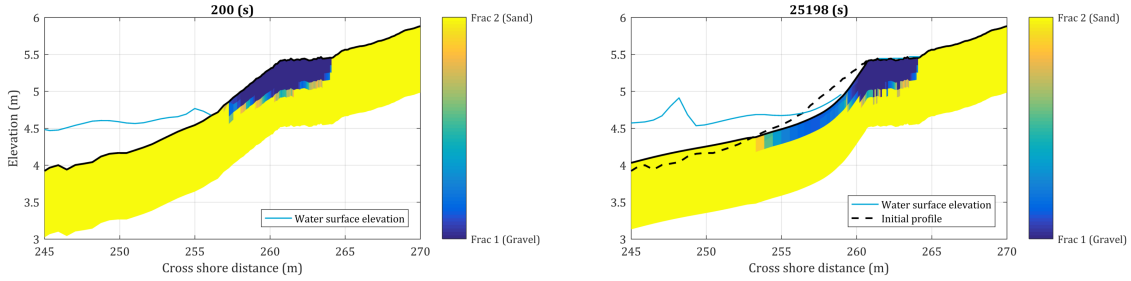

Figure D.1: Profile development of test MF1

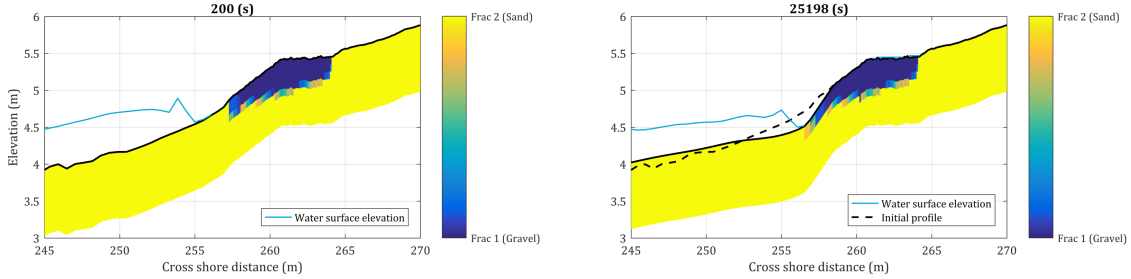

Figure D.2: Profile development of test MF2

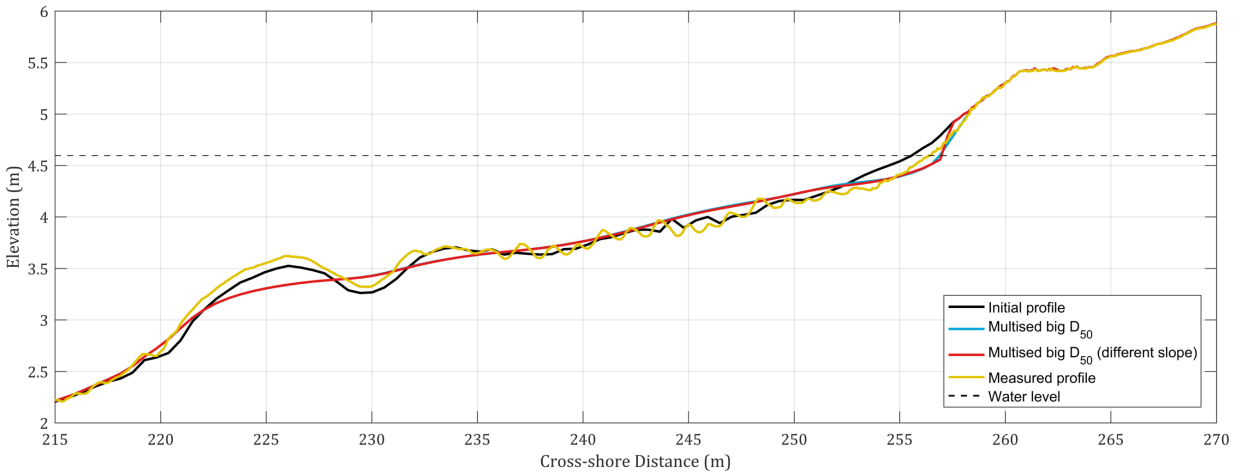

Figure D.3: XBeach multi-fraction result MF3

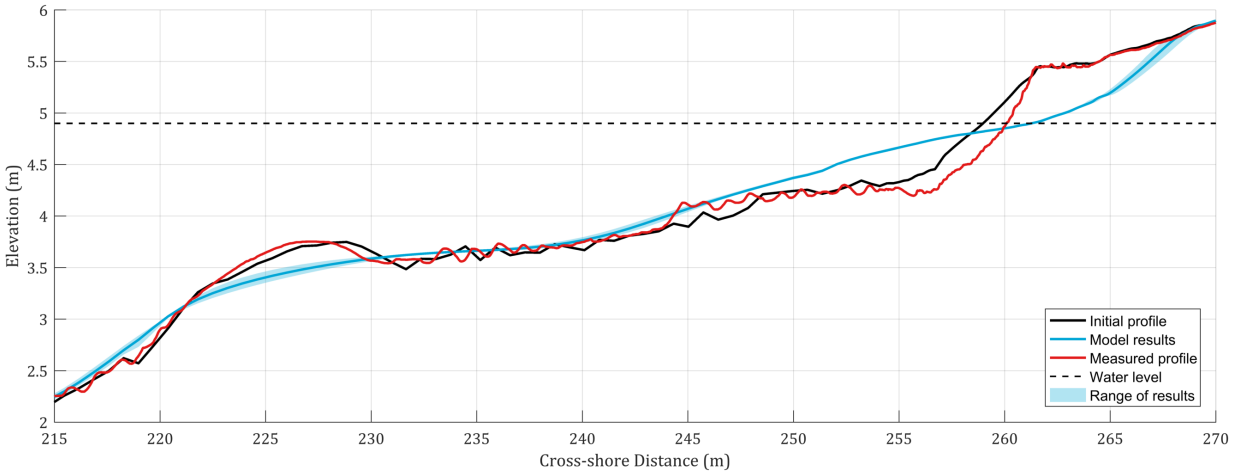

Figure D.4: XBeach multi-fraction result MF4

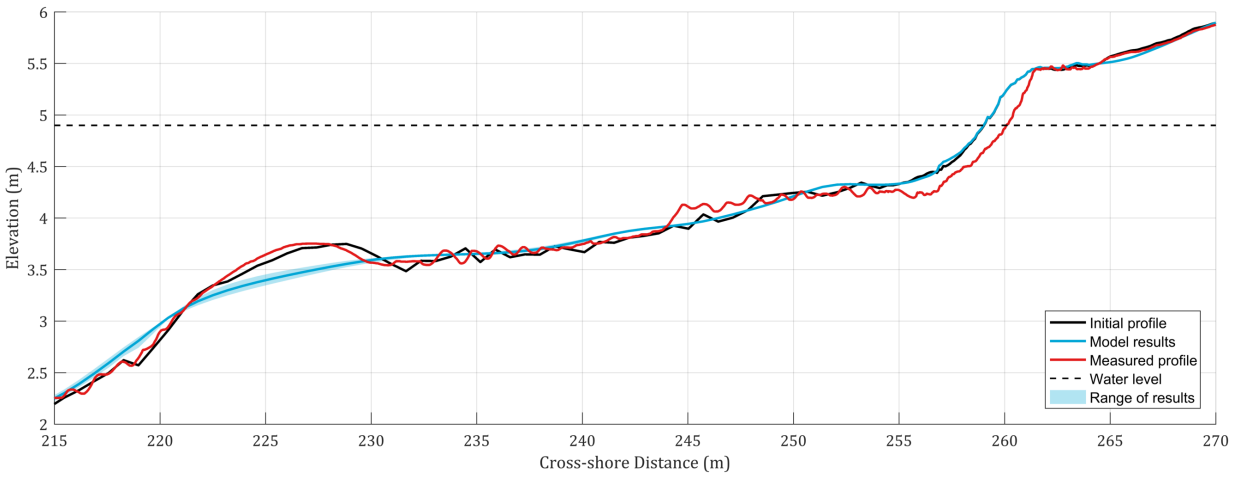

Figure D.5: XBeach multi-fraction result MF6

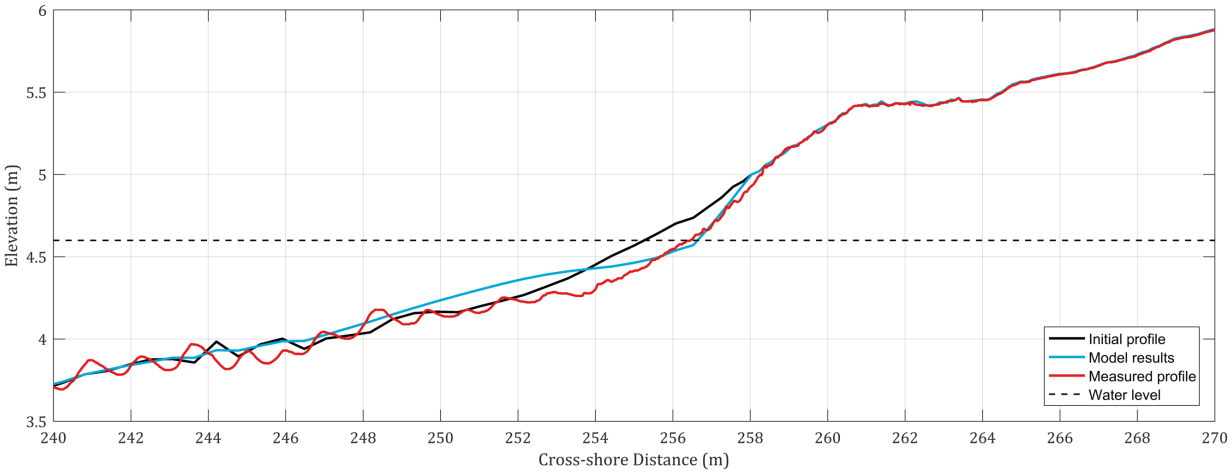

Figure D.6: XBeach multi-fraction result MFG1

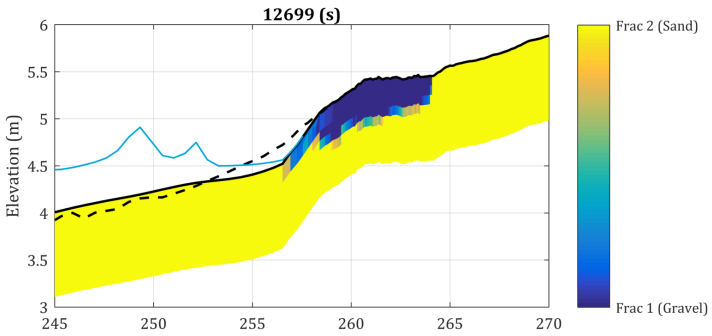

Figure D.7: Fraction distribution after MFG3 (DR1)

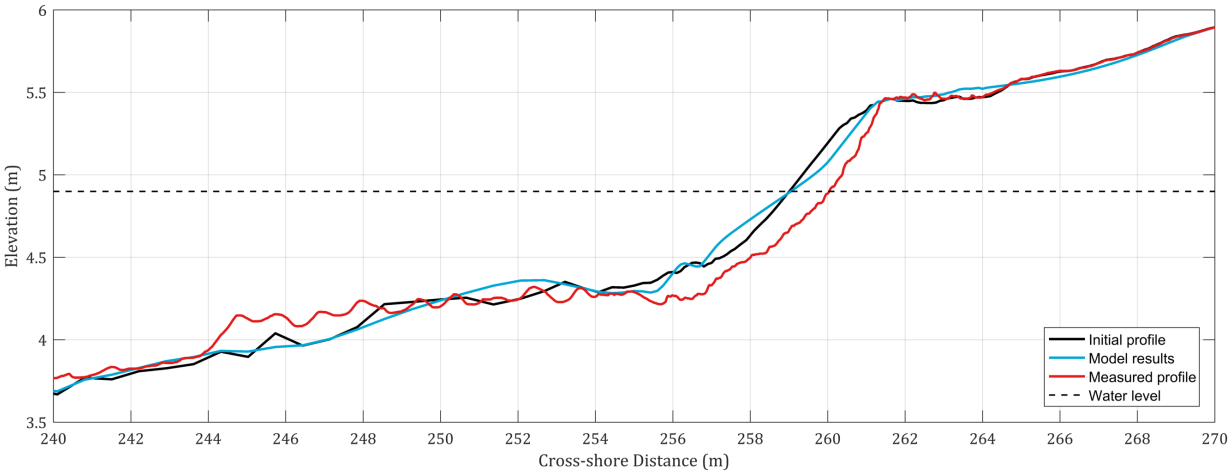

Figure D.8: XBeach multi-fraction result MFG4

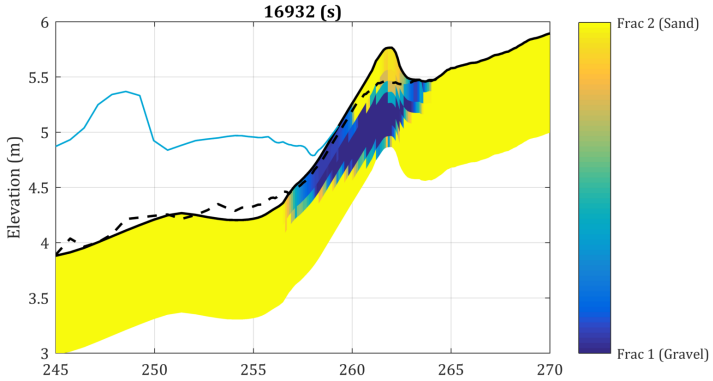

Figure D.9: Fraction distribution after MFG6 (DR4)

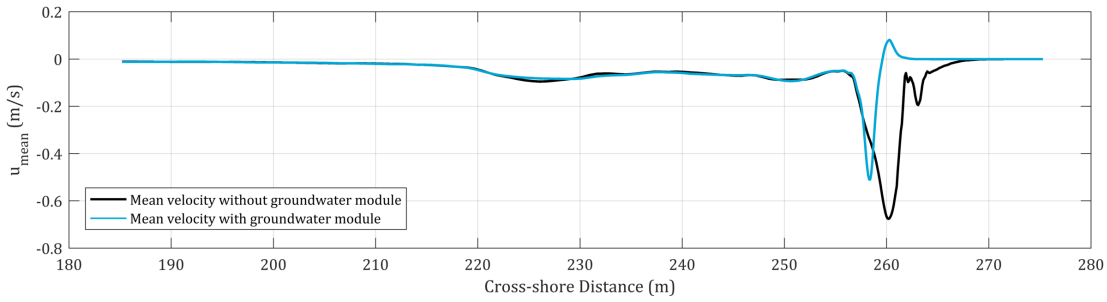

Figure D.10: Mean velocity differences with and without groundwater flow

E

SAND TRANSPORT INSIDE THE REVETMENT

E.1. SENSITIVITIES

Water level at revetment

When wave breaking is indeed important regarding where transports fluxes are significant, it can be expected that the transports fluxes would also change for different water levels. In order to inspect the influence of the water level on the transport two models are run. One model run is performed with a water level of 4.7 meter and one with 5.1 meter. The results are respectively shown in Figures E.7 and E.8.

Dimensionless friction factor c_f

A rough approximation was made for the c_f in the McCall-Van Rijn formulation. It is of interest to see how the transports react to different values for c_f. Two larger values are compared with the original c_f of 0.059, namely 0.1 and 0.2 (-). It has been chosen to evaluate larger values as larger values than 0.059 will give shear stresses, therefore larger transports. The latter is of interest for offshore transports.

Results show the expected results: transports are larger for both onshore as offshore directed. The shapes do not differ, just the magnitudes of the transports. The results changes for DR1 are the same as for DR4.

Calibrated variables Jacobsen

In the Jacobsen transport formulation two variables are calibrated variables. The calibration has been done by Jacobsen et al. (2017). Here C_1 was calibrated to be $10 \cdot 10^{-6}$, but in their report Jacobsen et al. (2017) also investigated C_1 to be $9 \cdot 10^{-6}$ and $11 \cdot 10^{-6}$. The variable $\Psi_{cr,0}$ was investigated for values between 0.080 and 0.150. The sensitivity of the transports have been investigated for these outer values. The changes of results for DR1 and DR4 were similar and minimal: larger values for C_1 give larger transports and lower values gives lower transports. For $\Psi_{cr,0}$ this is the other way around, larger values give lower transports and lower values give larger transports. These results are presented in Appendix E.

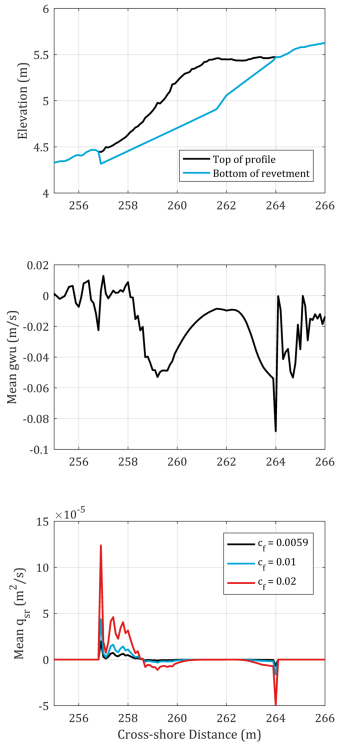

Figure E.1: Sensitivity of McCall-Van Rijn to c_f for DR4

E.2. RESULTS DR1

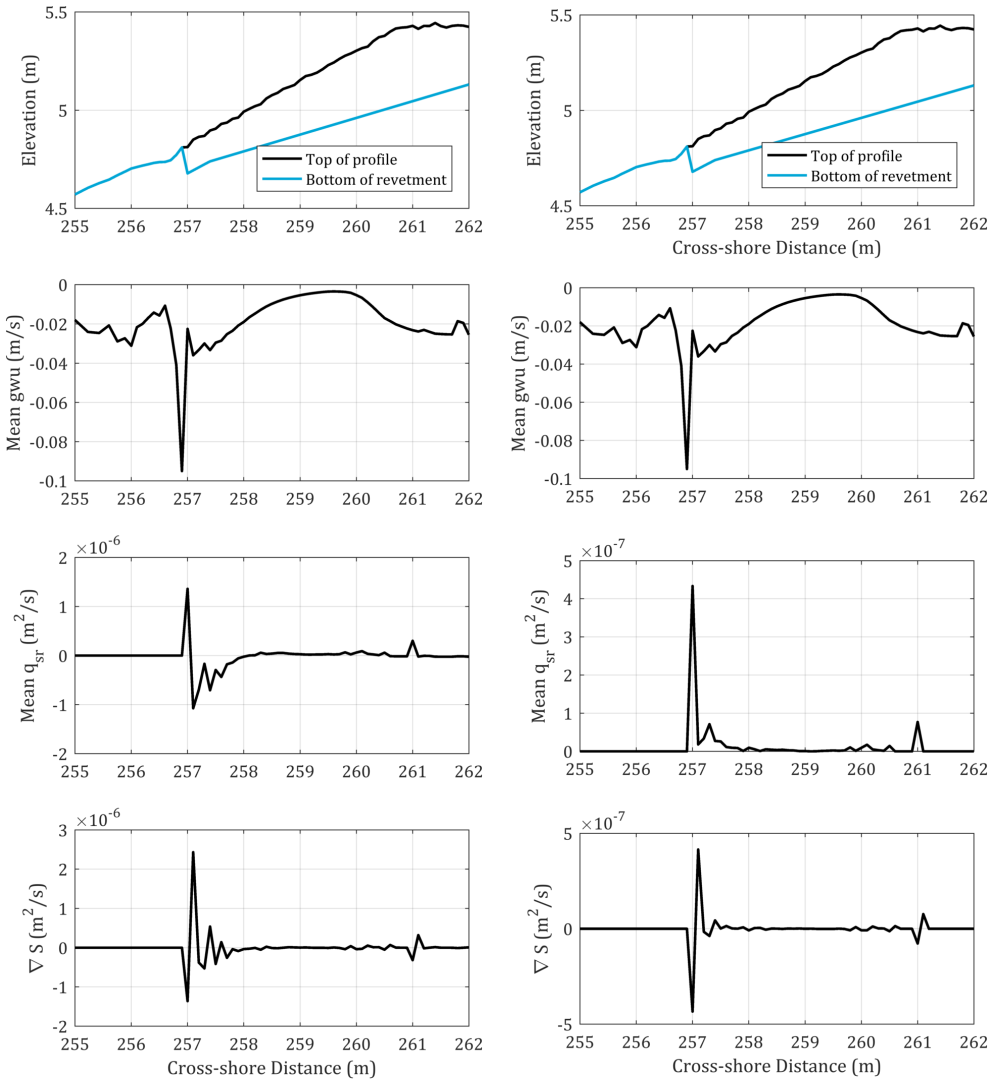

(a) Jacobsen (b) McCall-Van Rijn

Figure E.2: Overview of results with transport equations (DR1) - Left shows results with Jacobsen and right with McCall-Van Rijn. Top panel shows the revetment, second panel shows average horizontal groundwater velocity in each cell gwu, the one to last shows the bed transport fluxes at cell interfaces q_{sr} and bottom panel shows the transport gradients ∇S

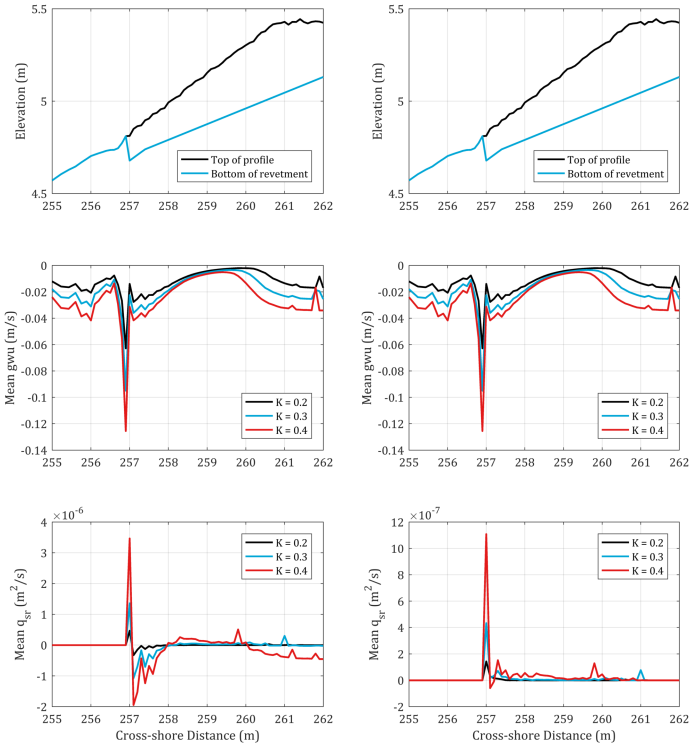

(a) Jacobsen (b) McCall-Van Rijn

Figure E.3: Sensitivity to hydraulic conductivity K for DR1

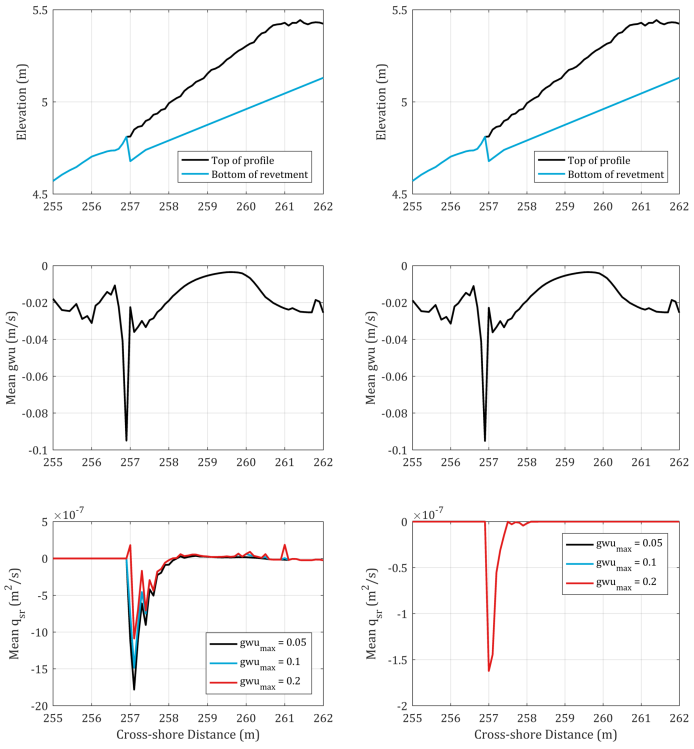

(a) Jacobsen (b) McCall-Van Rijn

Figure E.4: Sensitivity to gwu_{max} for DR1

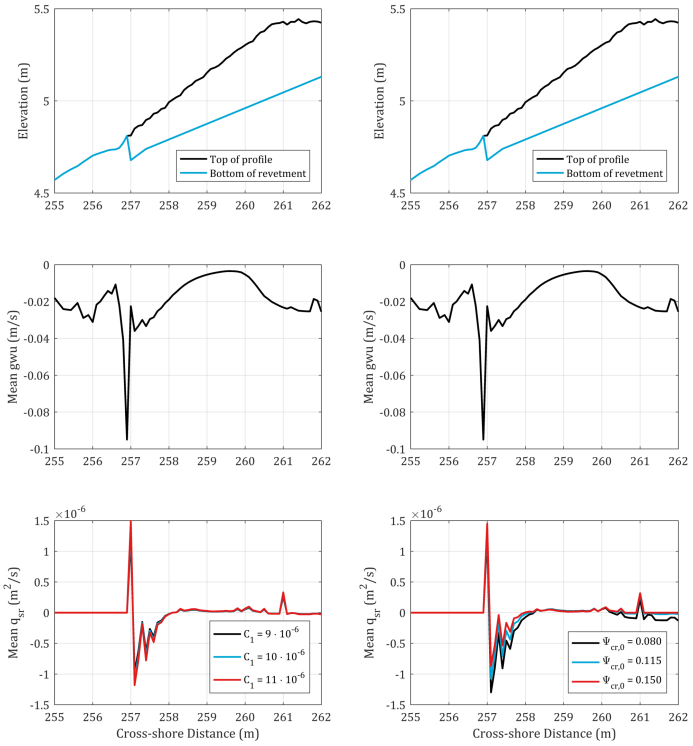

(a) C_1 (b) $\Psi_{cr,0}$

Figure E.5: Sensitivities variables C_1 and $\Psi_{cr,0}$ for DR1 - Applied in the Jacobsen transport formulation

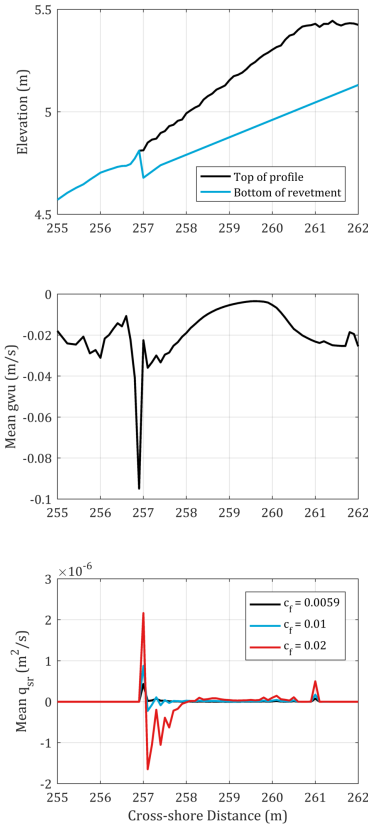

Figure E.6: Sensitivity of McCall-Van Rijn to c_f for DR1

E.3. RESULTS DR4

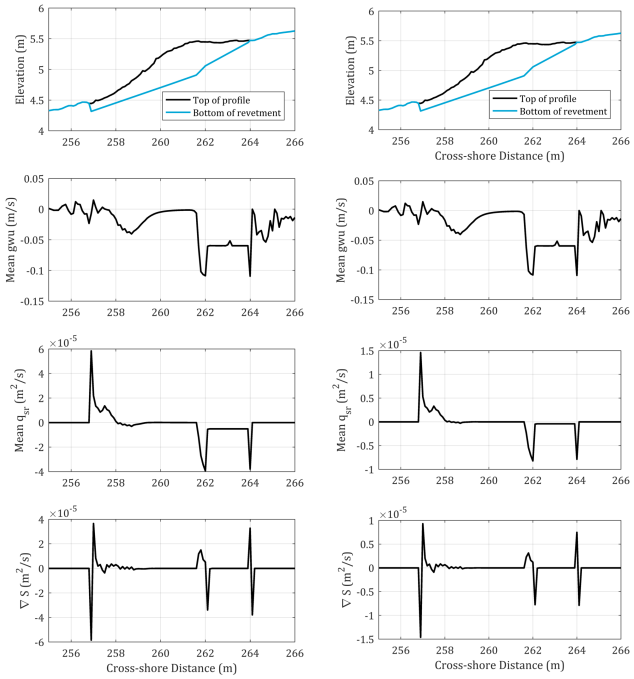

(a) Jacobsen (b) McCall-Van Rijn

Figure E.7: Overview of results with transport equations (DR4) with water level at 4.7 m

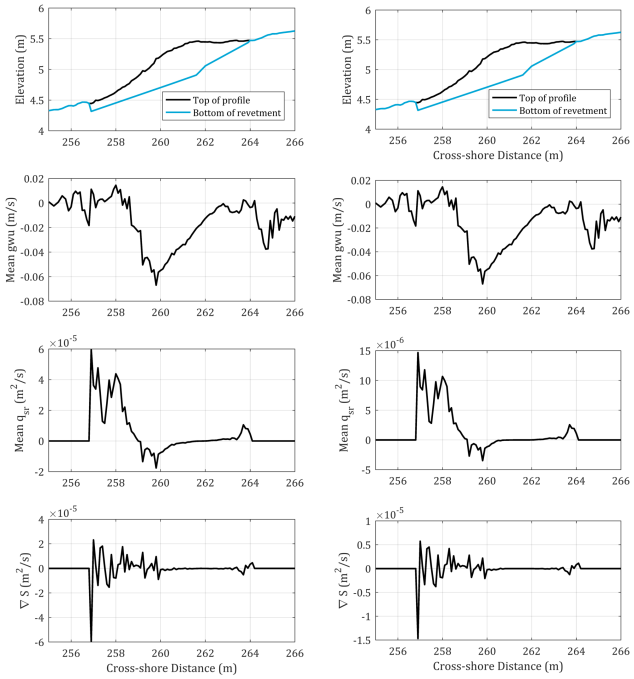

(a) Jacobsen (b) McCall-Van Rijn

Figure E.8: Overview of results with transport equations (DR4) with water level at 5.1 m

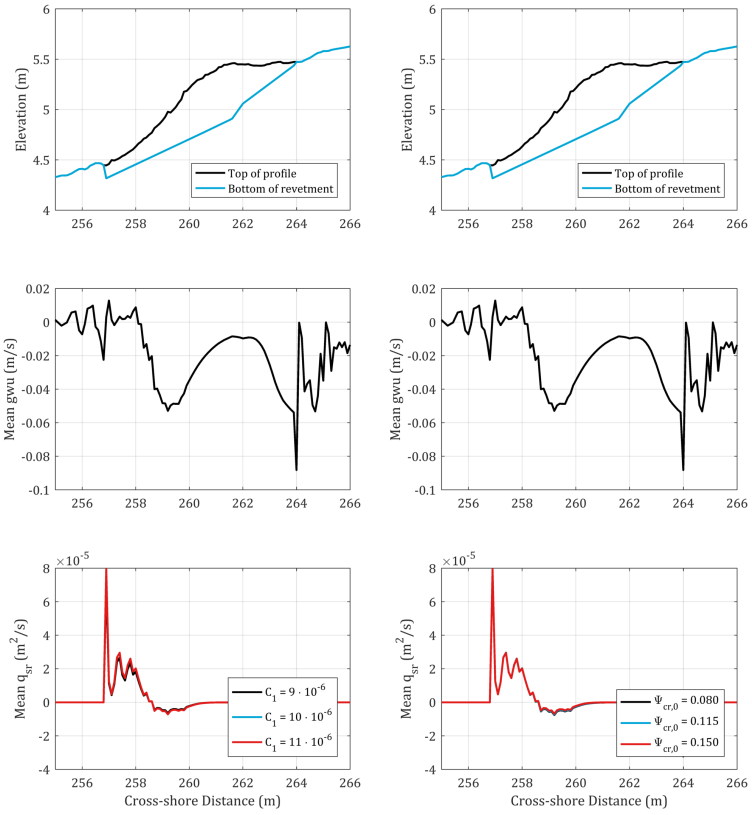

(a) C_1 (b) $\Psi_{cr,0}$

Figure E.9: Sensitivities variables C_1 and $\Psi_{cr,0}$ for DR1 - Applied in the Jacobsen transport formulation

E.4. FIGURES

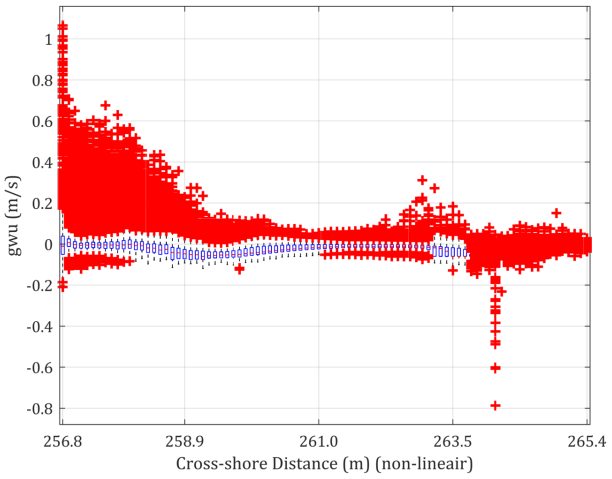

Figure E.10: Boxplot of gwu at cell interfaces - Within the blue box the 25 to 75 percentiles are shown. The center of these boxes are the medians. The whiskers show the maximum and minimum values. Red crosses describe outliners.

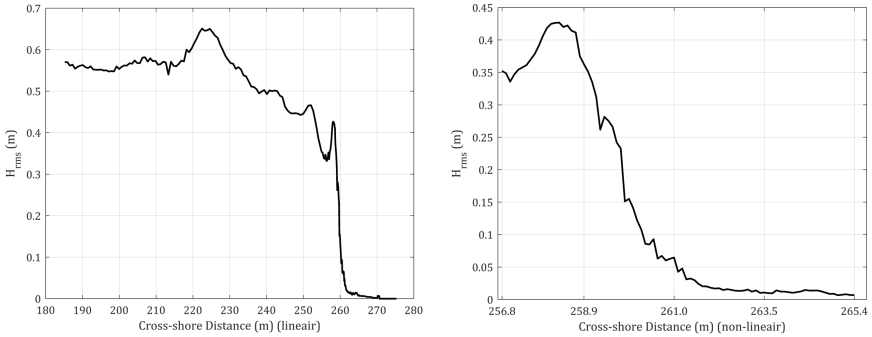

(a) H_{rms} at cross-section (b) H_{rms} at at revetment

Figure E.11: Root-mean squared wave heights H_{rms} throughout cross section and at revetment - Left panel shows H_{rms} throughout cross section. As can be seen, first a slight increase is seen in the wave height, which is the shoaling of waves. Thereafter the wave height decreases which is caused by wave breaking. Then around 259 m a peak is observed, which is also visible in the right panel, which shows the H_{rms} at the revetment. This peak is not expected, as wave breaking should continue and H_{rms} should decline. This peak is caused by the way H_{rms} is calculated. It is retrieved from the variance of the surface water elevation, which is equal to the bottom depth when cells are dry, causing extra variance in z_s when varying between wet and dry and therefore an increase in H_{rms}.

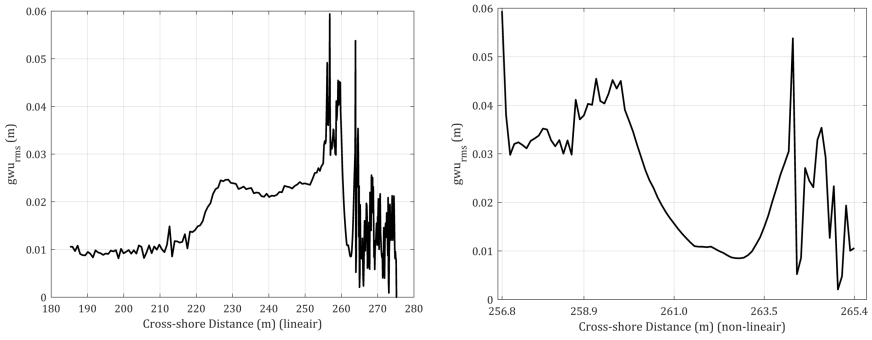

(a) gwu_{rms} at cross-section (b) gwu_{rms} at at revetment

Figure E.12: Root-mean squared groundwater velocities gwu_{rms} throughout cross section and at revetment

F

TWO-LINE MODEL

F.1. DIMENSIONLESS FRICTION FACTOR c_f

In the formulations for transports of sand or gravel on the interface of water to sand/gravel the bed shear stress is depended on the velocity profile in the water column. The velocity profile has a certain height and is dependent on the shape of the profile, which has often has a logarithmic form.

When interpolating the logarithmic form of this velocity profile one can find the mean velocity U divided by the shear velocity u^*. This equal to the square root of the dimensionless friction factor divided by one:

$$\frac{U}{u^*} = \frac{1}{\sqrt{c_f}} = \frac{1}{\kappa} \ln\left(e^{-1} \frac{d}{y_0}\right) \tag{F.1}$$

This formulation allows a crude assumption for the dimensionless friction factor c_f for the transport equation of sand in gravel. It is assumed that the velocity profile is still logarithmic and the height of the velocity profile is rather small compared to the grain size of gravel. It is assumed that the height d is about 5 mm compared to the 50 mm grain size. The Von Karman constant κ is 0.4 (-) and the roughness length y_0 is assumed to be 0.333 times the D_{50} of sand. This gives an indication of c_f:

$$c_f = \left(\frac{1}{\frac{1}{0.4} \ln\left(e^{-1} \frac{0.005}{0.333 \cdot 0.0003}\right)}\right)^2 = 0.0059(-)$$

F.2. NUMERICAL IMPLEMENTATION OF TWO-LINE MODEL

For the two-line model 4 variables are loaded into XBeach, namely *z_g* (thickness gravel layer), *z_s* (height of sand), *overlap* and *counter*. The following steps are undertaken in the two-linem model.

1. Calculate sand transport fluxes in u-point (cell-interfaces), $Susg$ and $Subg$ for $pb = 1$
2. Calculate gravel transport fluxes in u-point (cell-interfaces), $Subg\_g$ for $pb = 2$
3. Calculate sand transport under gravel fluxes in u-point (cell-interfaces), $Suss$ for $pb = 1$
4. Identify direction of fluxes and find availability of corresponding source (trans_inf)
5. Calculate sediment transport gradient
6. Calculate bed level change of gravel (rearrange sand height, overlap and counter)
7. Calculate bed level change of sand (rearrange sand height, overlap and counter)
8. Update total bed level for hydrodynamic calculations of model

F.2.1. TRANSPORT FORMULATIONS SAND UNDER GRAVEL

The transport of sand under gravel is done either by Jacobsen or similarly to the transport equation for gravel by McCall.

Instead of the current velocity the groundwater velocity gwu is used to calculate the transport. This gwu is retrieved from the groundwater module.

Jacobsen

First the slope of the bed relative to the direction of flow ϕ is calculated. The slope should be on the interface of the cell:

$$\phi^{i,j} = \text{atan}\left(\frac{z_b^{i,j} - z_b^{i+1,j}}{dsu^{i,j}} \frac{\pi}{180}\right) \tag{F.2}$$

Now the critical mobility numbers Ψ_{cr} can be calculated:

$$\Psi_{cr}^{i,j} = \Psi_{cr0} \frac{\sin\left(\phi_r - \phi^{i,j}\right)}{\sin\phi_r} \tag{F.3}$$

In which Ψ_{cr0} is a calibrated constant and $\phi_r = 35°$. Now where $z\_g > 0$ the local mobility number is calculated.

$$\Psi^{i,j} = \frac{\left(gwu^{i,j}\right)^2}{gD_{50}\Delta} \tag{F.4}$$

Here gwu is limited to a maximum speed, because these can get extremely large due to the wave breaking in the model. Now where $z\_g > 0$ and $\Psi > \Psi_{cr}$

$$q_{sr}^{i,j} = C_1\left(\Psi^{i,j} - \Psi_{cr}^{i,j}\right)^{1.5} \frac{gwu^{i,j}}{\left|gwu^{i,j}\right|} \tag{F.5}$$

Elsewhere:

$$q_{sr}^{i,j} = 0 \tag{F.6}$$

McCall

With the groundwater velocity the bed shear stress is calculated. Where $z\_g > 0$ and $z\_s \neq gwlevel$:

$$\tau_{suss}^{i,j} = \pm c_f \rho \left(\frac{gwu^{i,j}}{n_{p,g}}\right)^2 \tag{F.7}$$

Elsewhere:

$$\tau_{suss}^{i,j} = 0 \tag{F.8}$$

Here gwu is limited to a maximum speed, because these can get extremely large due to the wave breaking in the model.

The shields stress θ and critical shields stress equal :

$$\theta^{i,j} = \frac{\left|\tau_{suss}^{i,j}\right|}{\rho g D_{50} \Delta} \tag{F.9}$$

$$\theta_{crit} = \frac{0.30}{1+1.2D_*} + 0.055\left(1-\exp^{-0.020D_*}\right) \tag{F.10}$$

Now the transport flux q_{sr} is calculated

$$q_{sr}^{i,j} = C_{qb}\,\gamma D_{50} D_*^{-0.3} \sqrt{\frac{\left|\tau_{suss}^{i,j}\right|}{\rho}} \frac{\theta^{i,j}-\theta_{crit}}{\theta_{crit}} \frac{\tau_{suss}^{i,j}}{\left|\tau_{suss}^{i,j}\right|} \tag{F.11}$$

F.2.2. FLUX IDENTIFICATION

Sediment transport for suspended and bed-load transport of sand is only called if no gravel layer on top is present. Gravel transport and transport of sand underneath gravel is only called if a gravel layer is on top. This is done by checking the depth of the gravel layer, in the model *depthcheck*.

$$\text{depthcheck} = z\_g^{i,j} - \text{overlap}^{i,j} \tag{F.12}$$

$$\text{depthcheck} > 0.05 (\text{Gravel transport and sand transport below gravel}) \tag{F.13}$$

$$\text{depthcheck} \leq 0.05 (\text{Sand transport}) \tag{F.14}$$

In order to prevent sand erosion from a cell where a gravel layer is located (e.a. no sand transport) or gravel erosion from a cell where only sand transport can occur in the model, a variable is calculated that contains information about the cells present. Then the sediment fluxes S are multiplied with this variable, which is called $trans\_inf$:

If $u_{reps}^{i,j} > 0$

$$\text{trans\_inf}^{i,j} = 0 \quad \text{for depthcheck}^{i,j} > 0.05 \tag{F.15}$$

$$\text{trans\_inf}^{i,j} = 1 - \text{depthcheck}/0.05 \quad \text{for depthcheck}^{i,j} > 0 \,\text{and depthcheck}^{i,j} <= 0.05 \tag{F.16}$$

$$\text{trans\_inf}^{i,j} = 1 \quad \text{for depthcheck}^{i,j} < 0 \tag{F.17}$$

If $u_{reps}^{i,j} < 0$

$$\text{trans\_inf}^{i,j} = 0 \quad \text{for depthcheck}^{i+1,j} > 0.05 \tag{F.18}$$

$$\text{trans\_inf}^{i,j} = 1 - \text{depthcheck}/0.05 \quad \text{for depthcheck}^{i+1,j} > 0 \,\text{and depthcheck}^{i+1,j} <= 0.05 \tag{F.19}$$

$$\text{trans\_inf}^{i,j} = 1 \quad \text{for depthcheck}^{i+1,j} < 0 \tag{F.20}$$

Now multiply the sediment transport fluxes with trans_inf:

$$Susg^{i,j,1} = Susg^{i,j,1} \cdot \text{trans\_inf}^{i,j} \tag{F.21}$$

$$Subg^{i,j,1} = Subg^{i,j,1} \cdot \text{trans\_inf}^{i,j} \tag{F.22}$$

$$Subg\_g^{i,j,2} = Subg\_g^{i,j,2} \cdot (1 - \text{trans\_inf}^{i,j}) \tag{F.23}$$

For $Suss$ the exact same procedure is followed, with the difference that instead of u_{reps} the groundwater velocity gwu is used. Now the transport gradients for each cell is calculated.

$$(\nabla S_s)^{i,j} = \frac{Susg^{i,j}\Delta n_u^{i,j} - Susg^{i-1,j}\Delta n_u^{i-1,j} + Subg^{i,j}\Delta n_u^{i,j} - Subg^{i-1,j}\Delta n_u^{i-1,j} + Suss^{i,j}\Delta n_u^{i,j} - Suss^{i-1,j}\Delta n_u^{i-1,j}}{A_z^{i,j}} \tag{F.24}$$

$$\left(\nabla S_g\right)^{i,j} = \frac{Subg\_g^{i,j}\Delta n_u^{i,j} - Subg\_g^{i-1,j}\Delta n_u^{i-1,j}}{A_z^{i,j}} \tag{F.25}$$

F.2.3. BED LEVEL UPDATE OF GRAVEL LAYER

The first step is to update the gravel layer.

$$dz_g^{i,j} = MF \cdot \partial t \cdot \frac{\nabla S_g^{i,j}}{(1-n_{p,g})} \tag{F.26}$$

$$z\_g^{i,j} = \max\left(z\_g^{i,j} - dz_s^{i,j}, 0\right) \tag{F.27}$$

With the gravel layer increased or decreased the sand height and/or overlap / counter must adapted. A distinction is made between the situation where sand is on top of gravel and where it isn't. See respectively step 1 and step 2.

Step 1:
Here a sand layer is covering the gravel. Therefore the $counter > 0$. Still an incoming flux of gravel can be present. In that case the gravel layer is increased, the sand height is increased, the overlap increases and the counter decreases. A check must be done to see if the sand above the gravel is swallowed by the gravel (i.e. the sand fits within the pores of the newly added gravel). This is done with $mass\_check$.

$$mass\_check = mass1 - mass2 \tag{F.28}$$

In which *mass1* is the mass of the sand on top of the gravel.

$$mass1 = counter \frac{(1-n_{p,s})}{MF\,\partial t} \tag{F.29}$$

And *mass2* is the maximum amount of sand that could could fit within the newly accreted gravel (note accretion gives negative dz_g's):

$$mass2 = -dz_g n_{p,g} \frac{1-n_{p,s}}{MF\,\partial t} \tag{F.30}$$

Now if $mass\_check > 0$ (gravel does not swallow sand layer that is on top) and a gravel layer is present, the sand depth increases a bit, and the counter (reduced with respect to earlier timestep) and overlap (increased) must be updated:

$$dz_{s,extra} = dz_g + MF\,\partial t \frac{mass\_check}{1-n_{p,s}} \tag{F.31}$$

$$counter = MF\,\partial t \frac{mass\_check}{1-n_{p,s}} \tag{F.32}$$

$$overlap = z\_g \tag{F.33}$$

Now if $mass\_check <= 0$ (gravel does swallow sand layer that is on top) and a gravel layer is present, the sand depth increases a bit, and the counter and overlap must be updated:

$$dz_{s,extra} = -MF\,\partial t \frac{mass1}{(1-n_{p,s})n_{p,g}} \tag{F.34}$$

$$counter = 0 \tag{F.35}$$

$$overlap = z_g + MF\,\partial t \frac{mass\_check}{(1-n_{p,s})n_{p,g}} \tag{F.36}$$

Now lastly, update the sand elevation. Hereafter step 3 is proceeded.

$$z\_s = z\_s - dz_{s,extra} \tag{F.37}$$

Step 2:
Here no sand is covering a gravel layer. Thus step 3 is proceeded.

F.2.4. BED LEVEL UPDATE OF SAND ELEVATION

The update of z_s starts with the a *depthcheck* in order to discriminate locally between a the types of bottoms present:

$$depthcheck = z\_g - overlap \tag{F.38}$$

If the *depthcheck* is large a thick gravel layer is present. If *depthcheck* is small or zero, barely any gravel is present, no gravel is present or a fully filled gravel layer is present.

Two possibilities are regarded:

1. $depthcheck >$ Threshold depth:
   Gravel is present, such that no suspended and/or bed-load sand erosion from this cell is possible. Erosion of sand underneath gravel is possible, as well as gravel transport. Accretion is possible for all transports. Updates are explained in step 3.
2. $depthcheck <=$ Threshold depth:
   Little gravel is present, such that little to no bed-load gravel erosion from this cell is possible. Erosion of sand underneath gravel is not possible. Accretion is possible for all transports. Update are explained in step 4.

Step 3:
Step 3 is divided into 2 substeps. Either there is accretion ($\nabla S_s < 0$) or erosion ($\nabla S_s > 0$) of sand. If $\nabla S_s = 0$ there is no bed level change of the sand and thus $dz_s = 0$ and step 5 is executed.

Accretion:
Here sand is accreted, while a gravel layer is present. Therefore the sand bed changes with the Exner$^+$ equation.

$$dz_s = MF\,\partial t \frac{\nabla S_s}{1 - n_{p,s}} / n_{p,g} \tag{F.39}$$

$$overlap = overlap - dz_s \tag{F.40}$$

Now it is possible that more sand is accreted than there is space for in the gravel. This is done by checking the depth with the newly calculated *overlap*: $check = z\_g - overlap$. If $check < 0$ then a sand layer on top of the gravel is created (reset overlap, dz_s and counter:

$$dz_s = MF\,\partial t \frac{\nabla S_s + \left(\frac{depthcheck \cdot n_{p,g}(1-n_{p,s})}{MF\,\partial t}\right)}{1 - n_{p,s}} - depthcheck \tag{F.41}$$

$$overlap = z\_g \tag{F.42}$$

$$counter = dz_s - depthcheck \tag{F.43}$$

In which $depthcheck$ is the height of the gravel that has been with sand filled.

Erosion:
Here sand is eroded, while a gravel layer is present. Therefore the sand bed changes with the Exner$^+$ equation.

$$dz_s = MF\,\partial t \frac{\nabla S_s}{1 - n_{p,s}} / n_{p,g} \tag{F.44}$$

$$overlap = overlap - dz_s \tag{F.45}$$

Now it is possible that more sand is eroded than there is present in the gravel. If this occurs the new $overlap < 0$. If this occurs the bed level update must be adapted to include both Exner and Exner$^+$ and the overlap must be update to be zero.

$$dz_s = MF\,\partial t \frac{\nabla S_s + \left(\frac{overlap \cdot n_{p,g}(1-n_{p,s})}{MF\,\partial t}\right)}{1-n_{p,s}} - depthcheck \tag{F.46}$$

$$overlap = 0 \tag{F.47}$$

Step 4:
Step 4 is divided into 2 substeps. Either there is accretion ($\nabla S_s < 0$) or erosion ($\nabla S_s > 0$) of sand. If $\nabla S_s = 0$ there is no bed level change of the sand.

Accretion:
With the accretion of sand it is first checked whether some gravel is present or not. This is done by checking $depthcheck$ from equation F.38. If $depthcheck > 0$ this means a little layer of gravel is still present (this is still limited to be less than the threshold depth of gravel). When $depthcheck > 0$ it is also checked whether the transport gradient is large enough fill this last layer of gravel. This is done with $signcheck$. The following formulations arise for accretion:

If $depthcheck > 0$:

$$signcheck = \nabla S_s + \frac{depthcheck\, n_{p,g}(1-n_{p,s})}{MF\,\partial t} \tag{F.48}$$

If $signcheck > 0$, thus gradient was not large enough to fill the gravel, use the Exner$^+$ bed level update:

$$dz_s = MF\,\partial t \frac{\nabla S_s}{(1-n_{p,s})} / n_{p,g} \tag{F.49}$$

$$overlap = overlap - dz_s \tag{F.50}$$

When $signcheck <= 0$, thus the gradient was large enough to fill the gravel, use both Exner and Exner$^+$.

$$dz_s = MF\,\partial t \frac{\nabla S_s + \frac{depthcheck\, n_{p,g}(1-n_{p,s})}{MF\,\partial t}}{(1-n_{p,s})} / n_{p,g} - depthcheck \tag{F.51}$$

$$overlap = z\_g \tag{F.52}$$

$$counter = dz_s - depthcheck \tag{F.53}$$

If $depthcheck <= 0$:

$$dz_s = MF\,\partial t \frac{\nabla S_s}{1-n_{p,s}} \tag{F.54}$$

$$counter = counter - dz_s \quad \text{(Only if the sand is covering a gravel layer)} \tag{F.55}$$

Erosion:
Sand can be eroded from a cell where only sand is available (no gravel buried) or from a cell where sand is covering a gravel layer. The first situation can easily be done with the Exner equation:

$$dz_s = MF\,\partial t \frac{\nabla S_s}{(1-n_{p,s})} \tag{F.56}$$

If sand is covering a gravel layer it is possible that more sand is eroded than is present on top of the gravel. In that case both Exner and Exner$^+$ should be used. First the dz_s is calculated the same as in equation F.56. Then if $dz_s > counter$ use both Exner and Exner$^+$ (if not proceed to equation F.61).

$$dz_s = MF\,\partial t \frac{\nabla S_s - \frac{counter\,(1-n_{p,s})}{MF\,\partial t}}{(1-n_{p,s})} / n_{p,g} + counter \tag{F.57}$$

$$overlap = overlap - (dz_s - counter) \tag{F.58}$$

It could be possible that the transport gradient is sufficiently large to be able to erode all the sand inside the gravel and thus also sand underneath the gravel. If this is so, the $overlap$ from equation F.58 is negative. In that case the following equations are used:

$$dz_s = MF\,\partial t \frac{\nabla S_s - \frac{counter(1-n_{p,s})}{MF\,\partial t} - \frac{overlap\_old\; n_{p,g}(1-n_{p,s})}{MF\,\partial t}}{1-n_{p,s}} + overlap\_old + counter \tag{F.59}$$

$$overlap = 0 \tag{F.60}$$

The following equation is done. if partial erosion of a sand bed on top of a gravel layer has occurred.

$$counter = counter - dz_s \tag{F.61}$$

Step 5: The final step is to update the elevation of the sand bed elevation. After doing this one is also able to update the general bed level.

$$z\_s = z\_s - dz_s \tag{F.62}$$

$$z_b = z\_s + (z_g - overlap) \tag{F.63}$$

F.3. HORIZONTAL GROUNDWATER VELOCITY CALCULATIONS IN WET CELLS

Here the calculation of the horizontal groundwater velocities is discussed and it is discussed how this influences sand transport inside the revetment. In wet cells the horizontal groundwater velocities are calculated by the groundwater head gradient $\frac{\partial H}{\partial x}$. Here a situation is sketched for two grid cells with a surface water elevation with a gradient and with two different revetment depths, see figure F.1.

In groundwater module the head gradient is calculated on top of the revetment. This is the same for both grid cells. With this gradient the velocities are calculated within the revetment, see figure F.2. Because the velocities are the same, erosion is not larger for the cell with a lower depth. In shallow cells velocities should be larger for the same gradients. This will eventually erode the cell and then velocities reduce, smearing the bed (shown in the right figure).

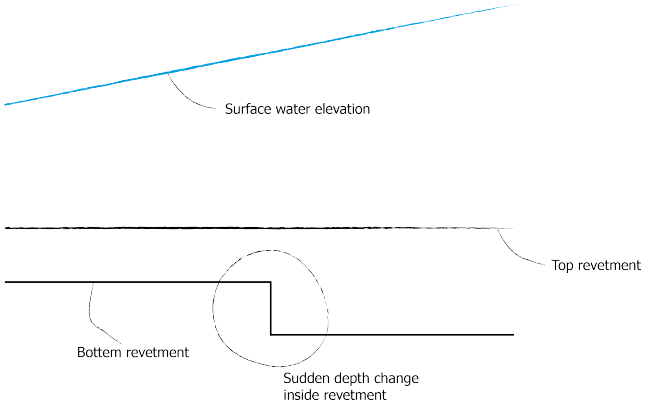

Figure F.1: Sketch of situation inside the revetment

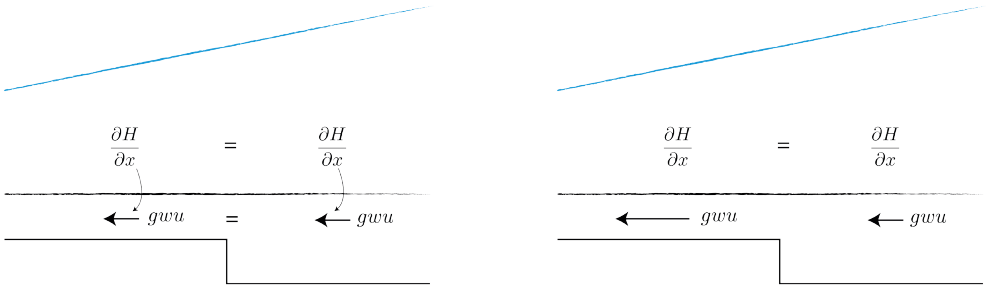

Figure F.2: Horizontal groundwater velocity calculation - Left shows impression of model calculation and right shows expected velocities.

F.4. MODEL RUNS AND RESULTS

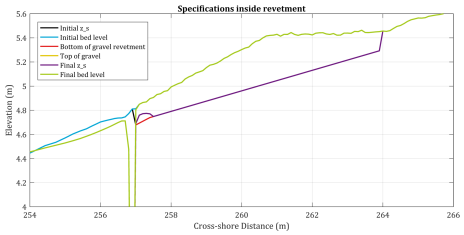

Figure F.3: Two-line model run DR1 - Specifics inside revetment

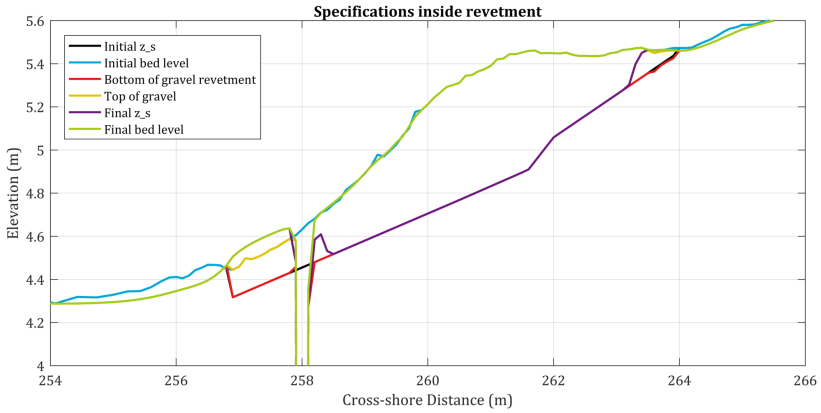

Figure F.4: Two-line model run DR4 - Specifics inside revetment

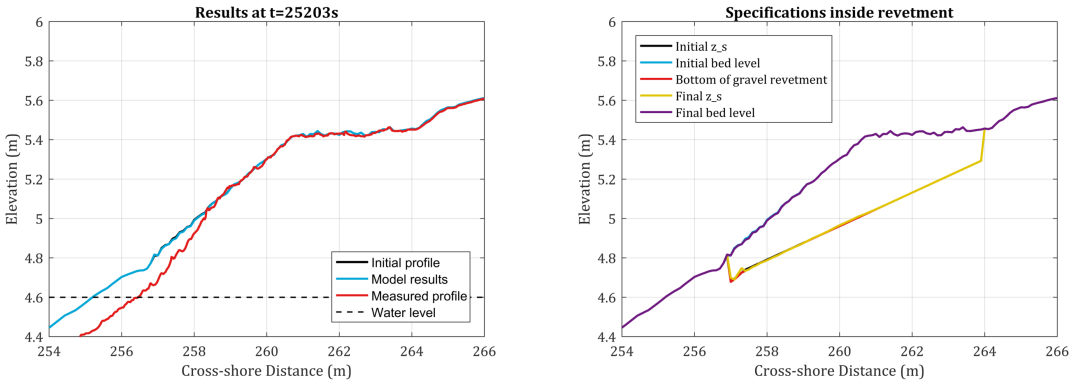

Figure F.5: Model run C1

Test	Reference wave set	Transport equation	K (ms^{-1})	gwu_{max} (ms^{-1})	Comment	Figure
C1	DR1	Jacobsen	0.2	100	-	F.5
C2	DR1	Jacobsen	0.3	100	-	9.4
C3	DR1	Jacobsen	0.4	100	-	9.5
C4	DR1	Jacobsen	0.3	0.05	-	F.6
C5	DR1	Jacobsen	0.3	0.1	-	F.7
C6	DR1	Jacobsen	0.3	0.2	-	F.8
C7	DR4	Jacobsen	0.2	100	Failed	F.9
C8	DR4	Jacobsen	0.3	100	Failed	9.6
C9	DR4	Jacobsen	0.4	100	Failed	F.10
C10	DR4	Jacobsen	0.3	0.05	-	9.7
C11	DR4	Jacobsen	0.3	0.1	-	F.11
C12	DR4	Jacobsen	0.3	0.2	Failed	F.12
C13	DR1	McCall-Van Rijn	0.2	100	-	F.13
C14	DR1	McCall-Van Rijn	0.3	100	-	F.14
C15	DR1	McCall-Van Rijn	0.4	100	-	F.15
C16	DR1	McCall-Van Rijn	0.3	0.05	-	F.16
C17	DR1	McCall-Van Rijn	0.3	0.1	-	F.17
C18	DR1	McCall-Van Rijn	0.3	0.2	-	F.18
C19	DR4	McCall-Van Rijn	0.2	100	-	9.8
C20	DR4	McCall-Van Rijn	0.3	100	Failed	F.19
C21	DR4	McCall-Van Rijn	0.4	100	-	F.20
C22	DR4	McCall-Van Rijn	0.3	0.05	-	F.21
C23	DR4	McCall-Van Rijn	0.3	0.1	-	F.22
C24	DR4	McCall-Van Rijn	0.3	0.2	-	F.23

Table F.1: Model runs with Jacobsen and McCall-Van Rijn for DR1 and DR4

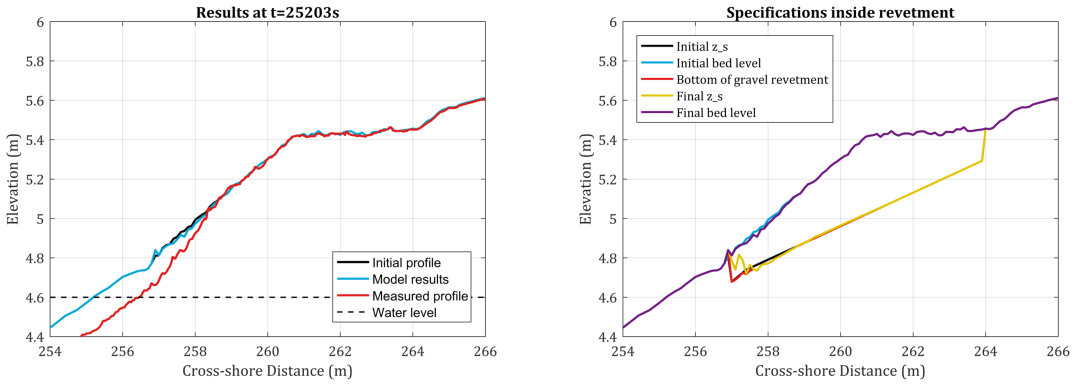

Figure F.6: Model run C4

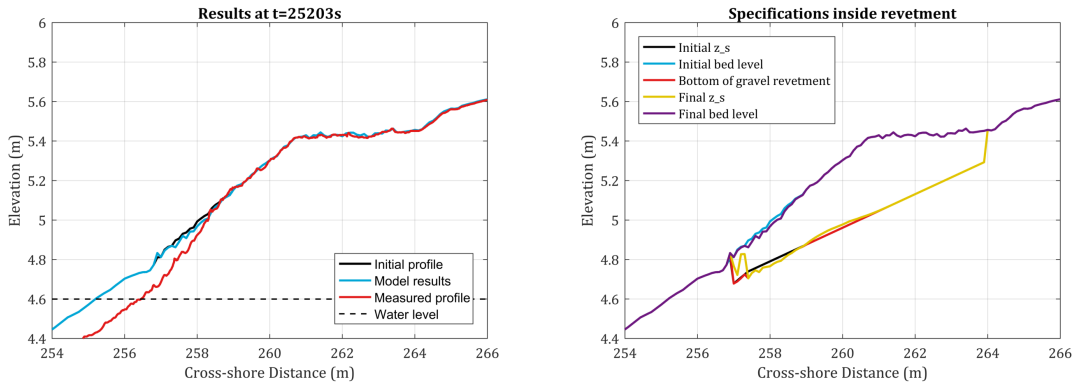

Figure F.7: Model run C5

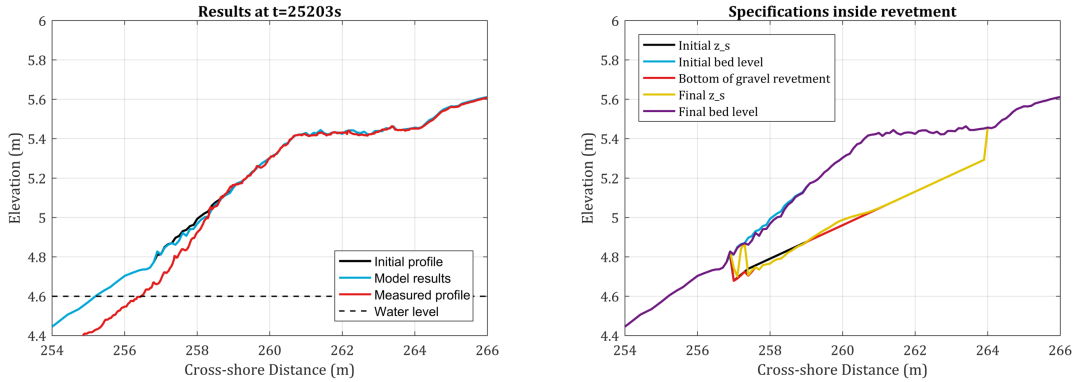

Figure F.8: Model run C6

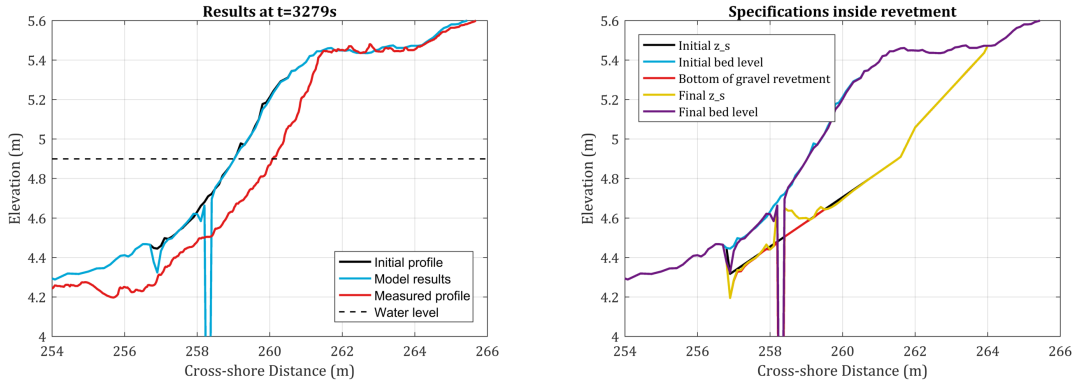

Figure F.9: Model run C7

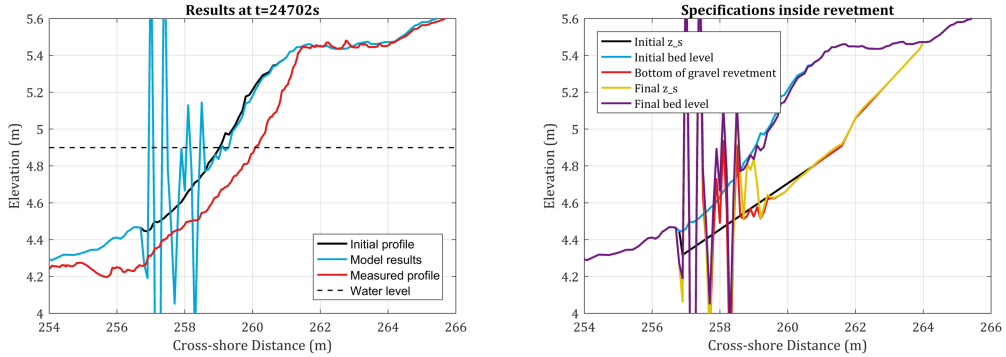

Figure F.10: Model run C9

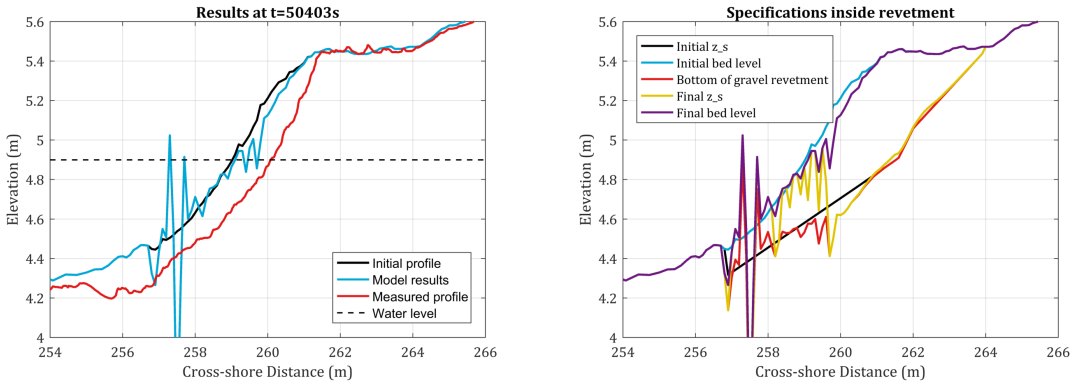

Figure F.11: Model run C11

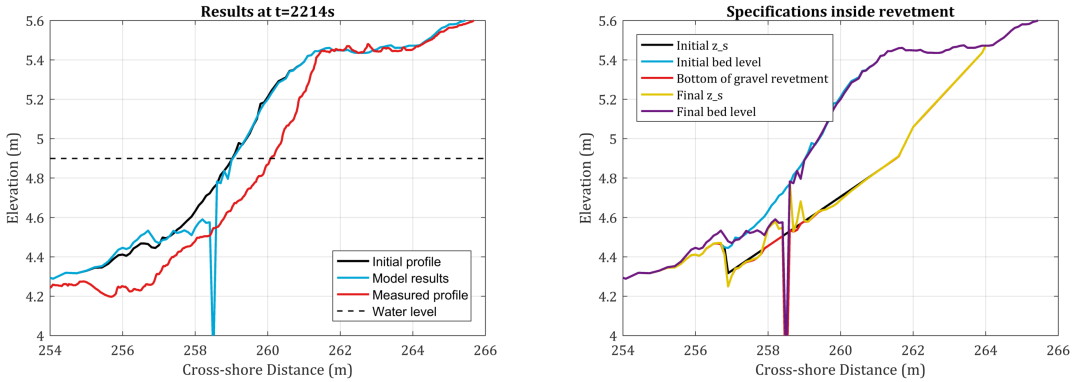

Figure F.12: Model run C12

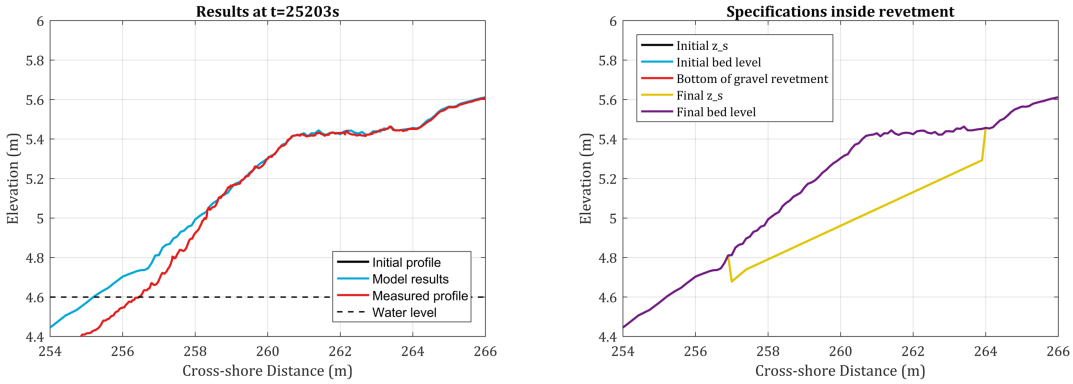

Figure F.13: Model run C13

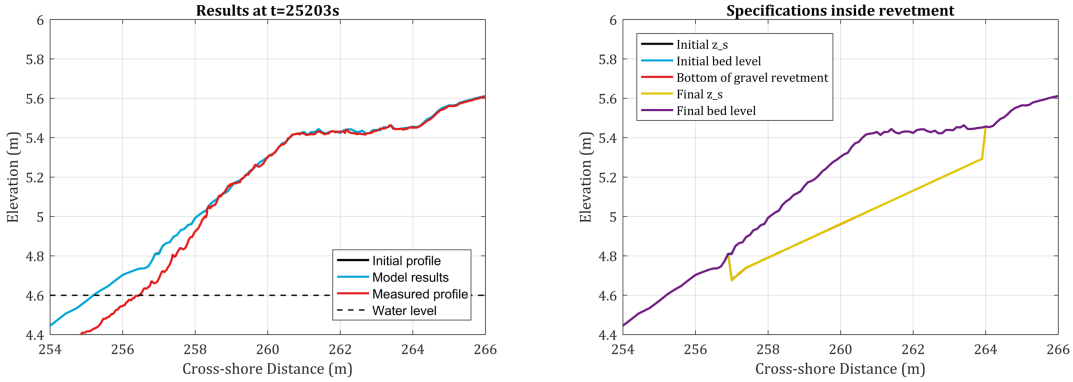

Figure F.14: Model run C14

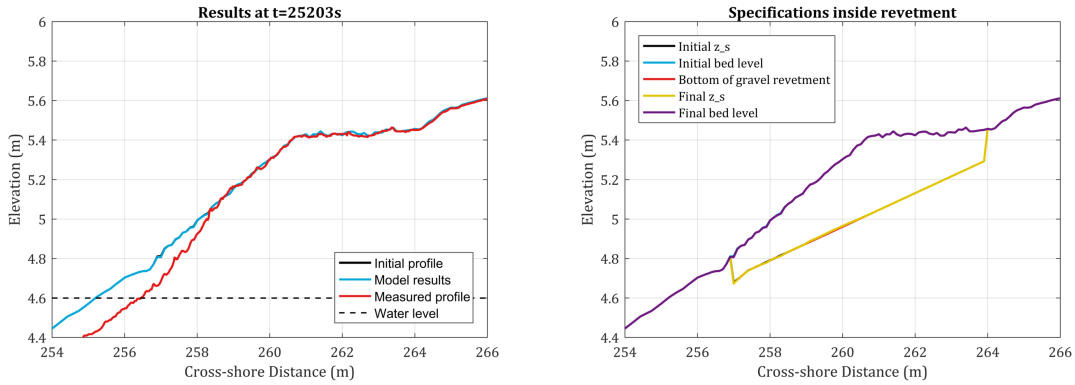

Figure F.15: Model run C15

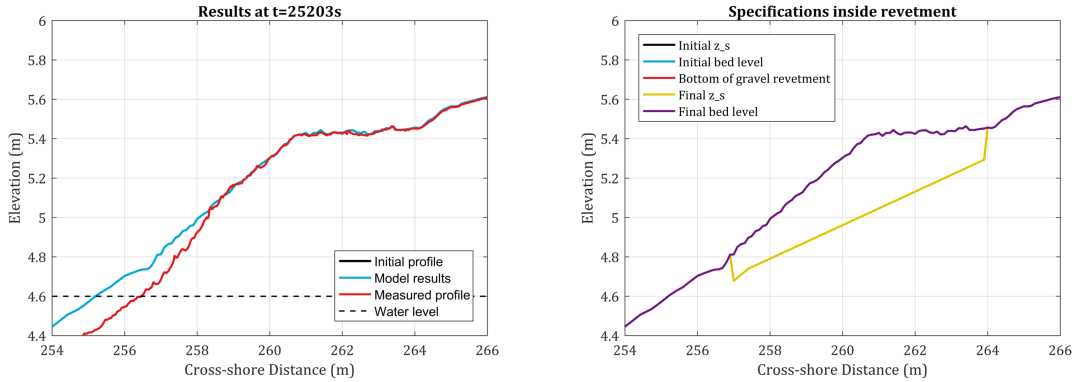

Figure F.16: Model run C16

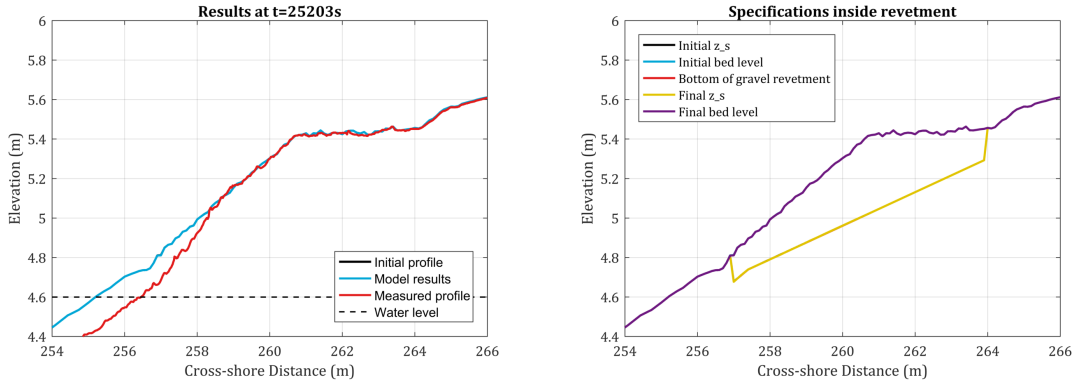

Figure F.17: Model run C17

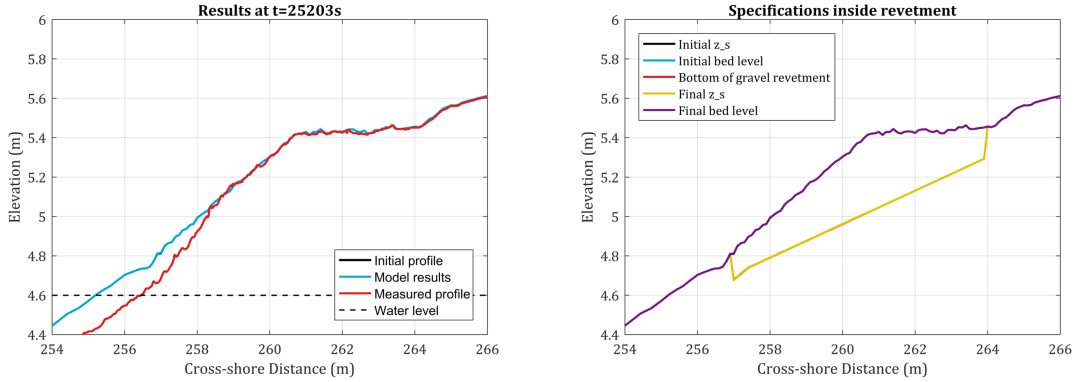

Figure F.18: Model run C18

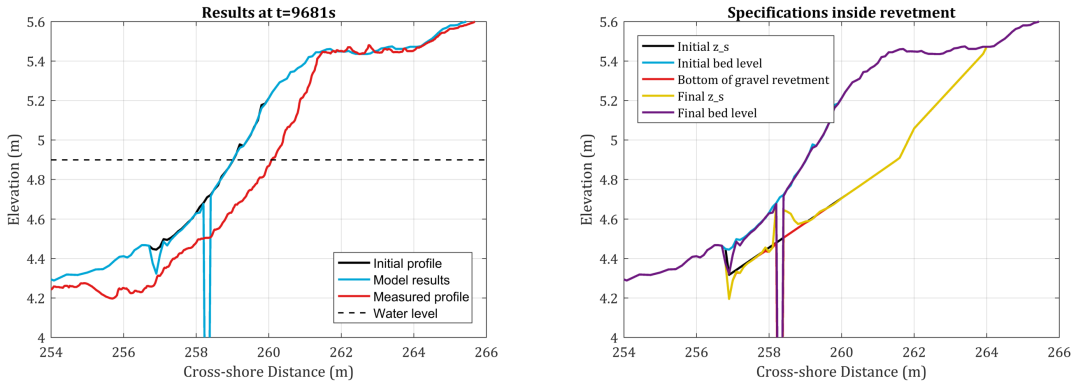

Figure F.19: Model run C20

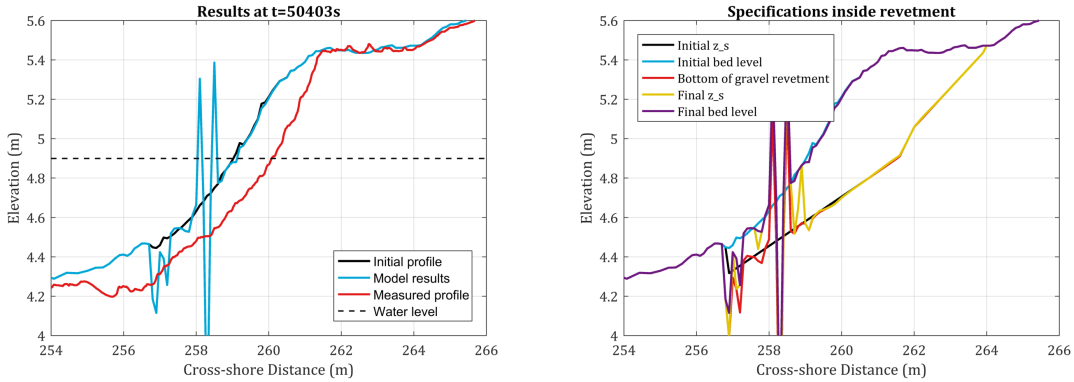

Figure F.20: Model run C21

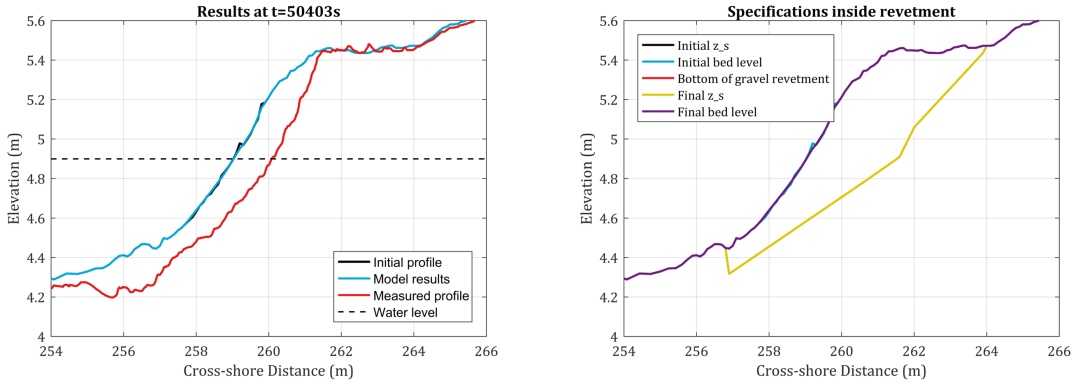

Figure F.21: Model run C22

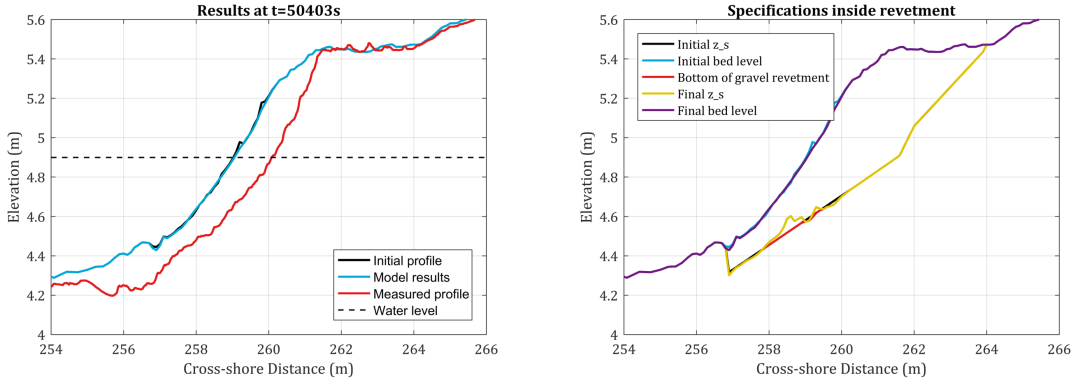

Figure F.22: Model run C23

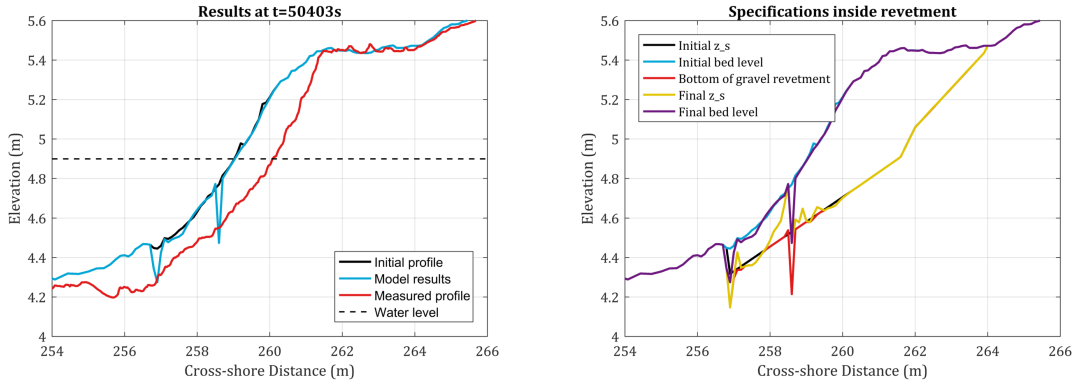

Figure F.23: Model run C24

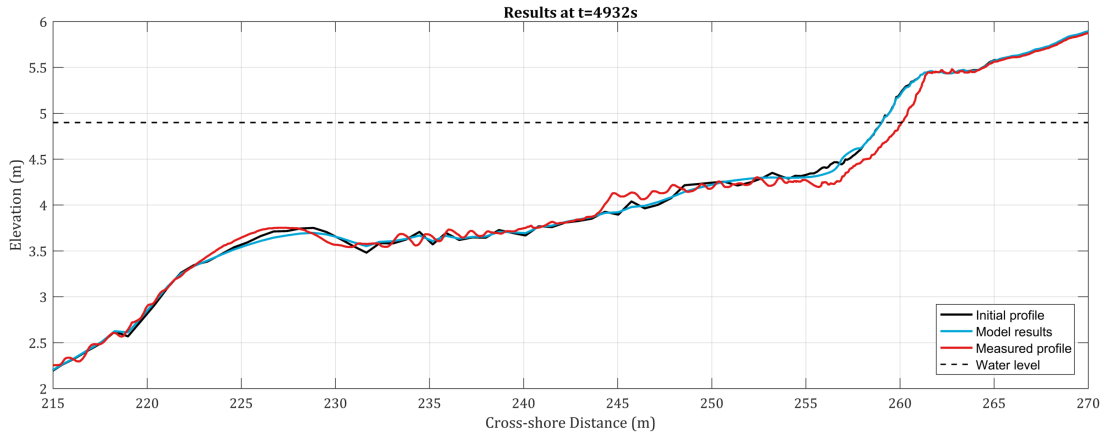

Figure F.24: Two-line model run DR4 before crash - All types of transport, including erosion in revetment

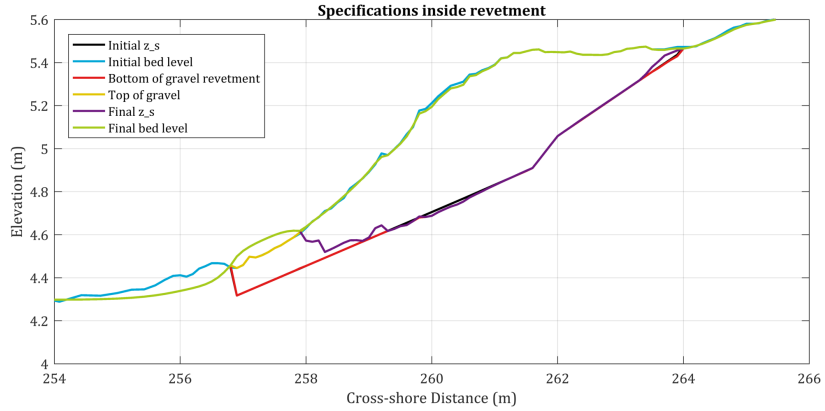

Figure F.25: Specifications inside revetment before crash - Model runs with all types of transports

REFERENCES

Ahrens, J. P. (2000). A Fall-Velocity Equation. *Journal of Waterway, Port, Coastal, and Ocean Engineering*, 126(April):99–102.

Allan, J. C., Geitgey, R., and Hart, R. (2005). Dynamic Revetments for Coastal Erosion in Oregon. Technical report.

Allan, J. C., Priest, G. R., and Komar, P. D. (2004). Coast hazards and management issues on the Oregon coast.

Battjes, J. (1974). Surf Similarity. In *Coastal Engineering 1974*, pages 466–480, New York, NY. American Society of Civil Engineers.

Bergillos, R. J., Masselink, G., McCall, R. T., and Ortega-Sánchez, M. (2016). Modelling overwash vulnerability along mixed sand-gravel coasts with XBeach-G: Case study of Playa Granada, Southern Spain. *Coastal Engineering*.

Blenkinsopp, C. (2016). Dynamic coastal protection: resilience of dynamic revetment under SLR. (Proposal).

Bosboom, J. and Stive, M. J. (2015). *Coastal Dynamics 1, Lecture notes CIE4305*. VSSD.

Conley, D. C. and Inman, D. L. (1994). Ventilated oscillatory boundary layers. *Journal of Fluid Mechanics*, 273(-1):261.

Darcy, H. (1856). *Les fontaines publiques de la ville de Dijon*. Victor Dalmont, Dalmont, Paris.

De Vet, P. L. M. (2014). Modelling sediment transport and morphology during overwash and breaching events.

Dean, R. G. (1991). Equilibrium Beach Profiles: Characteristics and Applications.

Downie, K. and Saaltink, H. (1983). An artificial cobble beach for erosion control. *Coastal Structues '83*, pages 846–859.

Engelund, F. and Fredsøe, J. (1976). A Sediment Transport Model for Straight Alluvial Channels. *Hydrology Research*, 7(5).

Forchheimer, P. (1901). Wasserbewegung durch boden. *Zeitschrift des Vereines Deutscher Ingenieure*, 45:1782 – 1788.

Fredsøe, J. and Deigaard, R. (1992). *Mechanics of Coastal Sediment Transport*, volume 3 of *Advanced Series on Ocean Engineering*. World Scientific.

Fuller, R. M. and Randall, R. E. (1988). The Orford Shingles, Suffolk, UK-Classic conflicts in coastline management. *Biological Conservation*, 46(2):95–114.

Galappatti, G. and Vreugdenhil, C. B. (1985). A depth-integrated model for suspended sediment transport. *Journal of Hydraulic Research*, 23(4):359–377.

Hallermeier, R. J. (1981). Terminal settling velocity of commonly occuring sand grains. *Sedimentology*, 28(6):859–865.

Hazen, A. (1911). Discussion of: dams in sand foundations, by A.C. Loenig. *Transactions of the American Society of Civil Engineers*.

Holthuijsen, L. (2007). *Waves in Oceanic and Coastal Waters*. Cambridge University Press, 1 edition.

Jacobsen, N. G., van Gent, M. R., and Fredsøe, J. (2017). Numerical modelling of the erosion and deposition of sand inside a filter layer. *Coastal Engineering*, 120:47–63.

Jennings, R. and Shulmeister, J. (2002). A field based classification scheme for gravel beaches. *Marine Geology*, 186(3):211–228.

Karunarathna, H., Horrillo-Caraballo, J. M., Ranasinghe, R., Short, A. D., and Reeve, D. E. (2012). An analysis of the cross-shore beach morphodynamics of a sandy and a composite gravel beach. *Marine Geology*, 299-302:33–42.

Komar, P. D. and Miller, M. C. (1975). On the comparison between the threshold of sediment motion under waves and unidirectional currents with a discussion of the practical evaluation of the threshold: Reply. *Journal of Sedimentary Research*, 45(1).

Lorang, M. S. (1991). An Artificial Perched-Gravel Beach as a Shore Protection Structure. *Coastal Sediments '91*, pages 1916–1925.

MacCormack, R. (1969). The Effect of Viscosity in Hypervelocity Impact Cratering. *AIAA Paper*, pages 69–354.

Mason, T., Voulgaris, G., Simmonds, D., and Collins, M. (1997). Hydrodynamics and Sediment Transport on Composite (Mixed Sand/Shingle) and Sand Beaches: A Comparison. *Coastal Dynamics 1997*, pages 48 – 57.

Masselink, G. and Li, L. (2001). The role of swash infiltration in determining the beachface gradient: A numerical study. *Marine Geology*, 176(1-4):139–156.

McCall, R. T. (2015). Process-based modelling of storm impacts on gravel coasts.

Meyer-Peter, E. and Muller, R. (1948). Formulas for bed-load transport. *Proceedings of the 2nd Meeting of the International Association for Hydraulic Structures Research*, pages 39–64.

Mulqueen, J. (2005). The flow of water through gravels. *Irish Journal of Agricultural and Food Research*, 44(1):83–94.

Mutlu Sumer, B., Cokgor, S., and Fredsøe, J. (2001). Suction Removal of Sediment from between Armor Block. *Journal of Hydrologic Engineering*, 127(April):293 – 306.

Nielsen, P. (2002). Shear stress and sediment transport calculations for swash zone modelling. *Coastal Engineering*, 45(1):53–60.

Pedrozo-Acuña, A., Simmonds, D. J., Chadwick, A. J., and Silva, R. (2007). A numerical-empirical approach for evaluating morphodynamic processes on gravel and mixed sand-gravel beaches. *Marine Geology*, 241(1-4):1–18.

Quick, M. C. and Dyksterhuis, P. (1994). Cross-shore transport for beaches of mixed sand and gravel. *International Symposium: Waves—Physical and Numerical Modeling. Canadian Society of Civil Engineers*, pages 1443–1452.

Roelvink, D., Reniers, A., Van Dongeren, A., Van Thiel De Vries, J., Mccall, R., and Lescinski, J. (2009). Modelling storm impacts on beaches, dunes and barrier islands. *Coastal Engineering*, 56:1133–1152.

Roelvink, D., van Dongeren, A., McCall, R., Hoonhout, B., van Rooijen, A., van Geer, P., de Vet, L., Nederhoff, K., and Quataert, E. (2015). XBeach Technical Reference : Kingsday Release. (April):1–141.

Ruiz de Alegria-Arzaburu, A., Williams, J. J., and Masselink, G. (2011). Application of Xbeach To Model Storm Response on a Macrotidal Gravel Barrier. *Coastal Engineering Proceedings*, 1(32):1–15.

Schiereck, G. (2001). *Introduction to Bed, bank and shore protection*. Delft University Press, 1 edition.

She, K., Horn, D., and Canning, P. (2006). Porosity and Hydraulic Conductivity of Mixed Sand - Gravel Sediment.

Shields, A. (1936). Anwendung der Aehnlichkeitsmechanik und der Turbulenzforschung auf die Geschiebebewegung. *PhD Thesis Technical University Berlin*.

Smit, P. B., Stelling, G. S., Roelvink, D., van Thiel de Vries, J., McCall, R., van Dongeren, A., Zwinkels, C., and Jacobs, R. (2010). XBeach: Non-hydrostatic model. *Report, Delft University of Technology and Deltares, Delft, The Netherlands*.

Soulsby, R. (1997). *Dynamics of marine sands: a manual for practical applications*. Thomas Telford.

Soulsby, R. and Whitehouse, R. (1997). Threshold of Sediment Motion in Coastal Environments. In *Pacific Coasts and Ports '97: Proceedings of the 13th Australasian Coastal and Ocean Engineering Conference and the 6th Australasian Port and Harbour Conference*, volume 1, pages 145–150, Christchurch, N.Z. Centre for Advanced Engineering, University of Canterbury.

Stevanato, F., Nielsen, A., Sumer, B., and Fredsøe, J. (2010). Flow Velocities and Bed Shear Stresses in a Stone Cover under an Oscillatory Flow. *International Conference on Scour and Erosion*.

US Army Corps of Engineers (2002). Coastal engineering eanual. *Engineer manual*, pages 2–1100.

USGS (2006). U.S. Geological Survey Open-File Report 2006-1195.

van Gent, M. and Wolters, G. (2015). Granular slopes with open filters under wave loading. *Coastal Engineering*, pages 135–150.

Van Rijn, L. C. (1984). Sediment transport, part III: bed forms and alluvial roughness. *Journal of hydraulic engineering*, 110(12):1733–1754.

Van Rijn, L. C. (2007a). Unified view of sediment transport by currents and waves. I: Initiation of motion, bed roughness, and bed-load transport. *Journal of hydraulic engineering*, 133(6):649–667.

Van Rijn, L. C. (2007b). Unified view of sediment transport by currents and waves. II: Suspended sediment. *Journal of hydraulic engineering*, 133(6):668–689.

Van Rijn, L. C. (2007c). Unified view of sediment transport by currents and waves. III : Graded beds. *Journal of hydraulic engineering*, 133(6):761–775.

Van Thiel De Vries, J., Van Eekelen, E., Luijendijk, A., Ouwerkerk, S., and Steetzel, H. (2016). Challenges in Developing Sustainable Sandy Strategies.

Van Thiel De Vries, J. S. M. (2009). *Dune erosion during storm surges*.

Vellinga, P. (1983). *Predictive computational model for beach and dune erosion during storm surge*. Waterloopkundig Laboratorium, Delft.

Vriend, H. J. D., Havinga, H., van Prooijen, B. C., Visser, P. J., and Wang, Z. B. (2011). River Engineering.

Walstra, D. J. R., Van Rijn, L. C., Van Ormondt, M., Brière, C., and Talmon, A. M. (2007). The Effects of Bed Slope and Wave Skewness on Sediment Transport and Morphology. *Coastal Sediments '07*, pages 137 – 150.

Wong, M. and Parker, G. (2006). Reanalysis and Correction of Bed-Load Relation of Meyer-Peter and Müller Using Their Own Database. *Journal of Hydraulic Engineering*, 132(11):1159–1168.

Zanen, A., Jansen, P. P., Van Bendegom, L., den Berg, J., and De Vries, M. (1994). Principles of River Engineering: The non-tidal alluvial river.